ISTANBUL TECHNICAL UNIVERSITY ★ GRADUATE SCHOOL

BETA, GAMMA AND NEUTRON ATTENUATION PROPERTIES OF PMMA/COLEMANITE COMPOSITES EXPOSED TO SPACE RADIATION IN LOW EARTH ORBIT

M.Sc. THESIS

Mehmet Orhan ŞİRİN

Nuclear Research Division

Radiation Science and Technology Programme

JUNE 2024

ISTANBUL TECHNICAL UNIVERSITY ★ GRADUATE SCHOOL

BETA, GAMMA AND NEUTRON ATTENUATION PROPERTIES OF PMMA/COLEMANITE COMPOSITES EXPOSED TO SPACE RADIATION IN LOW EARTH ORBIT

M.Sc. THESIS

Mehmet Orhan SIRIN
(302211006)

Nuclear Research Division

Radiation Science and Technology Programme

Thesis Advisor: Prof. Dr. Nilgun BAYDOGAN

JUNE 2024

ISTANBUL TEKNİK ÜNİVERSİTESİ ★ LİSANSÜSTÜ EĞİTİM ENSTİTÜSÜ

ALÇAK DÜNYA YÖRÜNGESİNDE UZAY RADYASYONUNA MARUZ KALAN PMMA/KOLEMANİT KOMPOZİTLERİNİN BETA, GAMA VE NÖTRON ZAYIFLATMA ÖZELLİKLERİ

YÜKSEK LİSANS TEZİ

Mehmet Orhan ŞİRİN
(302211006)

Nükleer Araştırmalar Anabilim Dalı

Radyasyon Bilim ve Teknoloji Programı

Tez Danışmanı: Prof. Dr. Nilgün BAYDOĞAN

HAZİRAN 2024

Mehmet Orhan SIRIN, a M.Sc. student of ITU Graduate School student ID 302211006 successfully defended the thesis entitled “BETA, GAMMA AND NEUTRON ATTENUATION PROPERTIES OF PMMA/COLEMANITE COMPOSITES EXPOSED TO SPACE RADIATION IN LOW EARTH ORBIT”, which he prepared after fulfilling the requirements specified in the associated legislations, before the jury whose signatures are below.

Thesis Advisor :	**Prof. Dr. Nilgün BAYDOĞAN** Istanbul Technical University	.....
Jury Members :	**Prof. Dr. Nesrin ALTINSOY** Istanbul Technical University	.....
	Prof. Dr. Selcan KARAKUŞ Istanbul University-Cerrahpasa	.....

Date of Submission : 24 May 2024
Date of Defense : 24 June 2024

To my mother,

FOREWORD

I would like to offer my gratitude to my thesis advisor Prof. Dr. Nilgun BAYDOĞAN for her guide, support and virtue as gave me strength during the performing of experiments and preparation of thesis.

I am also extremely thankful to the Research Assistants Onur ERBAY and Hilal MACUN for their understandings and supports while conducting the experiments.

May 2024

Mehmet Orhan ŞİRİN
(Metallurgical and Materials Engineer)

TABLE OF CONTENTS

Page

FOREWORD ..... **ix**
TABLE OF CONTENTS ..... **xi**
ABBREVIATIONS ..... **xiii**
SYMBOLS ..... **xv**
LIST OF TABLES ..... **xvii**
LIST OF FIGURES ..... **xix**
SUMMARY ..... **xxiii**
ÖZET ..... **xxv**
1. INTRODUCTION **1**
1.1 Purpose of Thesis 1
1.2 Literature Review 1
1.3 Hypothesis 2
2. GENERAL INFORMATIONS **3**
2.1 Radiation 3
2.1.1 Classification of radiation 4
2.1.2 Radiation in space 6
2.1.2.1 Solar particle events 7
2.1.2.2 Galactic cosmic rays 8
2.1.2.3 Secondary radiation 9
2.1.3 Radiation shielding in space 10
2.1.3.1 Van Allen belts 10
2.1.3.2 Active shielding 12
2.1.3.3 Passive shielding 13
2.1.4 Laboratory experiments of space radiation 14
2.2 Polymers 16
2.2.1 Classification of polymers 17
2.2.2 Structure of polymers 17
2.2.3 Polymerization 20
2.2.4 Polymers for radiation shielding 21
2.2.5 Poly (methyl methacrylate) 22
2.2.5.1 Poly (methyl methacrylate) for radiation shielding 24
2.3 Minerals 25
2.3.1 Classification of minerals 25
2.3.2 Colemanite 26
2.3.2.1 Colemanite for radiation shielding 26
3. METHODOLOGY **27**
3.1 Sample Preparation 27
3.2 Radiation Exposure of the Samples 28
3.3 Experimental Setups 30
3.3.1 Beta transmission experiment 31

3.3.1.1 Sr-90 31
3.3.2 Gamma transmission experiment 32
3.3.2.1 Cs-137 and Co-60 32
3.3.3 Neutron transmission experiment 33
3.3.3.1 Nuclear-Chicago NH3 howitzer 33
4. RESULT AND DISCUSSION 35
4.1 Beta Transmission Measurements 35
4.1.1 Comparison of irradiated and unirradiated sample for Sr-90 39
4.2 Gamma Transmission Measurements 40
4.2.1 Gamma transmission measurements via Cs-137 41
4.2.2 Comparison of irradiated and unirradiated sample for Cs-137 44
4.2.3 Gamma transmission measurements via Co-60 for 1.1732 MeV 45
4.2.4 Gamma transmission measurements via Co-60 for 1.3325 MeV 47
4.2.5 Comparison of HVL values for 1.1732 MeV and 1.3325 MeV 49
4.2.6 Comparison of irradiated and unirradiated sample for Co-60 50
4.3 Neutron Transmission Measurements 52
4.3.1 Comparison of irradiated and unirradiated sample for ^{239}Pu-Be 55
4.4 Comparison of Attenuation Properties 56
4.5 The Approach for Experimental Study 61
4.6 The Approach for Shielding Study 62
4.7 The Approach for Material Study 63
4.8 The Approach for PMMA/CMT Composites 64
5. CONCLUSION 65
REFERENCES 67
CURRICULUM VITAE 71

ABBREVIATIONS

ATARC **:** Prof. Dr. Adnan Tekin Materials Science and Production Technologies Applied Research Center

ATRP **:** Atom Transfer Radical Polymerization

CAS **:** Chemical Abstracts Service

CME **:** Coronal Mass Ejection

CMT **:** Colemanite

EBiB **:** Ethyl 2-bromoisobutyrate

EPDM **:** Ethylene propylene diene monomer

ExHAM **:** Exposed Experiment Handrail Attachment Mechanism

GCR **:** Galactic Cosmic Ray

GMA **:** Glycidyl Methacrylate

GMT **:** Greenwich Mean Time

HDPE **:** High-density polyethylene

HVL **:** Half-value layer

ISS **:** International Space Station

JAXA **:** Japan Aerospace Exploration Agency

JEM-PM **:** Japanese Experiment Module-Pressurized Module

LDPE **:** Low-density polyethylene

LEO **:** Low Earth Orbit

MMA **:** Methyl methacrylate

MWCNT **:** Multi Walled Carbon Nanotube

NASA **:** National Aeronautics and Space Administration

NCRP **:** National Council of Radiation Protection and Measurements

NRC **:** National Research Council

PMDETA **:** Pentamethyl diethylenetriamine

PMMA **:** Poly (methyl methacrylate)

SEP **:** Solar energetic particle

SPE **:** Solar particle event

TKSC **:** Tsukuba Space Center

UV **:** Ultraviolet

Wt. **:** Weight

SYMBOLS

e^+	: Positron
e^-	: Electron
n	: Neutron
p	: Proton
α	: Alpha particle
β	: Beta particle
β^-	: Negative beta particle
γ	: Gamma ray
π^+	: Positive pion
π^-	: Negative pion
π^0	: Neutral pion
I_0	: Initial intensity
I	: Transmitted intensity
x	: Thickness
μ	: Linear attenuation coefficient
Σ	: Macroscopic cross-section

LIST OF TABLES

Page

Table 2.1 : Element abundance of GCR, SPEs and CMEs. 7
Table 2.2 : Physical properties of PMMA 24
Table 2.3 : The typical constituents of colemanite..... 26
Table 4.1 : Linear attenuation coefficients of the samples against beta particles at energy 0.546 MeV / 2.28 MeV 55
Table 4.2 : Linear attenuation coefficients of the samples against gamma photons at energy 0.662 MeV 56
Table 4.3 : Linear attenuation coefficients of the samples against gamma photons at energy 1.1732 MeV 56
Table 4.4 : Linear attenuation coefficients of the samples against gamma photons at energy 1.3325 MeV 57
Table 4.5 : Comparison of the experimental and theoretical results. 57
Table 4.6 : Total macroscopic cross-sections of the samples against neutron particles at energy ~5 MeV 58
Table 4.7 : Comparison of the attenuation of the samples in percentage..... 59

LIST OF FIGURES

Page

Figure 2.1 : Classification of radiations 5
Figure 2.2 : Approximate particle flux of main constituentof primary cosmic radiation 8
Figure 2.3 : Classification of radiation 9
Figure 2.4 : Van Allen Belts 10
Figure 2.5 : Locations of the different satellites and Van Allen belts 11
Figure 2.6 : Basic visualization of the active shielding 12
Figure 2.7 : Basic representation of external field approach and local field approach 154
Figure 2.8 : Comparison of the energy spectra of free space and shielded zone in space 155
Figure 2.9 : Classification of Materials 16
Figure 2.10 : General representation of poylmer 18
Figure 2.11 : Representations of (a) crosslinked, (b) linear, (c) branched, and (d) network (three-dimensional) molecular structure of polymers 19
Figure 2.12 : Various representations ((a), (b), (c)) of linear polymers. 19
Figure 2.13 : Linear formula of PMMA. 22
Figure 3.1 : Diagram of in-situ polymerization process 27
Figure 3.2 : The attachment of the sample module to ExHAM in the ISS 28
Figure 3.3 : The Pictures of the front view of the a) Base PMMA, (b) PMMA/CMT 5 wt.%, (c) PMMA/CMT 15 wt.%, and (d) PMMA/CMT 5 wt.% with microspheres 29
Figure 3.4 : The Pictures of the side view of the a) Base PMMA, (b) PMMA/CMT 5 wt.%, (c) PMMA/CMT 15 wt.%, and (d) PMMA/CMT 5 wt.% with microspheres 29
Figure 3.5 : Pictures of the beta transmission experiment setup 31
Figure 3.6 : Pictures of the gamma transmission experiment setup 32
Figure 3.7 : Pictures of the neutron transmission experiment setup 33
Figure 4.1 : Representation of the front view of beta transmission experiment setup. 34
Figure 4.2 : The changes of the relative intensity with thickness for irradiated base PMMA for 0.546 MeV / 2.28 MeV 35
Figure 4.3 : The changes of the relative intensity with thickness for irradiated PMMA/CMT 5 wt.% for 0.546 MeV / 2.28 MeV 35
Figure 4.4 : The changes of the relative intensity with thickness for irradiated PMMA/CMT 15 wt.% for 0.546 MeV / 2.28 MeV 36
Figure 4.5 : The changes of the relative intensity with thickness for irradiated PMMA/CMT 5 wt.% with microspheres for0.546 MeV / 2.28 MeV 36
Figure 4.6 : The HVL values of the irradiated samples for 0.546 MeV / 2.28 MeV 37
Figure 4.7 : The comparison of the relative intensity with thickness for irradiated and unirradiated PMMA/CMT 15 wt.%. 38

Figure 4.8 : The HVL values of the irradiated and unirradiated PMMA/CMT 15 wt.%. 38
Figure 4.9 : Representation of the top view of gamma transmission experiment setup 39
Figure 4.10 : The changes of the relative intensity with thickness for irradiated base PMMA for 0.662 MeV 40
Figure 4.11 : The changes of the relative intensity with thickness for irradiated PMMA/CMT 5 wt.% for 0.662 MeV 40
Figure 4.12 : The changes of the relative intensity with thickness for irradiated PMMA/CMT 15 wt.% for 0.662 MeV 41
Figure 4.13 : The changes of the relative intensity with thickness for irradiated PMMA/CMT 5 wt.% with microspheres for 0.662 MeV 41
Figure 4.14 : The HVL values of the irradiated samples for 0.662 MeV 42
Figure 4.15 : The comparison of the relative intensity with thickness for irradiated and unirradiated PMMA/CMT 15 wt.% for 0.662 MeV 43
Figure 4.16 : The HVL values of the irradiated and unirradiated PMMA/CMT 15 wt.% for 0.662 MeV. 43
Figure 4.17 : The changes of the relative intensity with thickness for irradiated base PMMA for 1.1732 MeV 44
Figure 4.18 : The changes of the relative intensity with thickness for irradiated PMMA/CMT 5 wt.% for 1.1732 MeV 44
Figure 4.19 : The changes of the relative intensity with thickness for irradiated PMMA/CMT 15 wt.% for 1.1732 MeV 45
Figure 4.20 : The changes of the relative intensity with thickness for irradiated PMMA/CMT 5 wt.% with microspheres for 1.1732 MeV 45
Figure 4.21 : The changes of the relative intensity with thickness for irradiated base PMMA for 1.3325 MeV 46
Figure 4.22 : The changes of the relative intensity with thickness for irradiated PMMA/CMT 5 wt.% for 1.3325 MeV 46
Figure 4.23 : The changes of the relative intensity with thickness for irradiated PMMA/CMT 15 wt.% for 1.3325 MeV 47
Figure 4.24 : The changes of the relative intensity with thickness for irradiated PMMA/CMT 5 wt.% with microspheres for 1.3325 MeV 47
Figure 4.25 : The HVL values of the irradiated samples for 1.1732 MeV. 48
Figure 4.26 : The HVL values of the irradiated samples for 1.3325 MeV. 48
Figure 4.27 : The comparison of the relative intensity with thickness for irradiated and unirradiated PMMA/CMT15wt.% for 1.1732 MeV 49
Figure 4.28 : The comparison of the relative intensity with thickness for irradiated and unirradiated PMMA/CMT15wt.% for 1.3325 MeV 49
Figure 4.29 : The HVL values of the irradiated and unirradiated PMMA/CMT 15 wt.% for 1.1732 MeV. 50
Figure 4.30 : The HVL values of the irradiated and unirradiated PMMA/CMT 15 wt.% for 1.1325 MeV. 50
Figure 4.31 : The changes of the relative intensity with thickness for irradiated base PMMA for ~5 MeV. 51
Figure 4.32 : The changes of the relative intensity with thickness for irradiated PMMA/CMT 5 wt.% for ~5 MeV. 51
Figure 4.33 : The changes of the relative intensity with thickness for irradiated PMMA/CMT 15 wt.% for ~5 MeV. 52

Figure 4.34 : The changes of the relative intensity with thickness for irradiated PMMA/CMT 5 wt.% with microspheres for ~5 MeV. 52
Figure 4.35 : The HVL values of the irradiated samples for ~5 MeV. 53
Figure 4.36 : The comparison of the relative intensity with thickness for irradiated and unirradiated PMMA/CMT 15 wt.% for ~5 MeV. 54
Figure 4.37 : The HVL values of the irradiated and unirradiated PMMA/CMT 15 wt.% for ~5 MeV. 54

BETA, GAMMA AND NEUTRON ATTENUATION PROPERTIES OF PMMA/COLEMANITE COMPOSITES EXPOSED TO SPACE RADIATION IN LOW EARTH ORBIT

SUMMARY

Polymers are an important material group that has gained a prominent place in various fields of industry. The usage of polymers has been expanded in a wide range of products ranging from automotive to aerospace industry apart from plenty of various promising scientific research. It is inevitable to evaluate that with a comprehensive perspective, polymers have gained a place that is difficult to change in today's world, thanks to its several properties such as low cost, easy to process and suitability for composite production. However, it becomes clear that some polymer- based materials are more suitable than other material options for a number of sophisticated research areas. Poly (methyl methacrylate) (PMMA) is a polymer-based synthetic material that is widely used in today's world. It is possible to state PMMA is an important thermoplastic material and stands out with its mechanical properties such as transparency and hardness. The applications of PMMA can be intrinsically diversified due to the opportunity of using as matrix in a composite structure apart from its utilization solely based on some physical and chemical properties. In other words, there is no such an obstacle to improve the any properties of PMMA and creating the new material that is more favorable than its base form with reinforcement voluminous elements. The reinforcement elements must be determined by taking into account a number of purposes since introducing agents directly affects the properties of the composite to be produced. However, Colemanite (CMT) is a mineral that can be considered as a candidate reinforcement element for use in the field of radiation shielding due to its chemical constituent. It is a foreseeable fact that introducing the CMT as a reinforcement agent along with PMMA that has been used for radiation attenuation applications within the scope of various researches can improve the attenuation ability of base PMMA against different types of radiation. On the other hand, it is an extremely critical point that for a developed material to maintain the attenuation properties in long-term use and to prevent various operational restrictions in terms of functionality. For this reason, the targeted properties must also be preserved during using of the material in addition to achieving the cost and desired properties in the initial synthesis process. There is a huge amount of radiation dose for a matter due to the components of space environment such as galactic cosmic rays and solar energetic particles. It is possible to foresee that there may be a series of changes in the structure of material groups in an exceedingly harsh radiation environment of space. Thereby, the materials used in space studies must be able to ensure effective radiation shielding for long term uses even after even after receiving high doses of radiation. Moreover, it is clear that long-term use of material in space can be considered as enormously favorable by taking into account cost and operational difficulty. In this study, base PMMA, PMMA/CMT 5 wt.%, PMMA/CMT 15 wt.% and PMMA/CMT 5 wt.% with microspheres were produced by the atom transfer radical polymerization (ATRP) method. Synthesized samples have been exposed to space radiation on the

International Space Station for approximately a year. Afterwards, attenuation properties of the samples against various types of radiation were examined within the scope of the ground-based experiments. Experimental studies on the exposure to space radiation were performed in cooperation with the Japan Aerospace Exploration Agency (JAXA). The launch and landing operations were carried out by the Space-X company. The samples were directed to JAXA's Tsukuba Space Center (TKSC) after landing on Earth. Launching was carried out with the Falcon-9 rocket and samples were placed in the 'ExHAM' facility which is connected to the outside of the Japanese experiment module on the International Space Station. In addition, the absorbed dose amount for the samples that interacted with high-energy electrons and positrons along with galactic cosmic radiation and solar energetic particles was determined as thereabout 0.02 kGy. Within the scope of the ground-based experiments, Sr-90 radioisotope was used as the beta source while Co-60 and Cs-137 radioisotopes were used as the gamma source. Apart from radioisotopes, ^{239}Pu-Be neutron howitzer has preferred as the neutron source. Beta, gamma and neutron attenuation properties of PMMA/CMT composites that exposed to space radiation were examined. Furthermore, PMMA/CMT composites 15 wt. % concentrations were investigated for different radiation types to obtain the attenuation properties for both unirradiated and irradiated state in each experimental setup. Hence, the effects of both CMT reinforcement and radiation environment in low earth orbit on the beta, gamma and neutron attenuation properties were determined. Studies have shown that the increase in CMT ratio in the composite structure improves the attenuation properties of PMMA/CMT composites that exposed to space radiation. In addition, linear attenuation coefficients of the samples were determined through the different thicknesses and compared with theoretical values. PMMA/CMT 15 wt. % samples in both irradiated and unirradiated state were examined in the same experimental setup to understand the effects of open space radiation. It can be stated that there is no decrease in the attenuation properties of the irradiated PMMA/CMT 15 wt. %. It is possible to predict that the samples have meet a series of structural changes as they were exposed to radiation in low earth orbit. The ATRP technique in the synthesis of a material was preferred by considering the space radiation environment. It is considered that new reactive end groups and free radicals formed due to the high amount of radiation dose taken during the space experiments. The formation of molecular cross-links within the polymer matrix can be occurred as a result of these newly formed end groups. However, the network structure of the relevant composite can be strengthened via the creation of cross-links. It has been inferred that the strengthening and density increase of the composite structure can be deducted with the formation of cross-links.

ALÇAK DÜNYA YÖRÜNGESİNDE UZAY RADYASYONUNA MARUZ KALAN PMMA/KOLEMANİT KOMPOZİTLERİNİN BETA, GAMA VE NÖTRON ZAYIFLATMA ÖZELLİKLERİ

ÖZET

Polimerler, günümüzde endüstrinin çeşitli alanlarında kendine yer edinmiş önemli bir malzeme grubudur. Otomotivden sektöründen havacılığa kadar uzanan geniş bir ürün yelpazesinde yer alan polimerler aynı zamanda gelecek vadeden pek çok bilimsel araştırmanında odak noktası olmuştur. Kapsayıcı bir bakış açısıyla değerlendirildiğinde; düşük maliyet, kolay proseslerle üretim yapılabilme imkânı, kompozit üretimine elverişlilik gibi pek çok özelliği sayesinde günümüz endüstirisinde değiştirilmesi güç bir yer edinmiştir. Bununla birlikte ilgili polimer bazlı malzeme grubu daha detaylı incelendiğinde bazı polimerlerin özellikle bir dizi araştırma konusunda diğer malzeme seçeneklerinden daha kullanışlı olduğu ortaya çıkmaktadır. Poli(metil metakrilat) (PMMA) günümüzde tıpkı diğer polimerler gibi geniş bir ürün yelpazesinde kullanıma sahip sentetik bir malzemedir. Bu noktada, PMMA' nın çeşitki malzeme özellikleri incelendiğinde, amorf yapılı termoplastik bir malzeme olarak sınıflandırılmasının yanı sıra saydamlık ve sertlik gibi bir dizi mekanik özellikleri ile de dikkat çeken bir malzeme olduğunu ifade etmek mümkündür. Fiziksel ve kimyasal çeşitli özelliklerinin haricinde özellikle kompozit yapısı içerisinde bir matris olarak kullanımı ile birlikte kendi doğasından gelen özelliklerin haricinde birçok farklı kullanım alanına da dahil olması kaçınılmazdır. Diğer bir deyişle, çeşitli takviye elemanlarının kullanımı ile birlikte PMMA' nın birtakım özelliklerinin desteklenebilmesi, artırılabilmesi ve baz formundan daha elverişli bir hale getirilebilmesinin önünde herhangi bir engel bulunmamaktadır. Takviye elemanlarının sahip olduğu özellikler, oluşturulacak yeni bir kompozitin yapısını doğrudan etkileyeceğinden dolayı ulaşılması hedeflenen malzeme özellikleri göz önünde bulundurularak belirlenmelidir. Kolemanit (CMT) içeriği itibarı ile radyasyon zırhlama alanında kullanıma aday bir takviye elemanı olarak değerlendirilebilecek mineraller arasında yer almaktadır. Çeşitli araştırmalar kapsamında radyasyon zayıflatma özellikleri tespit edilip literatüre sunulmuş olan PMMA ile birlikte CMT' nin takviye elemanı olarak kullanımının tercih edilmesinin farklı radyasyon tiplerine karşı daha gelişmiş bir radyasyon zırhlama imkânı ortaya koyacağı öngörülebilir bir olgudur. Öte yandan radyasyon zırhlama amacı ile geliştirilen farklı malzemelerin uzun ömürlü kullanımında zayıflatma özelliklerinin korunması ve çeşitli operasyonel kısıtlamaların önüne geçilmesi ilgili malzemelerin fonksiyonel kullanımı açısından oldukça kritik bir unsurdur. Bu sebeple sentezleme süresince düşük maliyet ve hedeflenen özelliklerin elde edilmesinin yanı sıra; kullanım süresince de malzemenin sahip olduğu çeşitli kimyasal ve fiziksel özelliklerinin korunmasının da sağlanabiliyor oluşunun göz önünde bulundurulması gerekmektedir. Özellikle uzaydaki yoğun radyasyon ortamı değerlendirildiğinde, yüksek enerjili parçacıklar ile hedef malzemenin etkileşimi sonucunda azımsanamayacak seviyede bir doz maruziyeti söz konusudur.

Bahsi geçen radyasyon yoğunluğu bakımından üst düzey riskli ortamda bulunan malzeme gruplarının doğrudan yüksek doza maruz kalması sonucu yapısında bir dizi değişikliğin olabileceğini öngörmek mümkündür. Bununla birlikte, uzay çalışmalarında kullanıma sunulan malzemelerin aldığı yüksek dozlar sonucunda herhangi bir ışınlama işlemine maruz kalmamış formundaki gibi efektif bir zırhlama performansı gösterebilmesi beklenmektedir. Doz maruziyeti süresince, zırhlama performansında oluşabilecek herhangi bir yetersizlik sonucu alternatif yeni bir malzeme kullanımının operasyonel zorluğu ve maliyeti göz önünde bulundurulduğunda uzun süreli fonksiyonel yapıların kullanımının uzay çalışmaları açısından bir gereklilik olarak değerlendirilmesi kaçınılmazdır. Bu tez çalışması kapsamında, atom transfer radikal polimerizasyon (ATRP) yöntemi ile üretilmiş baz PMMA, %5 CMT takviyeli PMMA, %5 CMT ve mikroküre takviyeli PMMA ve %15 CMT takviyeli PMMA kompozitlerinin yaklaşık 1 yıl süre ile alçak dünya yörüngesinde konumlandırılmış olan Uluslararası Uzay İstasyonunda açık uzay radyasyonuna maruz kaldıktan sonra çeşitli radyasyon türlerine karşı sergilediği zayıflatma özellikleri incelenmiştir. Sentezlenen numunelerin uzay radyasyonuna maruz bırakılmasına ilişkin deneysel çalışmalar Japonya Havacılık ve Uzay Araştırma Ajansı (JAXA) ile iş birliği içinde gerçekleştirilmiştir. Fırlatma ve iniş işlemleri Space-X firması aracılığı ile gerçekleştirilmiş olup, ilgili numuneler dünyaya iniş yaptıktan sonra JAXA' ya ait Tsukuba Uzay Merkezi (TKSC)' ne yönlendirilmiştir. Falcon-9 roketi ile fırlatılan numuneler Uluslararası Uzay İstasyonunda Japon deney modülü Kibo' ya bağlı bir bağlantı mekanizması olan 'ExHAM' tesisine yerleştirilmiş olup 363 gün boyunca açık uzayda radyasyona maruz bırakılmıştır. Uzay deneylerinin gerçekleştirildiği yörünge itibari ile galaktik kozmik radyasyonla birlikte yüksek enerjili elektron ve pozitronlarla etkileşime girmiş olan numuneneler için absorbe edilen doz miktarı yaklaşık 0.02 kGy olarak tespit edilmiştir. Numuneler uzay radyasyonuna maruz bırakıldıktan sonra dünya ortamına getirilmiş olup çeşitli deneylere tabi tutulmuştur. Bu deneyler kapsamında Sr-90 beta kaynağı olarak, Co-60 ve Cs-137 radyoizotopları ise gamma kaynağı olarak kullanılmıştır. Radyoizotopların haricinde, ^{239}Pu-Be nötron howitzer de nötron kaynağı olarak tercih edilmiştir. Gerçekleştirilen deneysel çalışmalarda, uzay radyasyonuna maruz bırakılmış farklı CMT takviyelerindeki PMMA/CMT kompozitlerinin beta, gama ve nötron zayıflatma özellikleri incelenmiştir. Bununla birlikte, herhangi bir ışınlama operasyonuna maruz kalmamış %15 CMT takviyeli PMMA/CMT kompozitinin aynı kompozisyondaki alçak dünya yörüngesinde açık radyasyona maruz bırakılmış formu ile karşılaştırması her bir deney düzeneğinde ayrıca incelenmiştir. Böylelikle hem CMT takviyesinin hem de Uluslararası Uzay İstasyonunun bulunduğu yörüngedeki radyasyon ortamının ilgili malzemelerin beta, gama ve nötron zayıflatma özelliklerine etkisi deneysel olarak ortaya konmuştur. CMT takviyesindeki artışın uzay radyasyonuna maruz kalmış PMMA/CMT kompozitlerinin zayıflatma özelliklerini artırdığı yapılan çalışmalar neticesinde tespit edilmiştir. Farklı kalınlıklarda gerçekleştirilen ölçümlerle birlikte, lineer zayıflatma katsayıları elde edilmiş olup teorik değerlerle birlikte kıyaslanması yapılmıştır. Öte yandan, %15 CMT takviyeli PMMA/CMT kompozitinin Uluslararası Uzay İstasyonundan gelen formu ile herhangi bir doza maruz kalmamış formu aynı deney düzeneklerinde incelendiğinde ise; doza maruz kalan numunenin zayıflatma özelliklerinde herhangi bir azalma görülmemiş olmasının yanı sıra zırhlama kabiliyetinin arttığı da sayısal değerlerle birlikte açıklanmıştır. Numunelerin alçak dünya yörüngesinde radyasyona maruz kalmasıyla birlikte yapısal bir dizi değişikliğe uğradığı öngörülmektedir. ATRP tekniğinin özellikle uzay radyasyonuna karşı zırhlama amacı ile kullanımda alternatif olabilecek bir malzeme sentezinde tercih

edilmesi, kompozit yapısının ışınlama sonrası değişimine etki edebileceği tahmin edilmektedir. Bu noktada ilgili kompozitlerin yapısında açık uzay deneyleri süresince alınan yüksek doz ile birlikte yeni reaktif uç grupların ve serbest radikallerin oluşması beklenmektedir. Işınlama ile birlikte ortaya çıkan bu uç grupların polimer matris içerisindeki moleküler çapraz bağların oluşumunu desteklemesi ile birlikte ilgili kompozitin ağ yapısının değişiminin söz konusu olduğu değerlendirilmiştir. Çapraz bağların oluşumu ile birlikte kompozit yapısının sıkışması, güçlenmesi ve yoğunluk artışının oluşmasına dair çıkarımlar radyasyon temelli gerçekleştirilen deneysel çalışmalar sonucunda yapılmıştır.

1. INTRODUCTION

1.1 Purpose of Thesis

The effects of radiation on human health have been known for years. However, detailed studies on the effects of radiation have been carried out with the help of various classifications and used in a spate of industrial applications [1]. Its use in the field of health has become widespread over time. Radiation has been used as an auxiliary element in precious specific health problems such as brain tumors [2,3]. Nuclear reactors and space studies have also received their share of radiation research beyond the use of radiation in medicine [4]. Recent developments in space studies clearly demonstrate the importance of radiation shielding in space studies [5].

The aim of the thesis is to examine the applications of PMMA/CMT composites in the space environment. Experimental studies aimed to determine the effects of CMT reinforcement in the composite structure as well as the effects of the exposure to space radiation through beta, gamma and neutron attenuation coefficients.

1.2 Literature Review

It is known that the space environment contains a high level of radiation that can be harmful to human health. The effects of a mixed radiation containing different types of radiation in space should be minimized to pave the way for various manned space missions. Basically, suggestions about the shielding in space aimed to be achieved using active and passive shielding methods. In particular, the feasibility of active shielding currently can be considered as a debated issue [5]. On the other hand, passive shielding approach seems more convenient in terms of applicability in the short and medium term when supported by current scientific developments. In addition, Van Allen belts are composed of charged particles with different energies and types. Position of the International Space Station is just right at the bottom of the inner Van Allen belt. Although the inner belt and outer belt have similar charged particles, they are the zones in which particles of different energies and charges are trapped [5].

Van Allen belts can be investigated with two different zones as inner belt and outer belt. Both of them are available in different compositions in terms of charged particles and locations as distance from the Earth. However, the outer Van Allen belt basically consist of the electrons with high energy level. Energy of the electron in outer belt is in the range of 0.1 and 10 MeV. Moreover, protons with the energy range of 30 keV to 500 MeV can be found in relatively low amount in the outer Van Allen belt [5].

However, it may be more preferable to carry out studies in specific energy range to make a proper scientific comparison since it is known that the radiation environment in space varies regionally. Therefore, even if it is not very achievable a high degree of shielding against all radiation types, its preferability increases as a result of effective shielding against the type of radiation that most prevalent in the relevant orbit since the density of different types of radiation in specific orbits in space is known.

1.3 Hypothesis

It is possible to see a number of changes in the structure of a composite exposed to high doses since space has an extremely high level of radiation environment. The samples used in the thesis study were exposed to radiation in the open space environment on the International Space Station for approximately 1 year.

The effects of space radiation environment on the samples in terms of radiation shielding can be determined by several ground-based experiments with a comparison made by the irradiated and unirradiated forms of the regarding materials. The feasibility of using the relevant materials against the radiation of a certain energy can be demonstrated with the common combination of the energy range emitted by the used radioisotopes and the energy range in the specific space environment.

In this way, outputs coming from the experimental tests may contribute to the safety of various electronic equipment used in space or astronauts working in the harsh radiation environment of the space. Especially, a wide variety of electronic equipment used on satellites in various orbits that containing different types of radiation at different densities can be protected from radiation.

2. GENERAL INFORMATIONS

2.1 Radiation

Radiation is a form of energy that can be observed both in form of particle and wave. Humankind has been living with radiation since the beginning of historical ages, but awareness of radiation has a relatively short history. The accidental discovery of X-rays by Wilhelm Conrad Roentgen (1845-1923) in 1895 can be accepted as the starting point of consciously living with radiation. Thenceforward, many scientists including Nobel Prize laureates such as Marie Curie and Henri Becquerel, who were among the pioneers of radiation science, have focused on radiation studies [1].

It is possible to observe various applications of radiation science and technology in industry. Imaging systems for radiological diagnosis or nuclear medicine applications for cancer treatments are some of the examples in medical studies [2]. Positron emission tomography and single-photon emission computed tomography systems directly utilize from the radiation science and are accepted as significant cancer treatment tools for different kind of fatal diseases such as brain tumors [3]. Apart from the medical applications, space studies or nuclear reactors are directly associated with radiation.[4].

In brief, there are many ongoing applications that required working with radiation and it is likely that radiation science and technology is going to be essential for many upcoming scientific studies.

As mentioned above, radiation science has many application areas and thus it is inevitable to come across many scientific studies published by several scientists for years. However, developments on the space studies have become remarkable in recent years among others. Specifically, the goal of the National Aeronautics and Space Administration (NASA) about the Mars mission including the sending humans to Mars in 2030 could be one of the greatest examples of the outstanding potential of space studies for radiation science and technology [5].

2.1.1 Classification of radiation

Technically, classification of radiation can be done in many ways. However, radiation is basically categorized under 2 main headings which are ionizing and non-ionizing radiation. Non-ionizing radiation is the radiation that does not have the sufficient energy to ionize an atom. Basically, visible light or radio waves can be the examples of non-ionizing radiation. On the contrary, ionizing radiation is a type of the radiation that have the sufficient energy to ionize an atom. Galactic cosmic rays or high energy neutrons can be the examples of ionizing radiation [2].

Apart from these, ionizing radiation can also be categorized into 2 main headings as directly ionizing radiation and indirectly ionizing radiation. One of them, which is directly ionizing radiation is the radiation that consists of charged particles such as electrons, protons or heavy ions. Indirectly ionizing radiation consists of neutral/non-charged particles as neutrons or X-rays [2].

In addition to the previous statements, further classifications can also be made depending on the type of the particles in both charged and neutral particles. Directly ionizing radiation can be classified into 3 groups as light, intermediate and heavy charged particles. On the other hand, indirectly ionizing radiation can be classified into 2 groups as photons and neutrons [2]. Figure 2.1 shows the classification of radiation in detail.

The comprehensive view on the classification of radiation is essentially made to distinguish ionizing radiation from non-ionizing radiation. Ionizing radiation has huge amounts of benefits and advantageous for plenty of applications but it should not be forgotten that it is extremely hazardous and requires additional safety operations. All kinds of radiation within the scope of ionizing can cause incurable damages in case of unproper exposure [2].

These classifications may be considered as favorable depending on the field of study within the scope of nuclear research. In other respects, there is no obstacle to working with different classifications in different field-based studies. It is clear that for a nuclear research study based on charged and uncharged radiation, it may be more appropriate to evolve the classification as charged-uncharged radiation.

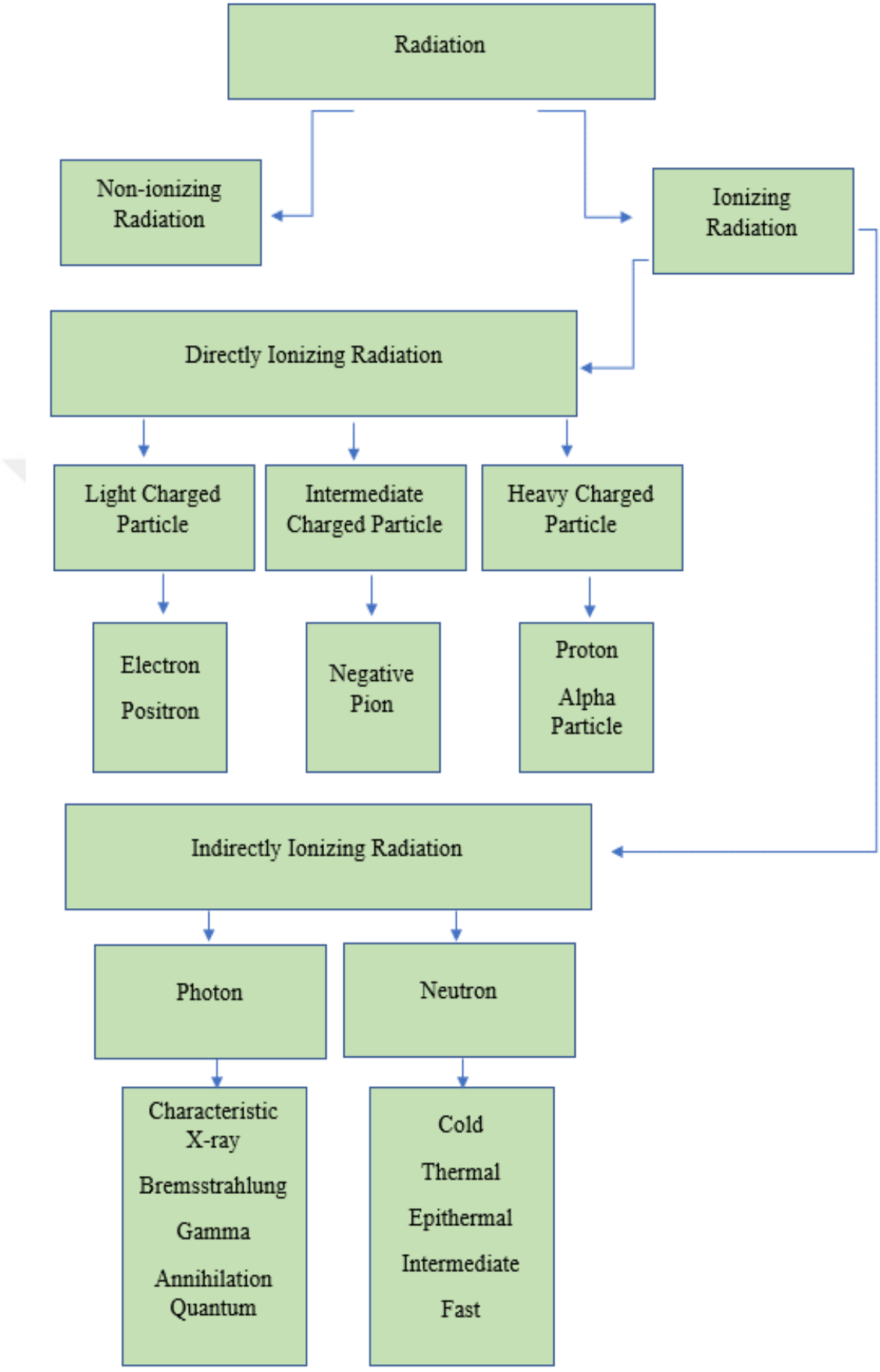

Figure 2.1 : Classification of radiation.

2.1.2 Radiation in space

The space environment is essentially full of with ionizing radiation. Basically, galactic cosmic rays (GCRs) and solar energetic particles (SEPs) are the main radiation types in the space environment. Their radiological effects cannot be ignored especially outside the low Earth orbit (LEO) which is possible to observe extremely high damage to deoxyribonucleic acid (DNA) including the irreparable damages [5].

Space radiation is one of the factors hindering various potential space explorations. A lot of regulations have been made by the relevant authorities within the framework of the 'As Low As Reasonably Achievable (ALARA)' principles to conduct space studies. There are several restrictions for astronauts taking part in space missions in order to eliminate the radiation risks to human health such as dose limits. National Aeronautics and Space Administration (NASA) has designated the acceptable radiation dose limits for astronauts in International Space Station (ISS) missions [6].

On the other hand, radiation is not homogeneously distributed in the universe. Particularly, damages caused by radiation significantly increase in places out of the Earth's magnetic field. Except for missions on the ISS, there are some other potential missions planned to take place far away from the effects of the Earth's magnetic field and Van Allen belts [5]. Thus, different parameters about the mission such as the location and duration of exposure should be scrutinized in order to decrease the risks based on radiation for missions beyond Earth's magnetic influence.

All things considered, it is extremely important to have comprehensive knowledge about the radiation environment of space so that human beings can carry out various studies in space and perhaps even live safely in colonies in the future. However, it might be more practical to examine the classification of space radiation separately from the generally used classification of radiation as Figure 2.1 in order to carry out a more specific study about the space radiation. It is more adequate to conduct investigations in more sophisticated areas of the subject with detailed classifications, thus paving the way for a more convenient study in terms of scientific comparison.

Hence, it possible to broadly classify space radiation into 2 main headings as GCRs and SEPs for further investigations. Among other things, it should be noted that solar energetic particles (SEPs) may also be named as solar particle events (SPEs).

2.1.2.1 Solar particle events

There are different ways to be witnesses of how sun carry out the acceleration and ejection processes of charged particles. However, impulsive Solar Particle Events and Coronal Mass Ejections (CMEs) are the 2 main mechanisms of the ejection and acceleration of the Sun. Impulsive SPEs are originated from the movements of sunspots and plasmas inside the Sun. Basically, movement of both sunspots and plasmas can be classified as convective movements and magnetic fields are rearranged as a result of the regarding convective movement. Relatively heavy elements are observed more in the composition of Solar Particle Events compared to Coronal Mass Ejections. Origins of the heavy elements can be accepted as the solar atmosphere. Additionally, angular dependency of SPE's is insignificant due to the effects of magnetic field and nature of the convection movement [5].

On the other side, CMEs may be considered as another critical issue for humans harnessed with the SPE since they are quite larger than the impulsive SPEs. The velocity of the materials released from CMEs is in the range of 100 to 3000 km/h. Releasing is carried out in extensive angular emission. General composition of the CME's is shown in Table 2.1[5].

Table 2.1 : Element abundance of GCR, SPEs and CMEs [5].

Element	Z	Photosphere (%)	CMEs (%)	Impulsive SPEs (%)	GCRs (%)
H	1	90.97	96.36	95.22	86.91
He	2	8.90	3.50	4.38	11.74
C	6	0.032	0.029	0.041	0.421
O	8	0.067	0.061	0.095	0.499
Ne	10	0.011	0.009	0.038	0.062
Mg	12	0.003	0.12	0.039	0.103
Si	14	0.003	0.009	0.034	0.098
Ti	22	0.000	0.000	0.000	0.002
Fe	26	0.003	0.008	0.103	0.003
Other	Other	0.012	0.013	0.054	0.167

2.1.2.2 Galactic cosmic rays

Galactic cosmic rays compose of highly energetic particles and origin of GCR can be based on solar system or extragalactic systems. Origins of the energetic particles can be estimated depending on the observed energy. It is possible to make an estimation as the energetic particles with less than 100 MeV are based on solar system and Sun. On the contrary, particles that have the energy over the 100 MeV can be accepted as the energetic particles that come from the galactic origins. Percentage of the elements in the composition of the GCR can be approximately listed as following: 1% heavy elements, 10% helium and 89% hydrogen [7]. Composition of the primary galactic cosmic rays is shown in Figure 2.2. It must be noted that the composition of the GCR's is changed depending on the interaction with the Earth's magnetic field which means that there is a possibility to observe various of composition of GCR's especially in the different measurement places [8]. Additionally, GCR's have electrons with explicitly lower density due to the nature of the electrons such as their properties against inverse Compton scattering on thermal photons. Thus, only high energetic electrons continue to be present in GCR, while low energetic electrons are scattered back to the depths of the galaxy [7].

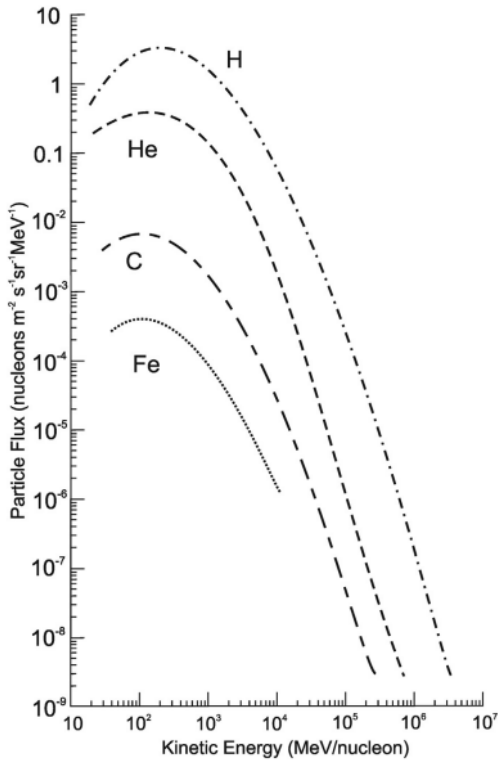

Figure 2.2 : Approximate particle flux of main constituent of primary cosmic radiation [8].

2.1.2.3 Secondary radiation

There is another term named as secondary radiation associated with the space radiation environment. GCR's and SPE's are considered as the primary radiations. However, the interactions of the primary radiation and the other matters can conclude with production of another radiation called secondary radiation [9]. These interactions can take place as various forms such as ionization, atomic excitation or both elastic and inelastic nuclear scattering [10]. In addition, secondary radiation can be observed several different types such as neutrons, protons, gamma and even baryons and mesons can be [11]. The formation of secondary cosmic radiation radiations within the atmosphere arising from a primary particle can be seen in Figure 2.3.

Neutrons can be considered the main source of the radiation-based problem compared to other types of secondary radiation due to the effects of neutrons on the effective dose inside the spacecraft [12]. Production of neutrons not only depends on the incoming primary charged particles but also depends on the design of spacecraft. However, neutron dose equivalent is about 140 μSv/d and total dose equivalent is 650 μSv/d according to the measurements onboard the ISS. Additionally, it should not be forgotten that these dose equivalents are strongly depends on the other parameters such as solar activity, latitude or thickness of shielding material [13].

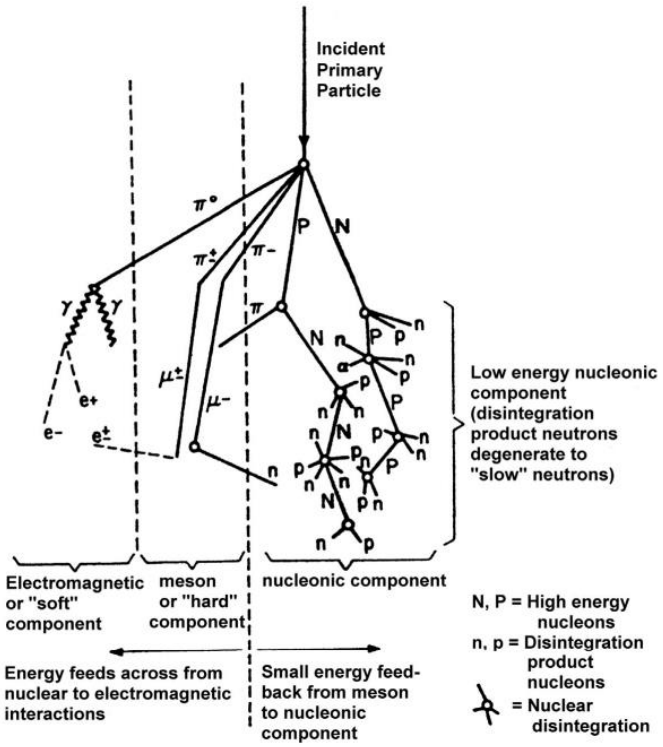

Figure 2.3 : Representation of the formation of secondary cosmic radiations [8].

Monte Carlo calculations are also used to make the estimations on the secondary radiations. Moreover, comparisons of the Monte Carlo calculations about the neutron spectra results and the real experimental outputs such as observations on the spacecrafts have already been performed [14]. In other words, there is an opportunity to correlate the simulations and the experimental results about the secondary neutron flux.

2.1.3 Radiation shielding in space

Radiation shielding is a basic requirement for space explorations depending on the As Low As Reasonably Achievable principles [6]. Probability of risks and uncertainties to determine the risks have been revealed with related reports issued by the National Research Council (NRC) and National Council of Radiation Protection and Measurements (NCRP) [6]. Major issue about the determining the exposure dose limits for astronauts is based on the lack of information of GCR [6].

2.1.3.1 Van Allen belts

Van Allen belts are the zones where electrons and protons with energies between 1-10 MeV are trapped [15]. They can be explained as toroidal shaped 2-layer belts surrounding the Earth. However, high energetic protons up to 100 MeV can be observed in Val Allen belts [16]. Figure 2.4 shows the Van Allen Belts in detail [16].

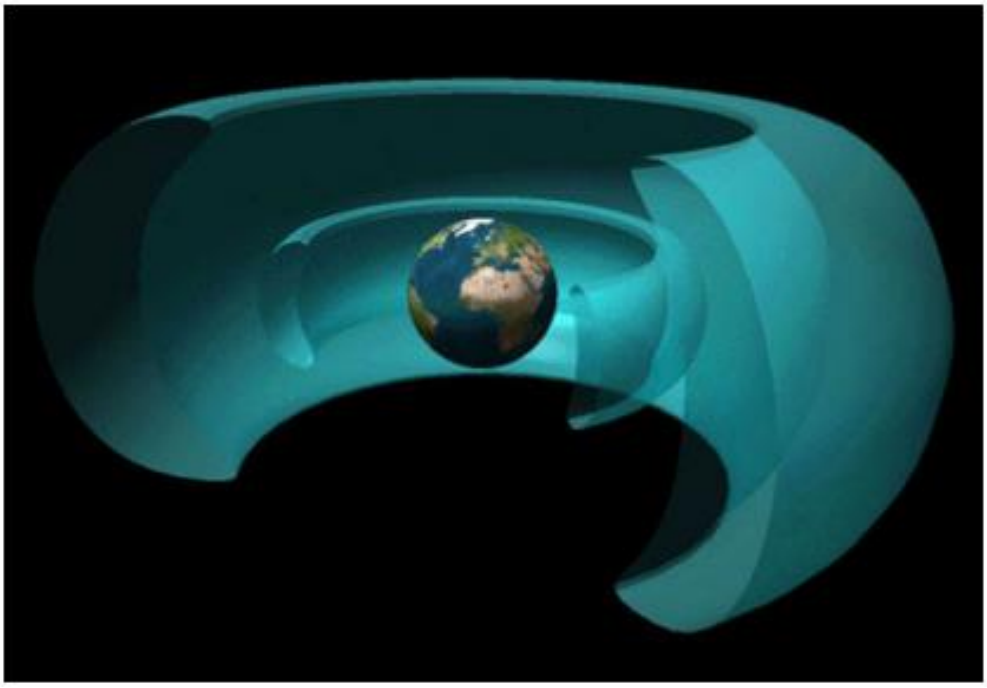

Figure 2.4 : Van Allen Belts [10].

Van Allen belts can be divided into two zones as inner belt and outer belt. The outer Van Allen belt mostly comprised of the high energy electrons. Energy of the electron in this zone is between 0.1 and 10 MeV. Additionally, protons can be found relatively low amount in the outer belt and energy of the protons that can be found in the outer belt is between 30 keV to 500 MeV [5].

Position of the outer belt starts nearly from 18000 km and goes on until approximately 60000 km depending on the latitude. Verge of the outer Van Allen belt can change based on the independent parameters such as activity of Sun and type of the particles coming from Sun [16]. On the contrary of the outer belt, high energy protons with the energies up to 100 MeV are the major constituent of the inner belt. Position of the inner belt can extend up to 6000 km depending on the latitude [16].

It must be noted that there are differences in the numbers describing the boundaries of both inner and outer Van Allen belts based on the latitude. Figure 2.5 shows the Van Allen belts and different satellite positions in detail.

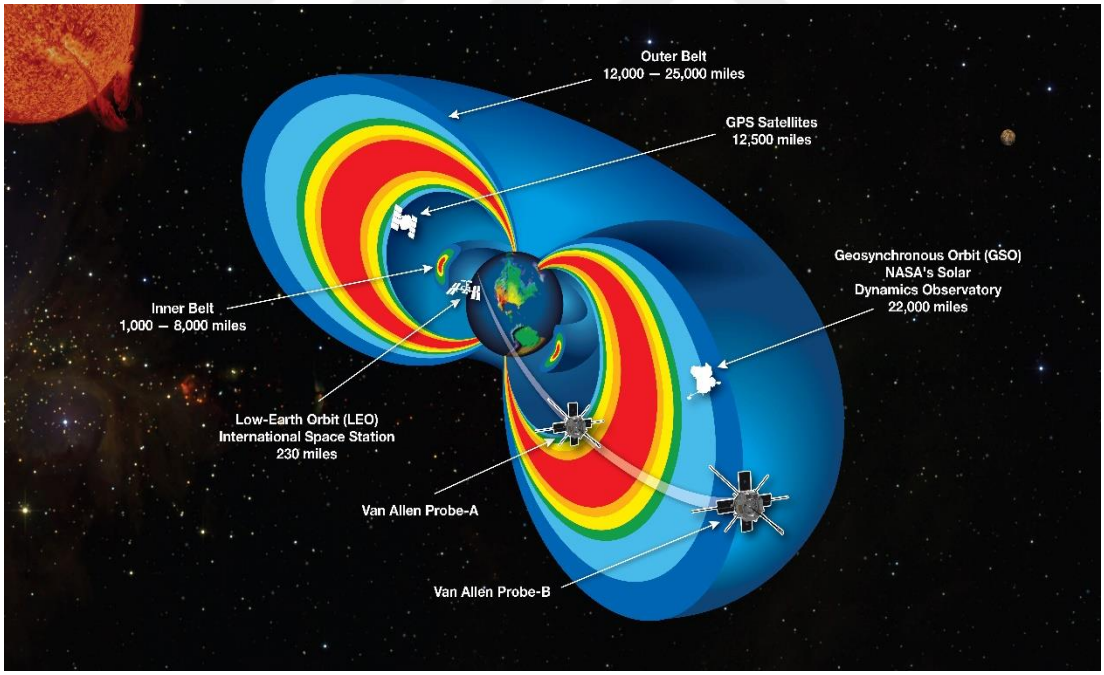

Figure 2.5 : Locations of the different satellites and Van Allen belts [17].

Van Allen belts are not only significant for protection of the Earth but also harmful for the crew and electronic devices on missions that Van Allen belts must be passed. LEO's are technically below the Van Allen belts so probability of the risk is low. However, since location of the belts depending on the latitudes ISS can also be affected from the belts when it comes closer to the belts during the movement on the orbit [16].

2.1.3.2 Active shielding

Active shielding focuses on the deflection of the incoming radiation from the shielded zone by using the electromagnetic fields. However, it is possible to consider electrostatic fields, plasmas and both confined and unconfined magnetic fields within the scope of active shielding [18].

Electrostatic shielding works with placing the charged spheres in an arranged orientation around the zone where desired to be shielded from coming radiation. There is a project under the development that aims to create a safe zone by using the principles of electrostatic shielding. Figure 2.6 shows the basic visualization of the proposal about active radiation shielding with supported gossamer membrane [19].

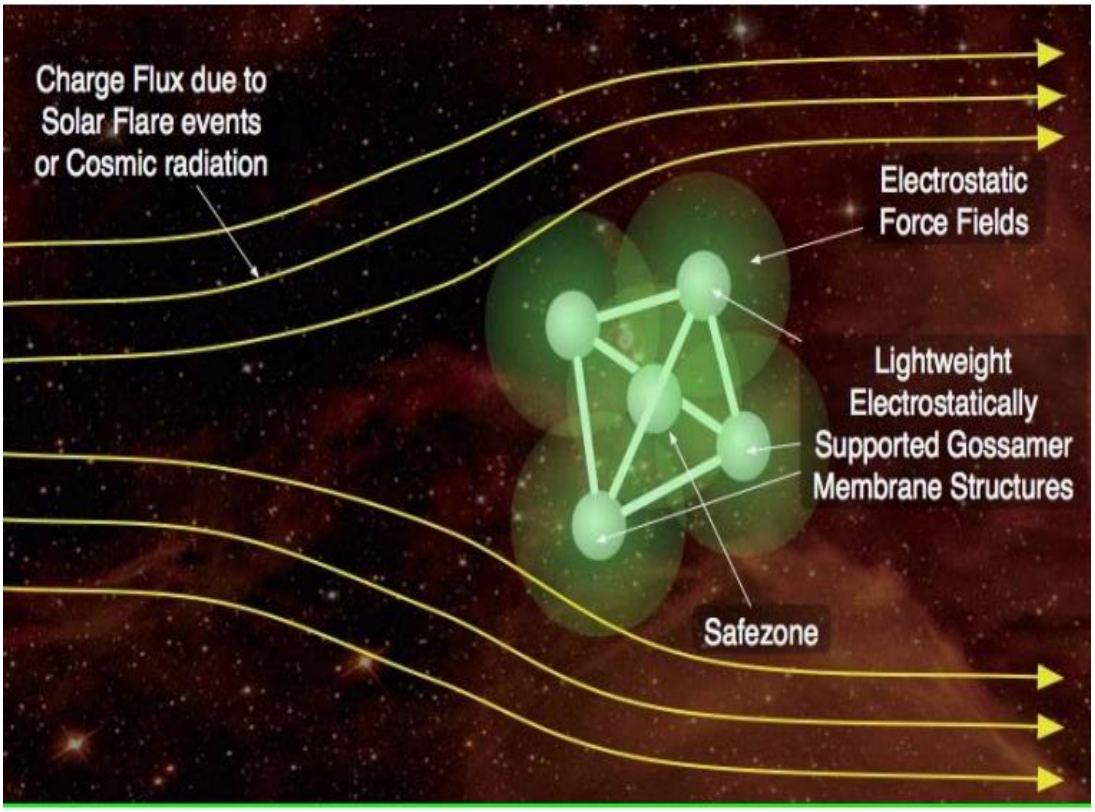

Figure 2.6 : Basic visualization of the active shielding [19].

Magnetic shielding principles are based on the force acting perpendicular to the incoming radiation in a magnetic field [5]. Additionally, shielding based on the electrostatic fields are not suitable for shielding against GCR's and SPE's as well as shielding based on plasmas. Also, required magnetic fields cannot be created by the conventional approaches. In particular, there are additional challenges such as limited operating area for a spacecraft that needed radiation shielding [20].

2.1.3.3 Passive shielding

Passive shielding can be considered as a traditional way for radiation attenuation applications. Basically, the use of materials such as aluminum or reinforced polymers is classified as passive shielding. The aim of passive shielding is to attenuate the incoming radiation and reduce the amount of radiation exposure. The required mass of material for effective radiation shielding varies according to the energy of the incident radiation. [21].

Passive shielding is more suitable against SPE's when compared to GCR due to high penetrating ability of the GCR's. Shielding of a spacecraft is predominantly accomplished by structural components used in the construction of the spacecraft. Structural elements not only provide shielding but also become the major factors of mechanical stability [18].

Passive shielding is the basic shielding mechanism of the space missions due to the excessive requirements of the applications of active shielding such as energy and cost. Therefore, there are many scientific publications about the radiation shielding properties of different material groups such as metal or composites within the scope of passive shielding.

At this point, it is possible to encounter with different elements that are suitable for use against various types of radiation in space. However, shielding capability of hydrogen against the protons and heavy nucleis is a well-known phenomenon [22]. Therefore, hydrogen-rich polymers can be considered as one of the most promising material groups for space radiation studies due to their feasibility.

Many industrial polymers such as PMMA which is the material used in this thesis study as a radiation shielding agent, HDPE, LDPE, EPDM have been evaluated as candidate material for radiation shielding applications. Additionally, since polymers can be used as matrices for composite manufacturing, there is a possibility to utilize from the other material group as additives in composite structure. Boron compounds such as boron carbide or boron nitride are the most preferred additives of the radiation shielding composites due to their neutron capture properties. Apart from the different forms of the boron-based compounds, there are many different candidate agents in material studies as additives for radiation shielding research e.g. gadolinium and graphite [23].

2.1.4 Laboratory experiments of space radiation

There are a few laboratories where can be used for ground-based experiments for space radiation research. These experiments are mostly performed at fixed energy level with ion beams both by using and not using degraders. Recently, experiments regarding to acceleration of the various beams with discrete energy level has performed. Additionally, switching time could be kept in the acceptable interval which is less than 120 seconds [24]. Therefore, mixed radiation spectrum which is more similar to space radiation environment can be simulated at least, in theory. Such advances in accelerator technology may be considered as milestones for ground-based space experiments.

There are 2 different approaches that have been discussed about the simulation of the GCRs as of today. These are called as external field and local tissue field approaches. As its name signifies external field approach focuses on the spectrum of the GCR outside the spacecraft while local tissue field approach focuses on the spectrum inside the spacecraft [24]. Figure 2.7 shows the basic representation of the differences between these two approaches [25].

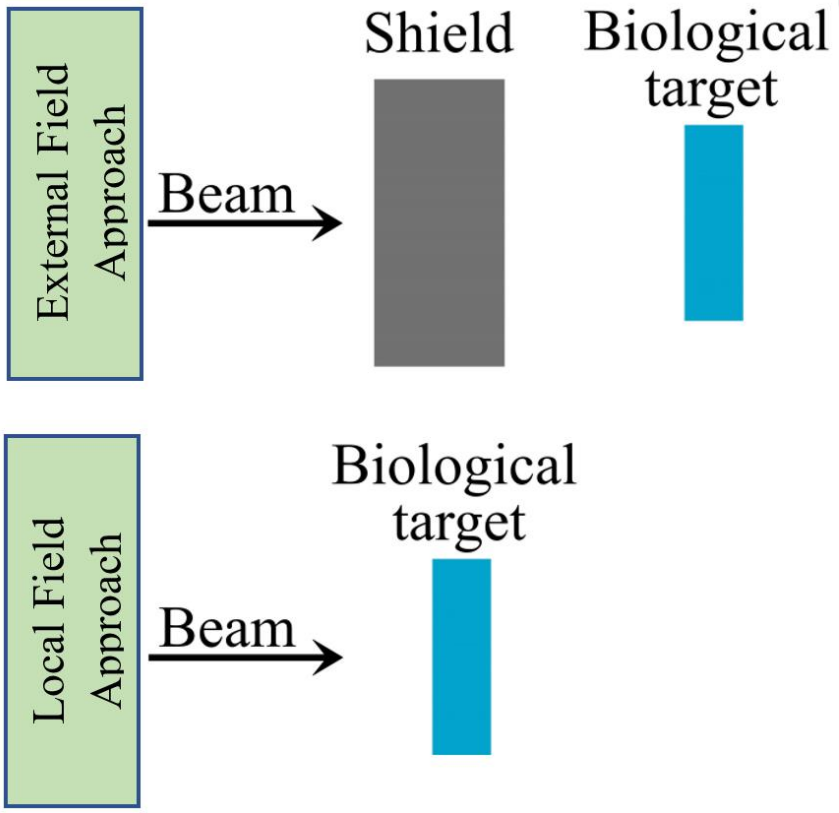

Figure 2.7 : Basic representation of external field approach and local field approach [25].

Setting up a mixed radiation environment is important to accurately represent the space environment. GCR consists of a broad spectrum which means that it is inevitable to encounter with difficulties to simulate the spectrum of all particles and energies. An example regarding to energy spectrum of GCR can be seen in Figure 2.8 [25].

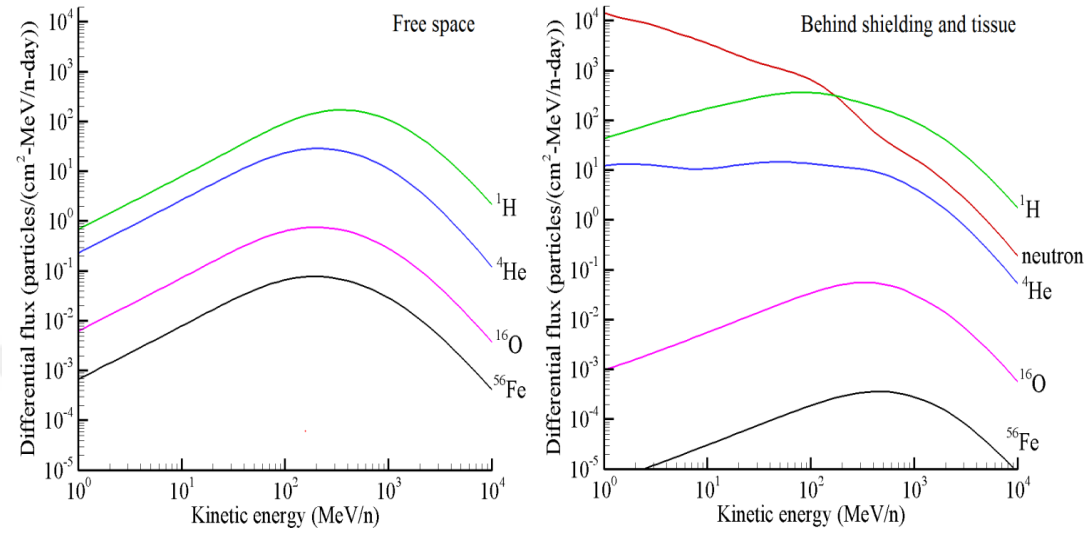

Figure 2.8 : Comparison of the energy spectra of free space and shielded zone in space [25].

Figure 2.8 shows the representation of an energy spectra of GCR in free space and energy spectra of the zone behind 5 g/cm^2 of aluminum and 30 g/cm^2 of water. Spectra has prepared with respect to solar minimum conditions. As it can be deduced from the graphics, the energy spectra of free space environment are suitable for the external field approach. On the contrary, the energy spectrum regarding the shielded zone is suitable for the local field approach. In other words, while free space represents the outside the spacecraft, shielded zone represents the inside the spacecraft.[25]

On the other hand, beam selection is another critical issue for ground-based experimental studies. Multiple beams can be used in experiments representing a mixed radiation environment, but in this case, it is not clear to specifically determine the effects of each beam. In this regard, it should not be forgotten that one of the main purposes of the ground-based experiments is to determine the biological effects of radiation on human health. However, the uncertainty about the effects of experimental outputs using multiple beams leads to deviation from this target since the effects of a mixed and separate ion energy environments are not the same [25].

To sum up, experiments using both single and multiple beams are needed to represent space radiation and to fully detect the effects of each beam regarding to health. However, most of the experiments about the space radiation environment still has performed with individual ion energies. Even though there are extraordinary improvements in accelerator technology, simulation of complete GCR still cannot be run in one experiment [25].

2.2 Polymers

Materials can be broadly classified into 4 main groups: polymers, ceramics, metals and composites. Figure 2.9 shows the main classification of the materials. However, it is possible to call polymers as a revolutionary material group. As a matter of fact, polymers replaced some other material groups such as metal for various reasons based on low cost. On the other hand, polymers have been used by mankind for a long time. While naturally occurring polymers have been used for centuries, synthetic polymers have a relatively short history. Some properties of synthetic polymers such as sufficient mechanical strength, processability, accessibility allow to create wide range of applications [26,27].

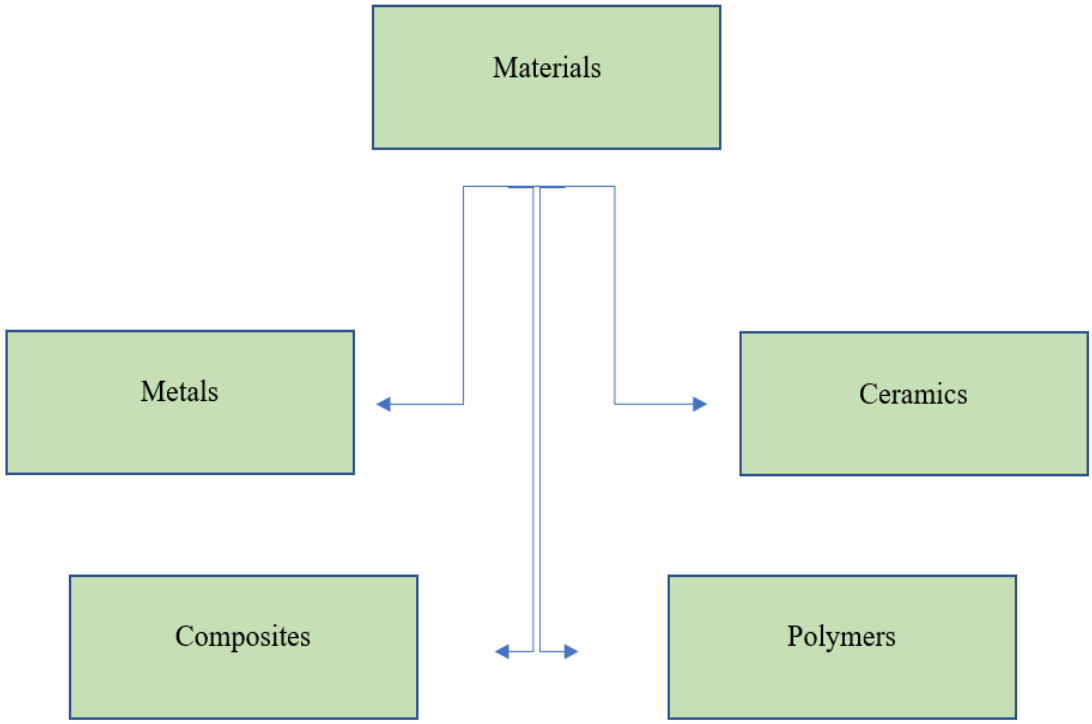

Figure 2.9 : Classification of Materials.

2.2.1 Classification of polymers

There are many classifications that has been made for polymers in order to define differences. However, classifications based on the structure, polymerization technique or biodegradability of the polymers are some of the approaches used in order to categorize the polymers. The functionality of the classification on polymer increases according to the purpose and approach to be studied. It must be noted that there are more classifications than the mentioned above in the literature [26,27]. Furthermore, there is no obstacle to have more classifications of polymers in the upcoming years.

2.2.2 Structure of polymers

Polymers composed of repeating units called monomers. Compositions of the units has a key role to identify the properties of the related material. Polymers can be accepted as a subgroup of materials that mostly encountered as organic compounds.

Hydrogen and carbon are two elements principally found in many organic compounds. The atomic number of a carbon atom is 6, while hydrogen is 1. So, there are 4 electrons for a carbon atom to participate the covalent bonding with hydrogen while hydrogen has just 1 electron to participate the same bonding. In brief, while a covalent bonding is formed between the carbon and hydrogen atom, the carbon atom still has 3 valence electrons to participate another bonding.

On the contrary, hydrogen is not required any additional bonding since there is no free valance electron. Therefore, amount of hydrogen and carbon defines the bonding mechanism of an organic material, e.g. acetylene, ethylene. Additionally, hydrocarbons with the same number of carbons and hydrogens do not always mean that they can be found in the same atomic order, e.g. butane, isobutane.

Polymers cannot be restricted with hydrocarbons since there are various polymeric materials composed of non-hydrocarbon units such as tetrafluoroethylene. Broadly, polymers can be represented with a generalized form that can be seen in Figure 2.10. The representation is suitable for some common polymers which means that it is not feasible to represent all the polymers with the generalized form in Figure 2.10. Homopolymers and copolymers are two different structural approximations that can be seen in literature of polymer science. Copolymers consist of at least two different repeating units while homopolymers consist of same repeating units [26].

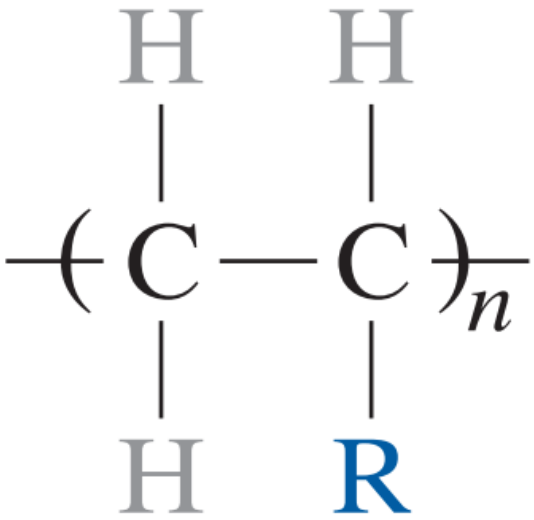

Figure 2.10 : General representation of polymer [26].

'R' can depict atoms or organic groups in the generalized representation. It may change depending on the repeating unit, e.g. Cl for Poly (vinyl chloride), OH for Poly (vinyl alcohol).

There are various types of molecular chains in polymeric structures (e.g. branched, network, linear and crosslinked). Linear polymers consist of monomer units that attach with each other and conclude as single chains. Long, continuous, and flexible chains containing the van der Waals and hydrogen bonding create the linear structure. Network polymers consist of multifunctional monomer units that create the three-dimensional networks. They can be obtained as a result of the chemical interaction between linear polymer chains and can be referred as highly crosslinked polymers. Branched polymers consist of as a result of the attaching of main chain and side chains with each other. Crosslinked polymers can be visualized the adjacent linear chains that attaching with each other by covalent bonding at different positions [26]. Figure 2.11 shows the schematic representations of molecular structure of polymers.

Polymer crystallinity can be considered more complex than the metals due to the molecular structure. However, crystalline structure can be observed in polymer-based materials via the consideration of the atomic arrangement consisting of the molecular chains. While metals can be considered completely crystalline, polymers are considered in terms of crystallinity in a range from the amorphous structure to almost crystalline structure [26].

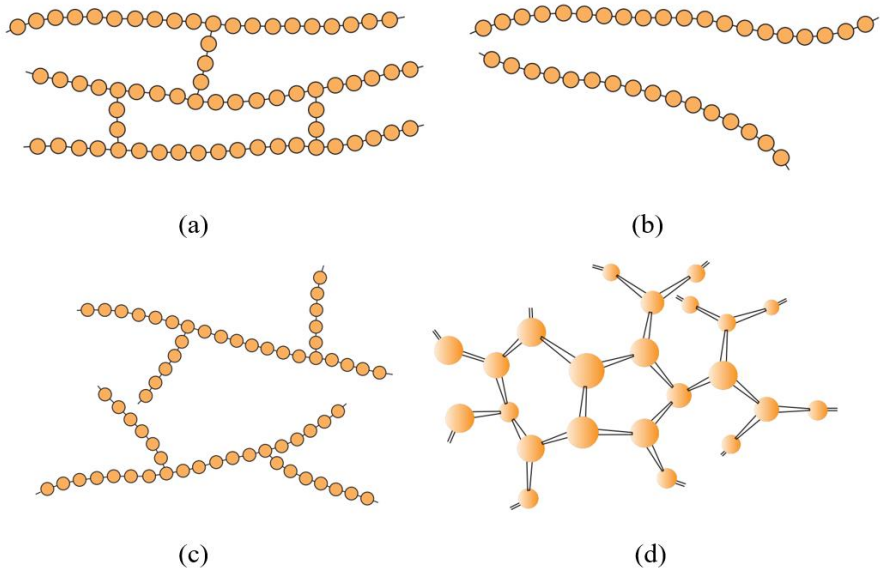

Figure 2.11 : Representations of (a) crosslinked, (b) linear, (c) branched, and (d) network (three-dimensional) molecular structure of polymers [26].

It should not be overlooked that there are separate representations for 4 different molecular structures in Figure 2.11. However, a structure within the same polymeric molecular structure can also exist in different forms. Figure 2.12 shows various representations of linear polymers in several forms.

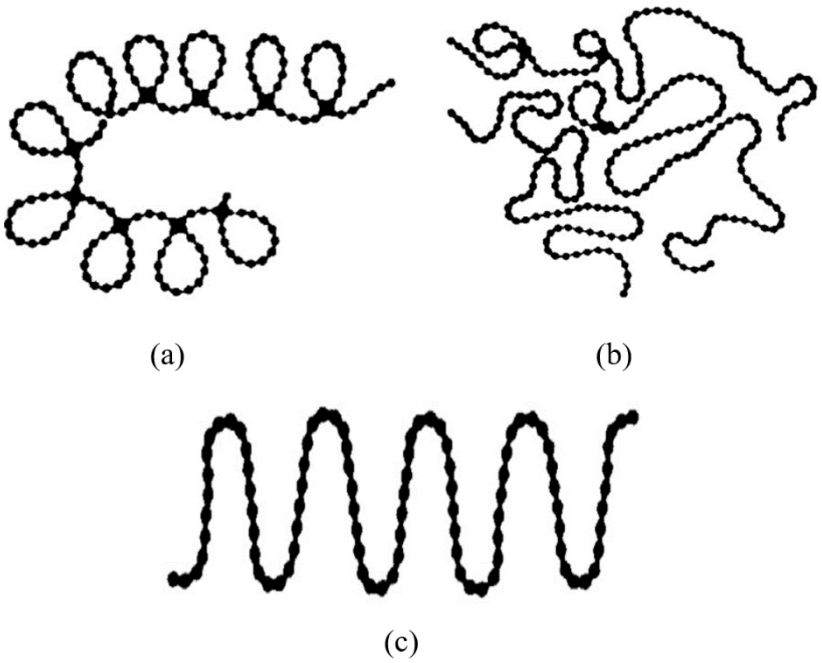

Figure 2.12 : Various representations ((a), (b), (c)) of linear polymers [28].

2.2.3 Polymerization

Polymerization is a term referred to synthesis of large molecules from the small units. Condensation polymerization and addition polymerization are two different reaction mechanisms for polymer synthesis. Condensation polymerization is named as step reaction while addition polymerization is named as chain reaction [29].

Condensation polymerization is performed by step-by-step reaction of smaller molecules or monomers with each other for the purpose of synthesizing of the regarding polymers. Formation of by products such as water can be observed in condensation polymerization and obtained by products are released during polymerization [29].

Addition polymerization is performed by attaching of the monomers one at a time in a chain-like fashion to synthesize the polymer structure [26]. Neither generation of byproducts nor elimination of molecules is observed in addition polymerization. The molecular weight of the synthesized polymers is same with monomers that are used for polymer synthesis. Also, at least one double bond is required for monomers to perform the addition polymerization [29].

There are 3 main steps in addition polymerization which are listed as: initiation, propagation, and termination. An active center is obtained during initiation process. Then propagation step has begun. It can be described as the growth of the polymer chain and is carried out by addition of monomer units to chain molecule that is growing. Ultimately, there is a termination stage that can be observed in different ways refer to disproportionation and combination [26].

Atom transfer radical polymerization (ATRP) is a technique that perform via controlled/ living polymerization to synthesize the polymeric structure in narrow molecular weight distribution and high degree of chain end functionality. It is possible to apply atom transfer radical polymerization technique to obtain several structures including homopolymer and copolymer as well as several topologies such as linear and network polymers.

Essential inputs of atom transfer radical polymerization basically can be listed as follows: initiator, monomer, catalyst and optionally the additive. In addition, temperature and solvent are two of the extremely critical factors effects the polymer synthesis via atom transfer radical polymerization technique [30].

2.2.4 Polymers for radiation shielding

Within the scope of radiation shielding research, shielding properties of many materials have investigated. Various material development studies have been carried out considering many parameters such as weight, attenuation, absorption, cost, processability of the regarding materials and type of radiation to be shielded [31]. For example, materials with higher atomic number and density are preferred for gamma radiation due to the higher probability of interactions with gamma rays of the material [32]. On the contrary, materials with lower atomic number and density can also be used by changing design parameters such as increasing the thickness of the materials [31]. It must be noted that the results may not be as expected when working with space radiation. In particular, the shielding efficiency decreases as the thickness of the shielding material increases due to the secondary particles formed as a result of the interaction of the GCR with the shielding material [33].

Polymers can be considered as a promising material group in the field of radiation shielding due to their lightweight, machinability, design flexibility and radiation shielding properties. In addition, it is an advantageous situation that polymers can be used as a matrix in composite construction, so that it provides the opportunity to obtain an effective shielding with a single material against different radiation types [31].

At this point, it is possible to see many polymers that have been researched in radiation shielding studies. Some of the popular polymers can be listed as followings: poly (methyl methacrylate), polyvinylidene chloride, high-density polyethylene, polytetrafluoroethylene, emulsion polyvinyl chloride, polyphenylene sulfide, polyacrylonitrile, polyoxymethylene, polyethylene terephthalate and polyvinyl chloride [31].

On the other hand, since polymers can be used as a matrix in the composites, many nano-micro-sized particles or fibers have been studied in polymer matrix composites for radiation shielding research. Some of the popular reinforcement agents of the composites can be listed as followings: boron carbide (B_4C), molybdenum oxide (MoO), bismuth oxide (Bi_2O_3), tungsten oxide (WO_3), titanium dioxide (TiO_2), lead oxide (PbO), lead tetraoxide (Pb_3O_4), zinc oxide (ZnO), zirconium dioxide (ZrO_2), cadmium oxide (CdO) [31].

In fact, it is possible to see application of many more polymers and reinforcement agents different from the above-mentioned materials in the field of radiation shielding according to the intended use. Additionally, the expected properties from a candidate material can be further elaborated without any restriction. For example, only limited amount of material can be able to be transported in long-distance space travel. Also, the necessity of living in an environment that is self-sufficient and does not require a constant supply from the Earth is essential for long term space missions beyond the Earth such as colonization on Mars. In this context, it is might be required that the materials used in such critical missions have recyclability properties as well as effective protection against radiation and lightweight [34].

2.2.5 Poly (methyl methacrylate)

PMMA is a thermoplastic polymer that consists of monomers called methyl methacrylate (MMA). The historical beginning of PMMA can be started with the preparation of acrylic acid carried out towards the end of the first half of the 19th century while first commercial manufacture is carried out in 1936 [35]. CAS name of the PMMA is 2-propenoic acid, 2-methyl-, methyl ester, homopolymer while trade names of is Plexiglas [36]. The linear formula of PMMA can be found in Figure 2.13.

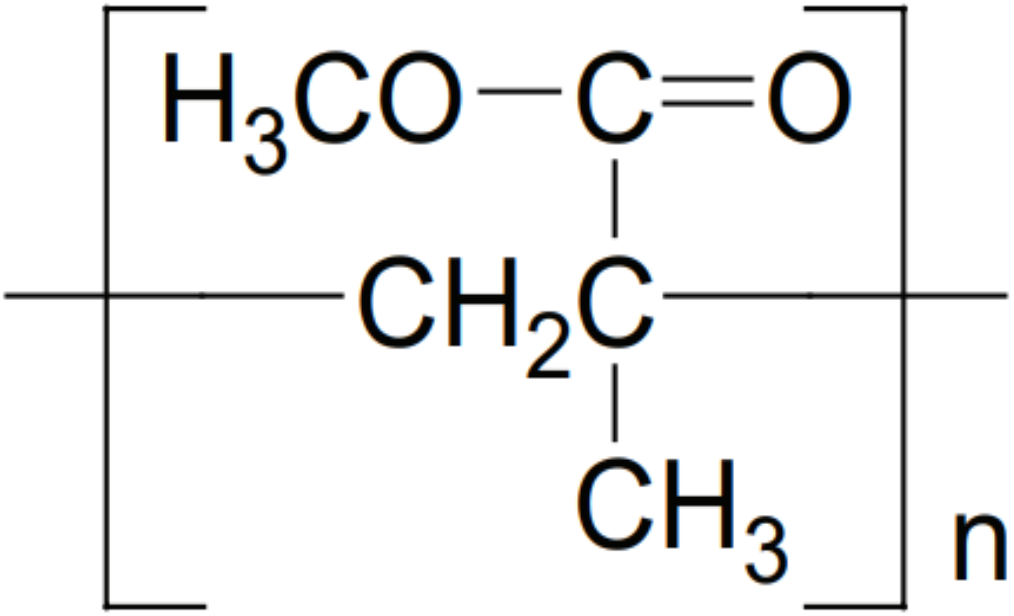

Figure 2.13 : Linear formula of PMMA [36].

PMMA is one of the remarkable polymers since it has various application areas. Basically, PMMA has been used in optical applications in industry such as automobile taillight lenses due to its transparency. However, it is possible to see other applications of PMMA such as automobile visors thanks to its features such as durability and shock resistance [37]. Apart from these, neurosurgical applications [35], polymer electrolyte making, pneumatic actuation or sensor applications are the examples of other usage areas of the PMMA [38]. Optical behavior, resistance to UV exposure and thermal stability are some of the notable properties of PMMA. In other words, these properties have a key role to determine the most feasible applications of PMMA. Additionally, detailed properties of PMMA can be found in Table 2.2. [38].

Table 2.2 : Physical properties of PMMA [38].

Property	PMMA
Density(g/cm^3)	1.18
Tensile Strength (MPa)	72
Tensile Modulus (GPa)	3.10
Elongation at Break (%)	5
Melting Point (°C)	220-240
Water Absorption (%)	0.3
Hardness (Rockwell)	M92, M90-M100
Glass Transition Temperature (Tg)	110 to 120
Color	Courless
Thermal Expansion Coefficient 20 °C (x10-4 k-1)	1.8
Thermal Conductivity at 20 °C(k(W/mK)	0.12,0.17

PMMA synthesis can be performed with different production methods such as radical polymerization of MMA, anionic polymerization of MMA, coordination polymerization of MMA. Apart from the polymerizations of MMA, PMMA can be manufactured via esterification of PMMA. Although it is possible to produce PMMA by various methods, radical polymerization of MMA is mostly preferred for PMMA synthesis. In addition, bulk, emulsion and solution polymerization approaches are utilized within the scope of manufacturing via radical polymerization method [37,38].

However, it can be stated that suspension polymerization is generally more useful when production is carried out with the radical polymerization method. PMMA powders are obtained as a result of the reaction between the radical initiator and small MMA droplets by suspension polymerization technique. In this way, the powders are become ready for the next steps of manufacturing such as extrusion and molding. In addition, other production techniques can be preferred according to the application area e.g. bulk polymerization is widely used for the production of flat PMMA sheets [37].

2.2.5.1 Poly (methyl methacrylate) for radiation shielding

It is possible to see many applications of PMMA in various radiation shielding studies. However, it is commonly used as a matrix in a composite rather than as a base polymer. PMMA has considered as one of the remarkable polymers that have been preferred in radiation shielding studies for a long time as well as PE. In particular, both PMMA and PE were also proposed as materials that can be used for radiation shielding applications inside the spacecraft in order to protect the astronauts from the hazardous environment of space [39].

There are many articles about the shielding properties of PMMA matrix composites with different reinforcement agents against different radiation types e.g. the bismuth trioxide (Bi_2O_3) reinforced PMMA composite against gamma radiation [40], the multi-walled carbon nanotubes (MWCNTs) reinforced PMMA nanocomposite against proton radiation [41].

Moreover, PMMA-based composites have also been studied for space radiation environment. The beta transmission of the PMMA/CMT composites before and after space radiation environment at LEO has tested. It has revealed that PMMA/CMT composites are the promising materials for radiation environment in space [42].

2.3 Minerals

Raw materials such minerals and rocks are extremely handy reserves for industrial developments and scientific research. There are a lot of applications of minerals for engineering and technical works. Minerals are the inorganic materials that naturally occurring in a homogeneous form. However, minerals usually are found in a crystalline and solid phase with several exceptions such as natural water. The Earth's crust consists of a spate of various minerals as well as rocks. There are nearly 3800 different minerals discovered on Earth. Therefore, this diversity provides the great opportunity to do different studies via minerals. For example, calcite is one of the widely known minerals and is used in different sectors such as the construction industry and defense industry.

Radiation research has also had its share of studies carried out using a variety of minerals. Lead based minerals such as cerussite ($PbCO_3$) and galena (PbS) are two of the examples of the minerals used in radiation studies for shielding applications [43] as well as aluminum-based spinel minerals such as pleonaste, gahnite, hercynite, galaxite and ceylonite [44]. In addition, minerals occurred in oxide or hydroxide form such as chromite ($FeCr_2O_4$) and hematite (Fe_2O_3) as well as barite ($BaSO_4$) as a sulfate form are the other remarkable examples of minerals with different occurrence forms experienced for the radiation shielding applications [45].

2.3.1 Classification of minerals

Minerals can be subject to different types of classification depending on their usefulness in distinguishing them. For instance, valuable minerals in terms of price are practically separated from the others depending on the commercial applications in industry. Classification of the minerals according to the being metallic or non-metallic form can be considered as the basic type of classification that is widely used in the literature [43].

As can be deducted from their names, metallic minerals contain metallic elements in their chemical composition, while nonmetallic minerals do not contain any type of metal in their composition. Various physical and mechanical properties of minerals such as color, hardness and specific gravity vary depending on the presence or absence of metallic elements in the chemical composition [43].

2.3.2 Colemanite

Colemanite with a general formula as following '$CaB_3O_4(OH)_3H_2O$' is a borate mineral discovered by William T. Coleman. The origin of the name of the colemanite comes from its discoverer. Colemanite is usually preferred for the synthesis of boric acid. Recently, the colemanite mineral has attracted the attention of research with the increasing demand for boron compounds in several industries such as nuclear studies and ceramic technologies [46]. The typical constituents of colemanite minerals can be found the Table 2.3 [47].

Table 2.3 : The typical constituents of colemanite [47].

Compound	Wt.
B_2O_3	44.5
CaO	27.0
MgO	2.0
Fe_2O_3	0.05
SiO_2	4.5

2.3.2.1 Colemanite for radiation shielding

Colemanite is one of the promising minerals for radiation shielding applications thanks to the hydrogen and boron in its chemical formula. It is especially used for the neutron shielding due to the effective radiation shielding properties of the boron. Additionally, colemanite shows better shielding against the neutrons compared to other boron contained minerals such as ulexite and tincal [48]. Therefore, it is possible to see various usage of the colemanite to support the development of the materials in terms of radiation shielding such as additive material introduced into the epoxy resin or barite concrete [47,49]. Colemanite has been tested not only against neutrons but also as a shielding material against gamma radiation. Gamma transmission experiments with Cs-137 has applied to the PMMA/CMT composites. The study has shown that the increasing of the colemanite amount in the composite structure, improves the radiation shielding properties of the PMMA/CMT composites against gammas emitted from the Cs-137 radioisotope [50].

3. METHODOLOGY

3.1 Sample Preparation

The monomer and the purified colemanite were mixed homogenously with the in-situ polymerization. The addition of the initiator has started the polymerization. Tubes and required materials were placed to the AtmosBag and magnetic stirrer was used for mixing. Synthesis was carried out in an inert environment provided by the pure Argon. Catalysts of the process were CuBr and Bu4NBr. CuBr was weighted as 0.067 g and 0.47 mmol and Bu_4NBr was weighted as 1.211 g and 3.76 mmol. Percentage of the colemanite added to tubes was 0%, 5% and 15%. Eventually, tubes were placed to another AtmosBag and sealed. The gas-tight syringe was used for the mixing process and amount of the MMA added to tubes was weighted as 0.282 mol and 28.2 g. Obtained mixture was degassed argon for 180 seconds and PMDETA with 47mmol and 0.081 g. was used a ligand. EBiB was used as an initiator to commence the polymerization. The amount of EBiB was 0.47 mmol and 0.092g. Tubes inside the AtmosBag were sealed with parafilm and removed. In this study, 4 different samples in terms of chemical concentrations were studied for radiation-based experiments. The samples are base PMMA, PMMA/CMT 5 wt.%, PMMA/CMT 15 wt.% and PMMA/CMT 5 wt.% with microspheres which is Glycidyl Methacrylate (GMA) loaded microcapsules. Density of the samples were measured as 1.187, 1.256, 1,378 and 1.1259 g/cm^3, respectively. Synthesis was carried out in ITU ATARC lab. Bel et al. presented the details of the production [50]. Figure 3.1 shows the production steps.

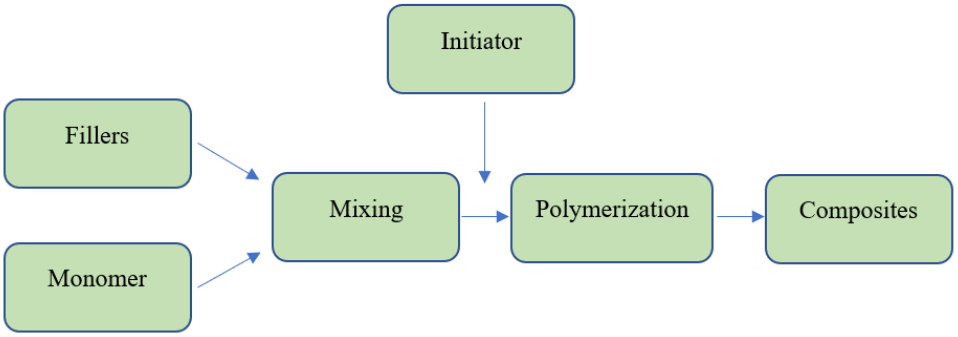

Figure 3.1 : Diagram of in-situ polymerization process.

3.2 Radiation Exposure of the Samples

The synthesized samples have prepared for the space compliance and space environment tests. Experiments have been conducted with the collaboration of the Japan Aerospace Exploration Agency (JAXA). Samples have placed the regarding module and launching of the module was carried out by Falcon-9 rocket. Launching was performed on 20:30, April 2, 2018, with GMT. The module containing samples was stored inside of Japanese Experiment Module-Pressurized Module (JEM-PM). Initiation of the exposure was carried out via ExHAM.

Duration of the experiment was 363 days between May 23, 2018- May 21, 2019. Irradiation of the regarding samples with positrons and trapped high-energy electrons was carried out at the outer ring of Van Allen Belts. Absorbed dose was determined as at ~0.02 kGy in ISS orbit. Experiment has achieved accomplishedly, and module was landed with Space-X CRS-18 (SpX-18) cargo to the Tsukuba Space Center (TKSC) [42].

Figure 3.2 shows the attachment of the sample module to ExHAM in the ISS.

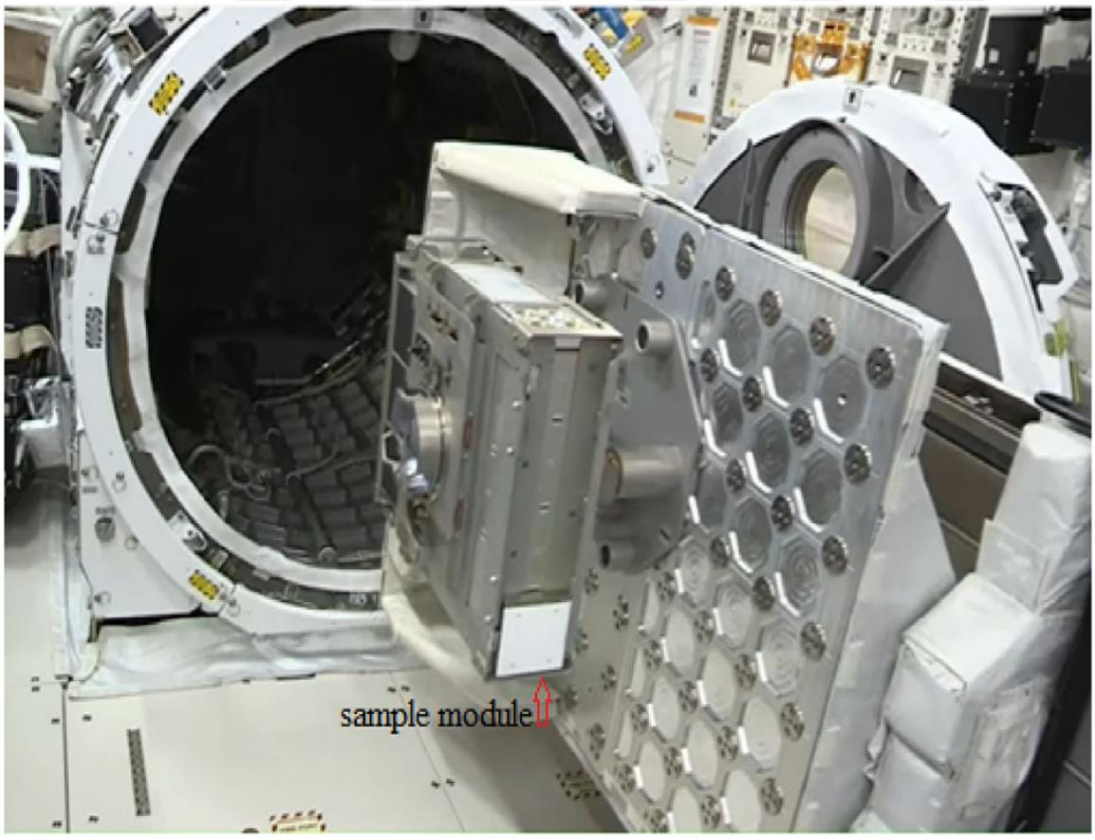

Figure 3.2 : The attachment of the sample module to ExHAM in the ISS [42].

Pictures of the front view and side view of irradiated samples after the exposure can be seen in Figure 3.3 and Figure 3.4 respectively.

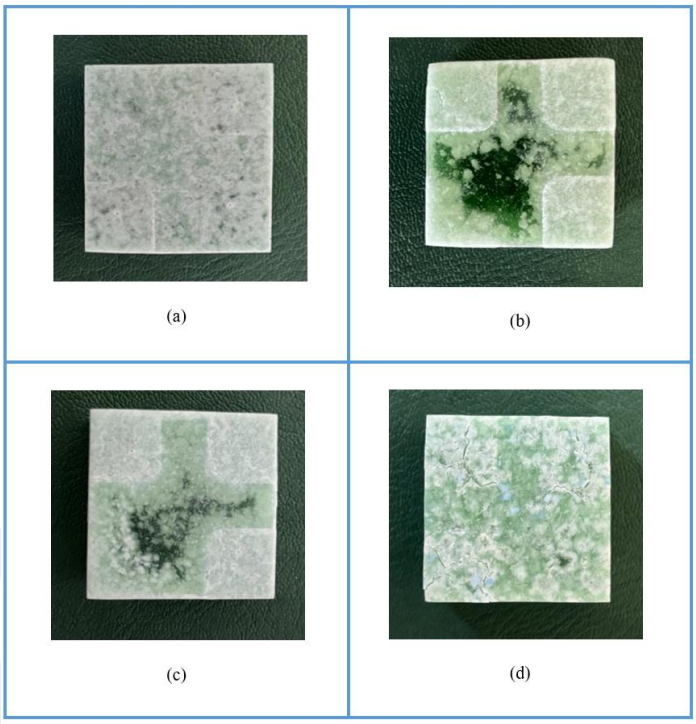

Figure 3.3 : The Pictures of the front view of the a) Base PMMA, (b) PMMA/CMT 5 wt.%, (c) PMMA/CMT 15 wt.%, and (d) PMMA/CMT 5 wt.% with microspheres

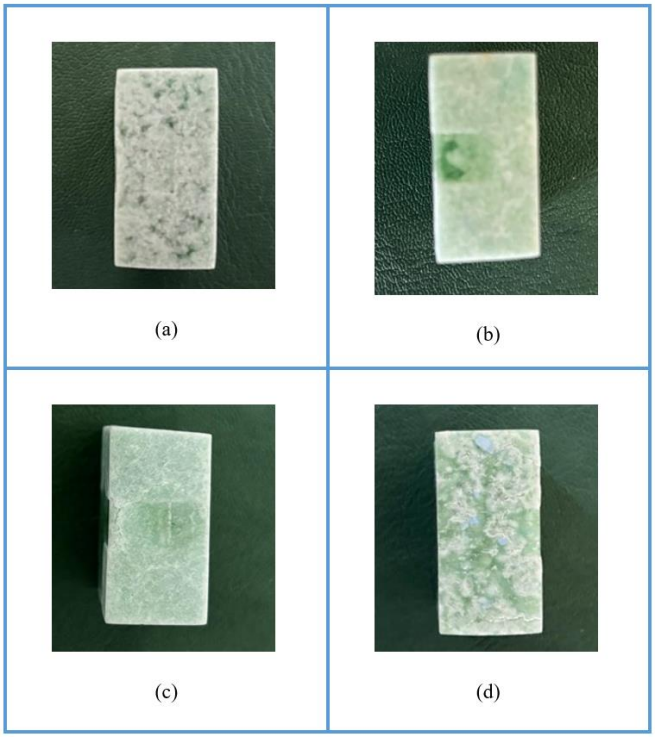

Figure 3.4 : The Pictures of the side view of the a) Base PMMA, (b) PMMA/CMT 5 wt.%, (c) PMMA/CMT 15 wt.%, and (d) PMMA/CMT 5 wt.% with microspheres

3.3 Experimental Setups

In experimental studies, radiation shielding properties of the relevant irradiated and unirradiated PMMA/CMT samples against betas(β), gammas(γ) and neutrons(n) were examined using the transmission technique. Sr-90 radioisotopes is used for beta transmission while Cs-137 and Co-60 radioisotopes were used for gamma transmission. Neutron howitzer NH3 (^{239}Pu-Be) produced by Nuclear Chicago Corporation is preferred for the neutron transmission measurements. Collimators were used to get narrow beam geometry and to minimize the scattering effects on the measurements. Therefore, Lamberts Beer equation has been made available in calculations. All the experiments were applied at least 3 times and results that differ by 10 percent from the average value are not included in the study. Then, the experiments were repeated to obtain results less than 10 percent for all measurements. The logarithmic relative radiation intensity value with respect to the thickness of the sample was calculated with the Lamberts Beer equation (2.1).

I_0 is the initial intensity while I in the same equation illustrates the transmitted intensity passing through the sample. Thickness is represented with 'x' while the linear attenuation coefficient is represented with 'μ'.

$$I = I_0 \, e^{-(\mu.x)} \tag{3.1}$$

Half-value layer (HVL) of the materials was identified to investigate the effects of the thickness on the shielding of the incoming radiation from the source. The thickness with respect to logarithmically half decreasing of relative intensity (2. 2).

$$HVL = \ln (0.5) / \mu \tag{3.2}$$

Attenuation coefficient of neutrons was calculated similar with linear attenuation coefficient from equation below:

$$I = I_0 \, e^{-(\Sigma_{total}.x)} \tag{3.3}$$

'I', 'I_0' and 'x' represent the same inputs as Equation 2.1.

Except for those mentioned in Equation 2.1, Σ_{total} represents the total macroscopic cross-section of neutrons.

3.3.1 Beta transmission experiment

Beta transmission technique is an experimental approach to identify beta attenuation properties of the samples. In this study, Sr-90 radioisotope with a diameter 0.015 cm was used as a radiation source. Experiments were carried out in a plexiglass cell at vacuum. The plexiglass cell was surrounded by the discs made by aluminum. The collimator preferred for the regarding experiments has inner and outer diameter as 6cm and 13cm, respectively. Counting was performed by the PM1405 Geiger-Muller detector. Measurements were performed from different thicknesses at least 15 minutes and less than 10% error ratio of the detector in the Radiation Applications Laboratory-B of ITU Energy Institute. Pictures of the beta transmission experiment can be seen below in Figure 3.5.

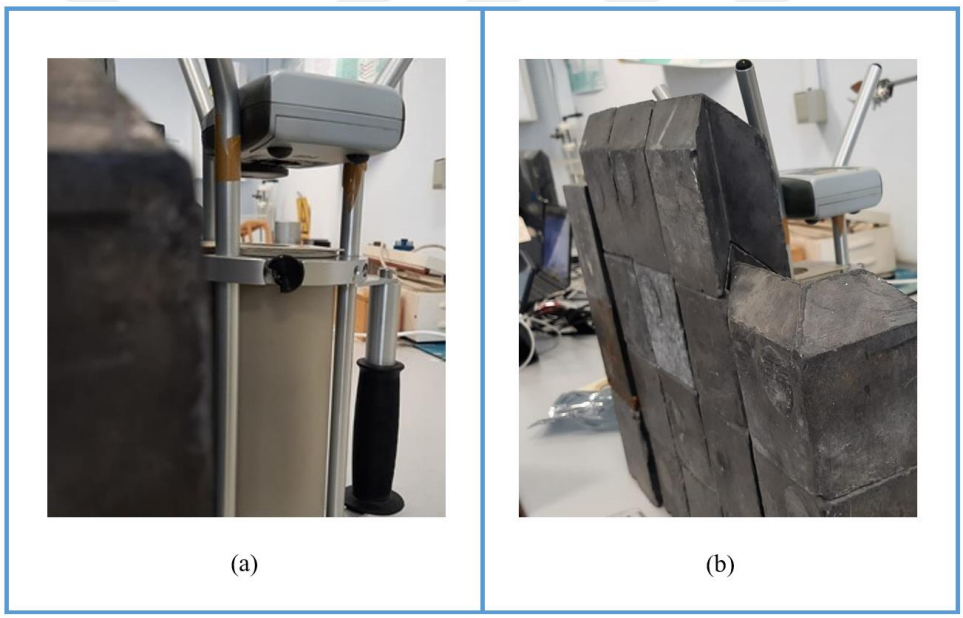

Figure 3.5 : Pictures of the beta transmission experiment setup.

3.3.1.1 Sr-90

Strontium has 4 isotopes in nature as followings Sr-84, Sr-86, Sr-87, Sr-88. Sr-90 can be produced manually in production facilities. It is mostly obtained via the nuclear fission process of the uranium and plutonium. Sr-90 is a radioisotope that emits beta particles with 0.546 MeV. Half-life and activity of the Sr-90 is 28.1 years and 3.58 mCi respectively [51]. Yittrium-90 radioisotope with 64 h half-life occurs from the decay of Sr-90 and emits beta particles with 2.28 MeV. The activity of Sr-90 radioisotope used for the beta transmission experiments of this study has calculated as 2.86mCi.

3.3.2 Gamma transmission experiment

Gamma transmission technique is an experimental approach to identify gamma attenuation properties of the samples. In this study, Cs-137 and Co-60 radioisotopes with 6 cm diameter were used as radiation source. Experimental setup can be seen in Figure 3.6 in detail. The gamma ray intensity counting system used for the transmission experiments was 'Canberra Bicron of Model: 802-2X2' connected with the multi-channel Analyzer holding 1024 channels. Diameter of the detector has measured as 20mm. In addition, the collimator hole had 7mm diameter and 10 mm thickness. Samples were placed to the setup with distance 30 mm and 15 mm for Cs-137 and Co-60, respectively. The setup has shielded with lead blocks to eliminate the incoming potential background radiation to the system from outside. Measurements were performed from different thicknesses of the relevant samples during 30 minutes in the Radiation Applications Laboratory-B of ITU Energy Institute.

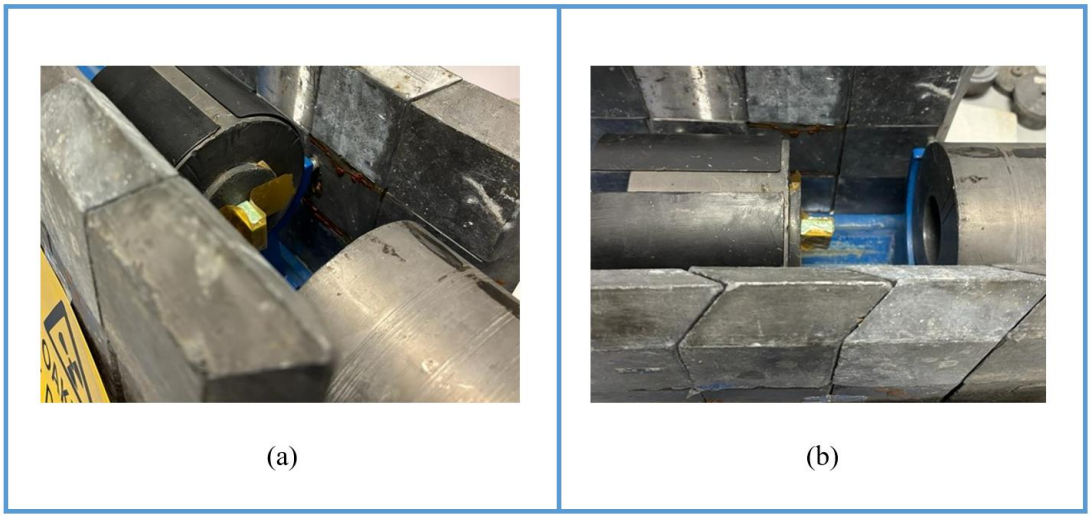

Figure 3.6 : Picture of the gamma transmission experiment setup.

3.3.2.1 Cs-137 and Co-60

Cs-137 is one of the most large-scale produced isotopes of cesium due to its more half-life compared to other radioisotopes of cesium such as Cs-134. Half-life and energy peak of the emitted photons of the Cs-137 is 30.17 years and 0.662 MeV, respectively [52]. Co-60 is a synthetic radioisotope of the cobalt. There are several isotopes of the cobalt with different half-lives as follows: CO-56, Co-58, Co-61 etc. Energy of the emitted photons of Co-60 can be observed for 2 distinct energy peaks at 1.17 MeV and 1.32 MeV and the half-life of it is known as 5.3 years [53].

3.3.3 Neutron transmission experiment

Neutron transmission technique is an experimental approach to identify the attenuation properties of the samples against neutrons. In this study, neutron howitzer NH3 (^{239}Pu-Be) produced by Nuclear Chicago Corporation was used as a radiation source. Distance between material and detector was measured as 20 cm. He-3 proportional counter named as Atomtex BDKN-02 was used as detector for neutron counting. Measurements were made until the detector error rate reached less than 1%. The experiments have carried out with lead blocks surrounding to the detector in order to minimize the background radiation. Pictures of the neutron transmission experiment can be seen in Figure 3.7.

Figure 3.7 : Picture of the neutron transmission experiment setup.

3.3.3.1 Nuclear-Chicago NH3 howitzer

Neutron howitzers are the type of irradiation instruments and sources of neutron for nuclear applications. It is a cylindrical drum made by aluminum that consists of two irradiation channels called vertical and horizontal irradiation channels. The activity of the neutrons released from the NH3 (^{239}Pu-Be) source is 5 Ci. Generation of neutrons is achieved by favor of (α, n) reaction. The flux of the generated neutrons via NH3 is 106 n/cm^2 with the average neutron energy at 5 MeV [54].

4. RESULT AND DISCUSSION

4.1 Beta Transmission Measurements

Representation of the front view of beta transmission experiment setup can be seen in Figure 4.1. Beta attenuation properties of the regarding composites can be seen in Figure 4.2, Figure 4.3, Figure 4.4 and Figure 4.5. Samples irradiated at LEO which are base PMMA, PMMA/CMT 5 wt.%, PMMA/CMT 15 wt.% and PMMA/CMT 5 wt.% with microspheres are shared respectively in figures as a function of the penetration depth. HVL values of the regarding materials has calculated and can be seen in Figure 4.6. In addition, comparison of the beta attenuation properties and HVL values of the irradiated-unirradiated samples has shown in Figure 4.7 and Figure 4.8 respectively.

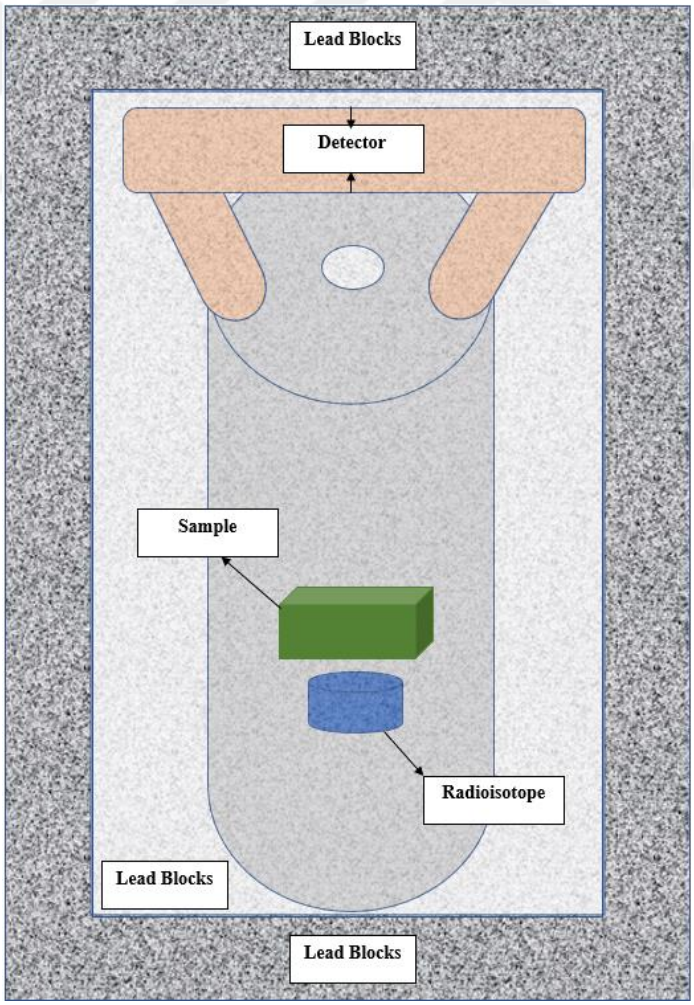

Figure 4.1 : Representation of the front view of beta transmission experiment setup.

Figure 4.2 and Figure 4.3 have explained the intensity drop as a function of the penetration depth for irradiated base PMMA and PMMA/Colemanite 5 wt.% respectively. Linear attenuation coefficients of the relevant samples were calculated as 0,198 mm^{-1} and 0,201mm^{-1} in turn.

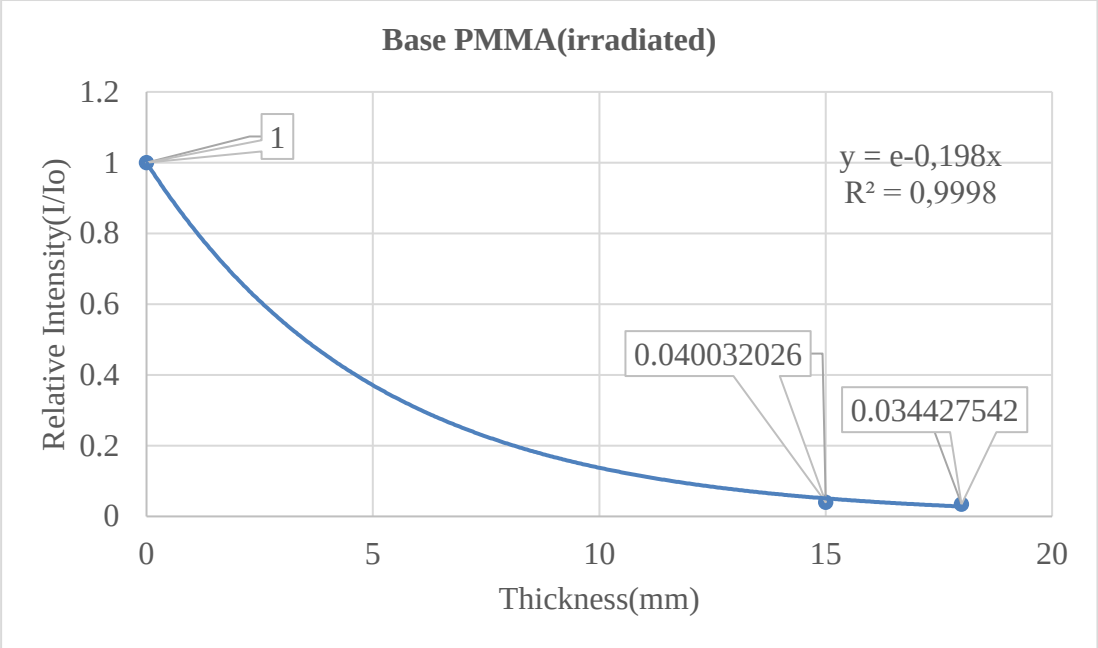

Figure 4.2 : The changes of the relative intensity with thickness for irradiated base PMMA for 0. 0.546 MeV / 2.28 MeV.

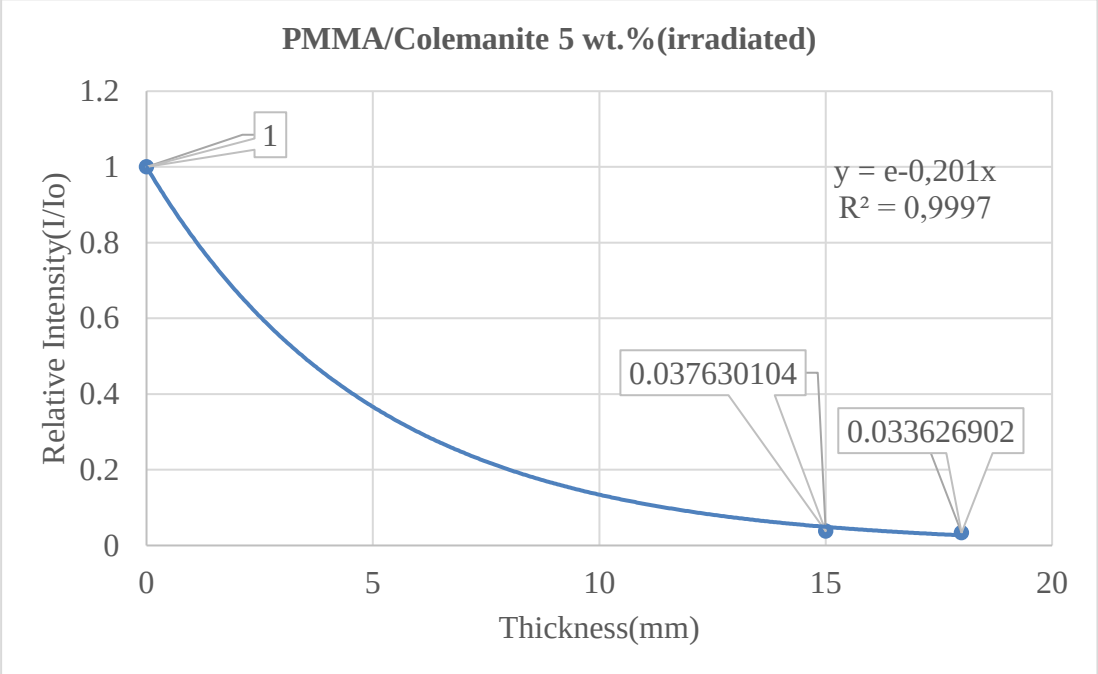

Figure 4.3 : The changes of the relative intensity with thickness for irradiated PMMA/CMT 5 wt.% for 0.546 MeV / 2.28 MeV.

Figure 4.4 and Figure 4.5 have explained the intensity drop as a function of the penetration depth for irradiated PMMA/Colemanite 15 wt.%. and PMMA/Colemanite 5 wt.% with microspheres respectively. Linear attenuation coefficients of the relevant samples were calculated as 0,209 mm^{-1} and 0,201mm^{-1} in turn.

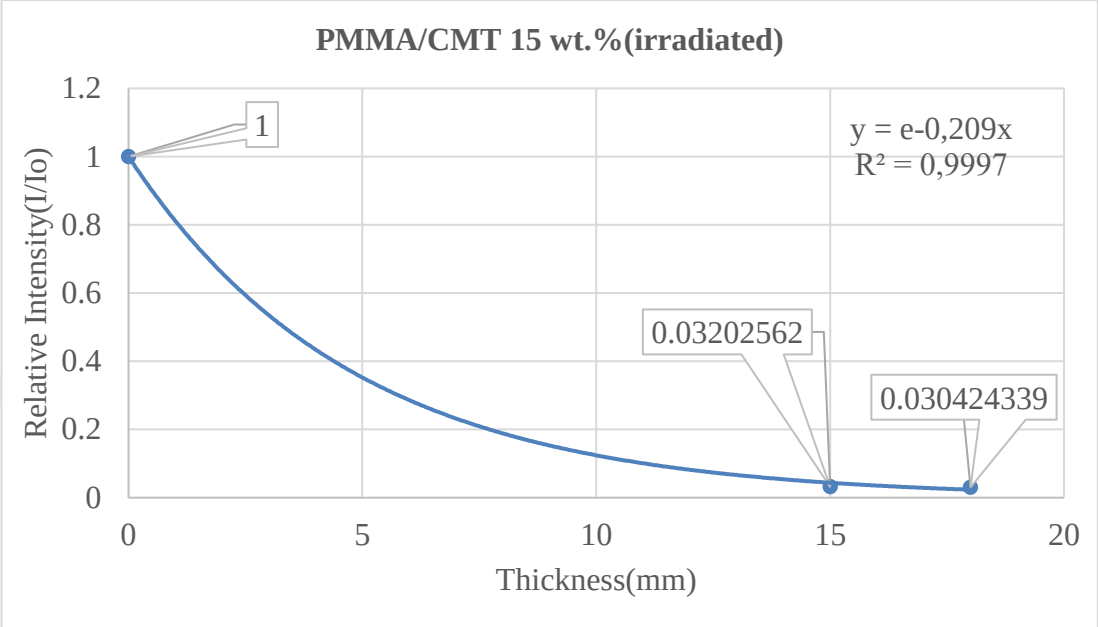

Figure 4.4 : The changes of the relative intensity with thickness for irradiated PMMA/CMT 15 wt.% for 0.546 MeV / 2.28 MeV.

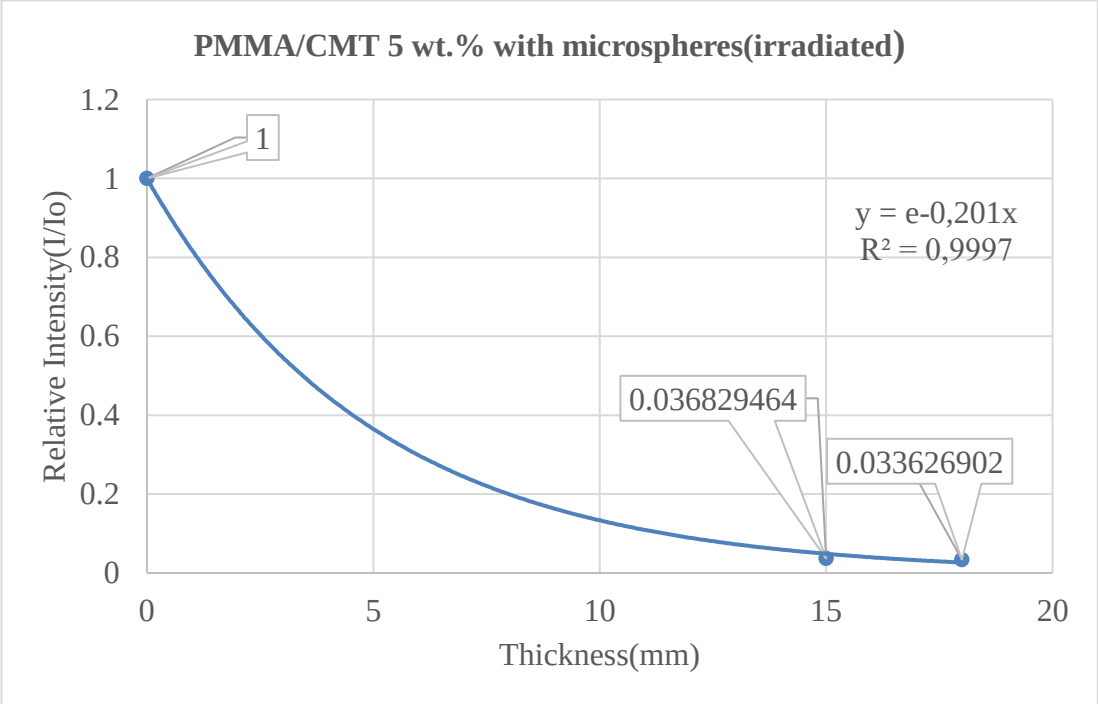

Figure 4.5 : The changes of the relative intensity with thickness for irradiated PMMA/CMT 5 wt.% with microspheres for 0.546 MeV / 2.28 MeV.

HVL values of the irradiated samples can be seen in Figure 4.6. As the amount of colemanite in the structure of the composite increased, the HVL value has decreased. However, there is no significant difference between the HVL values of PMMA/Colemanite 5 wt.% and PMMA/Colemanite 5 wt.% with microspheres samples. HVL values of base PMMA, PMMA/Colemanite 5 wt.%, PMMA/Colemanite 15 wt.% and PMMA/Colemanite 5 wt.% with microspheres has calculated as 3.5, 3.44, 3.31 and 3.44 respectively for 0.546 MeV / 2.28 MeV in terms of mm unit.

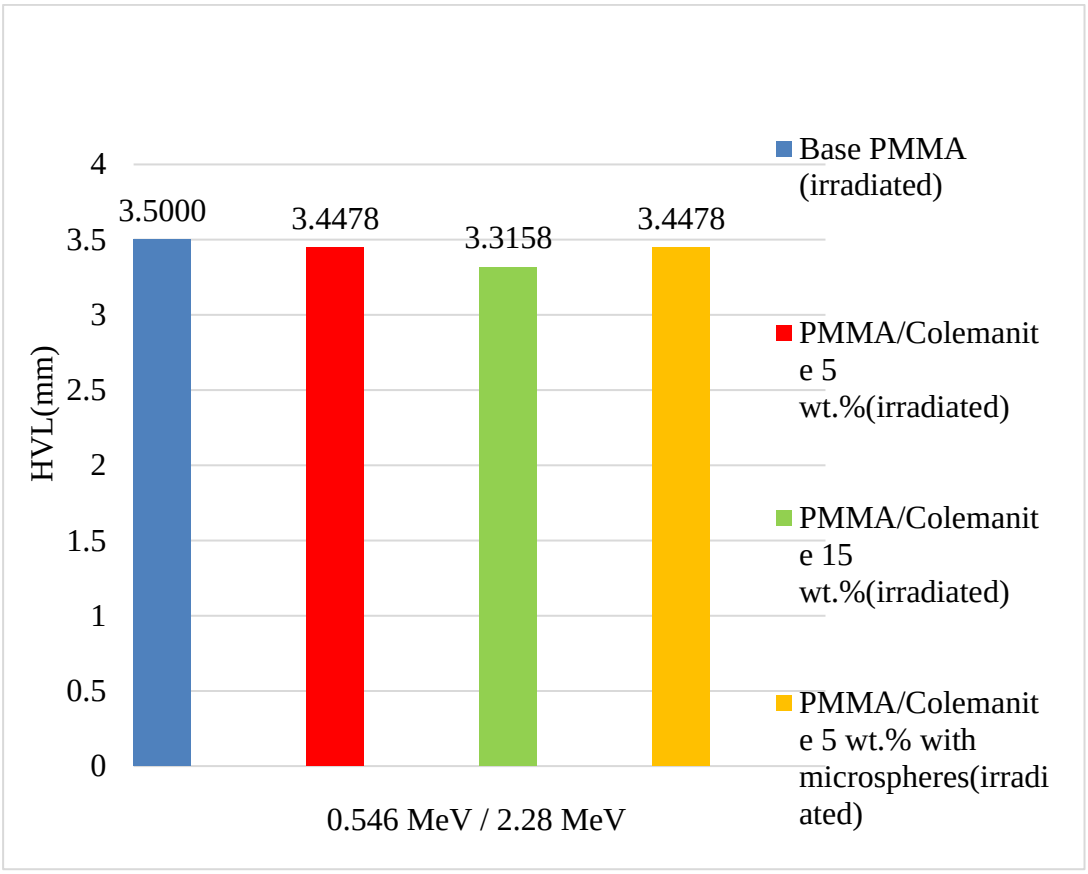

Figure 4.6 : The HVL values of the irradiated samples for 0.546 MeV / 2.28 MeV.

On the other hand, it must be noted that within the scope of calculations of beta transmission experiments; taking the 'mm' was preferred instead of taking the 'cm' as the unit system for the representation of relative intensity-thickness and HVL in regarding figures due to the passage of beta particles with an energy of 0.546 MeV / 2.28 MeV emitted from the Sr-90 radioisotope through samples for the specified thicknesses were extremely low. Since these observations have happened in different 'radiation source-material-detector' distance iterations, the calculations were made with the set-up used in this study in terms of mm unit.

4.1.1 Comparison of irradiated and unirradiated sample for Sr-90

Figure 4.7 has explained the difference between the relative intensity with thickness for both irradiated and unirradiated sample. However, linear attenuation coefficient of the unirradiated sample has slightly less than the irradiated sample. Therefore, it can be concluded that the radiation shielding properties and linear attenuation coefficient of PMMA/Colemanite 15 wt.%. sample exposed to space radiation for approximately 1 year at LEO have increased.

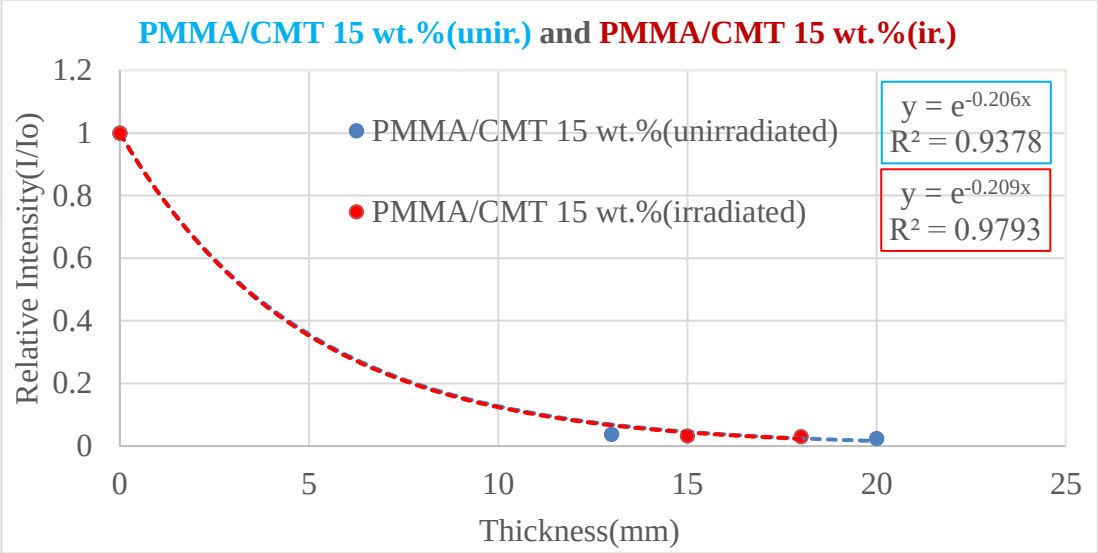

Figure 4.7 : The comparison of the relative intensity with thickness for irradiated and unirradiated PMMA/CMT 15 wt.% for 0.546 MeV / 2.28 MeV.

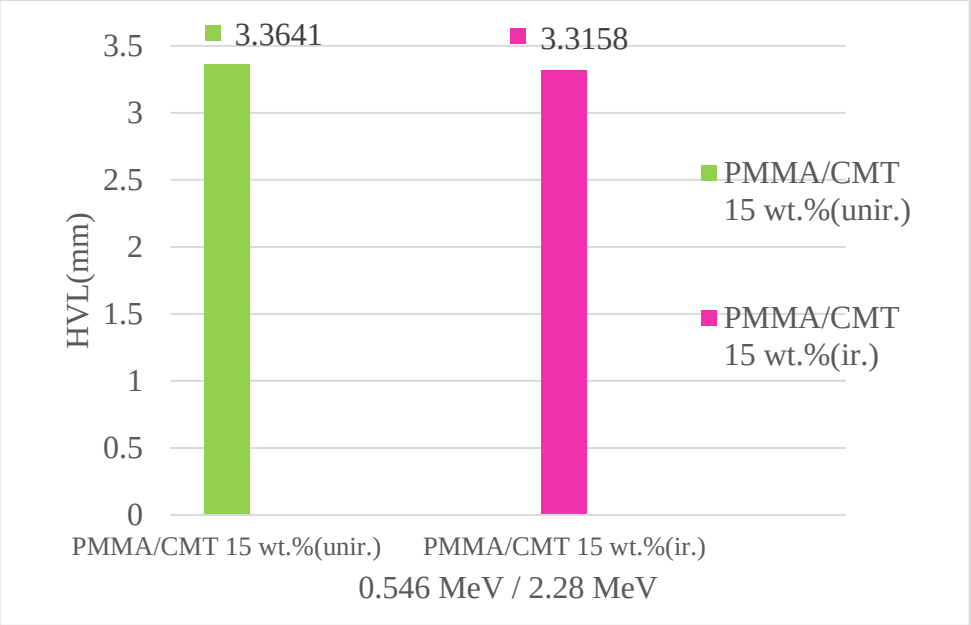

Figure 4.8 : The HVL values of the irradiated and unirradiated PMMA/CMT 15 wt.% for 0.546 MeV / 2.28 MeV.

4.2 Gamma Transmission Measurements

Samples irradiated at LEO which are base PMMA, PMMA/CMT 5 wt.%, PMMA/CMT 15 wt.% and PMMA/CMT 5 wt.% with microspheres are shared respectively in figures as a function of the penetration depth. Representation of the top view of gamma transmission experiment setup can be seen in Figure 4.9.

Gamma attenuation properties of the regarding composites can be seen in Figure 4.10, Figure 4.11, Figure 4.12 and Figure 4.13 in turn. In addition, attenuation properties of the relevant samples can be found in the regarding figures with different energy levels for Cs-137 and Co-60 as followings 0.662 MeV, 1.1732 MeV and 1.3325 MeV.

HVL values of the regarding materials have been calculated and can be seen in regarding figures with respect to energy levels for both radioisotopes used during the experimental studies. In addition, comparison of the gamma attenuation properties and HVL values of the irradiated-unirradiated samples for each energy level observed for Cs-137 and Co-60 have shown respectively in Figure 4.16, Figure 4.29 and Figure 4.30.

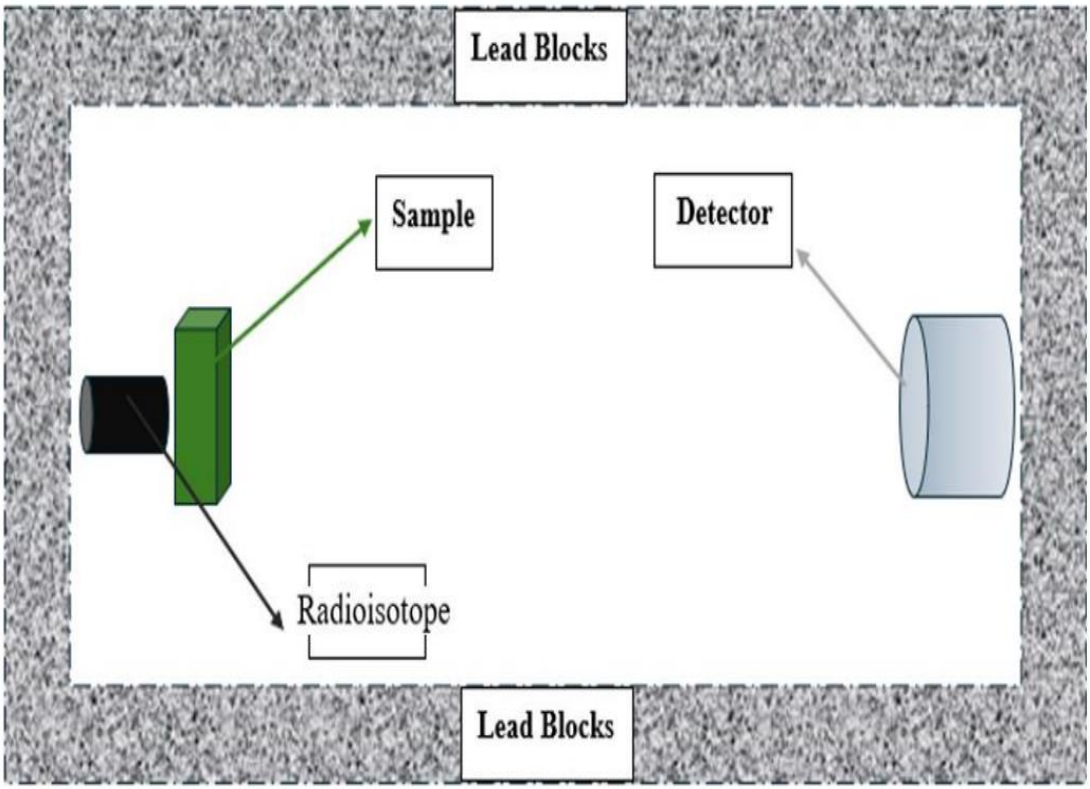

Figure 4.9 : Representation of the top view of gamma transmission experiment setup.

4.2.1 Gamma transmission measurements via Cs-137

Figure 4.10 and Figure 4.11 have explained the intensity drop as a function of the penetration depth for irradiated base PMMA and PMMA/Colemanite 5 wt.% respectively. Linear attenuation coefficients of the relevant samples were calculated as 0,099 cm^{-1} and 0,104 cm^{-1} in turn.

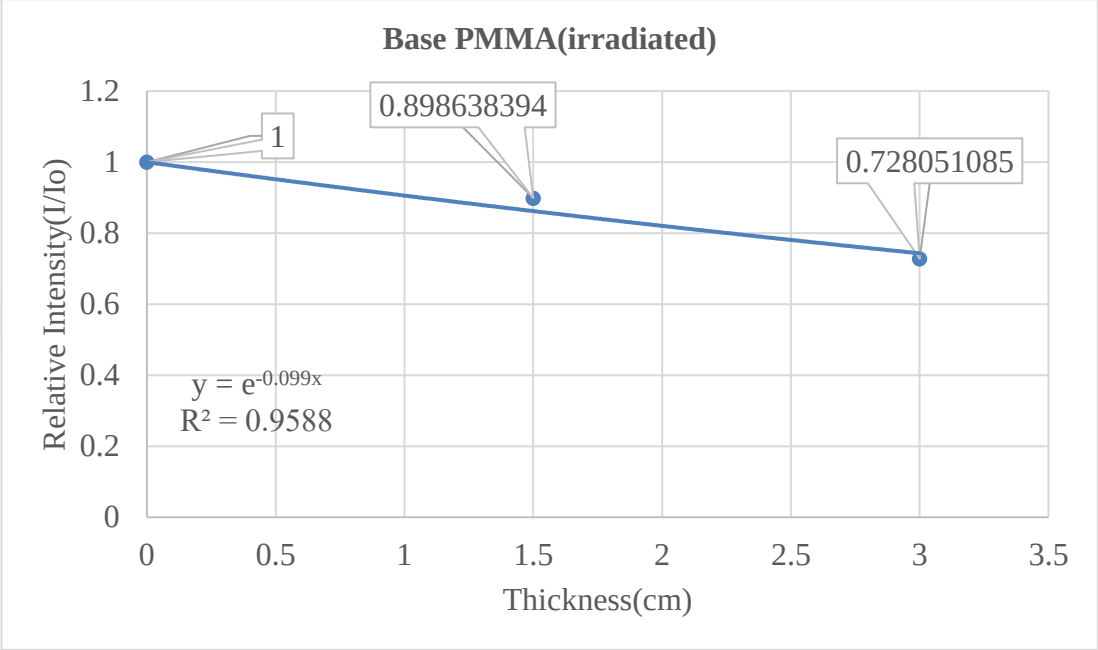

Figure 4.10 : The changes of the relative intensity with thickness for irradiated base PMMA for 0.662 MeV.

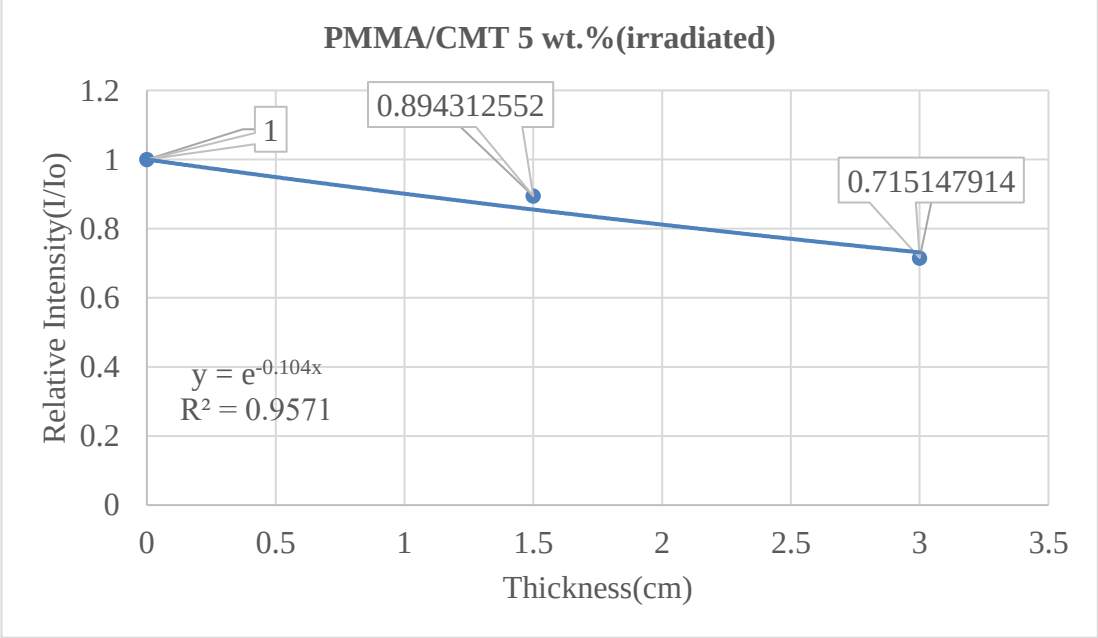

Figure 4.11 : The changes of the relative intensity with thickness for irradiated PMMA/CMT 5 wt.% for 0.662 MeV.

Figure 4.12 and Figure 4.13 have explained the intensity drop as a function of the penetration depth for irradiated PMMA/Colemanite 15 wt.%. and PMMA/Colemanite 5 wt.% with microspheres respectively. Linear attenuation coefficients of the relevant samples were calculated as 0,113 cm^{-1} and 0,104 cm^{-1} in turn.

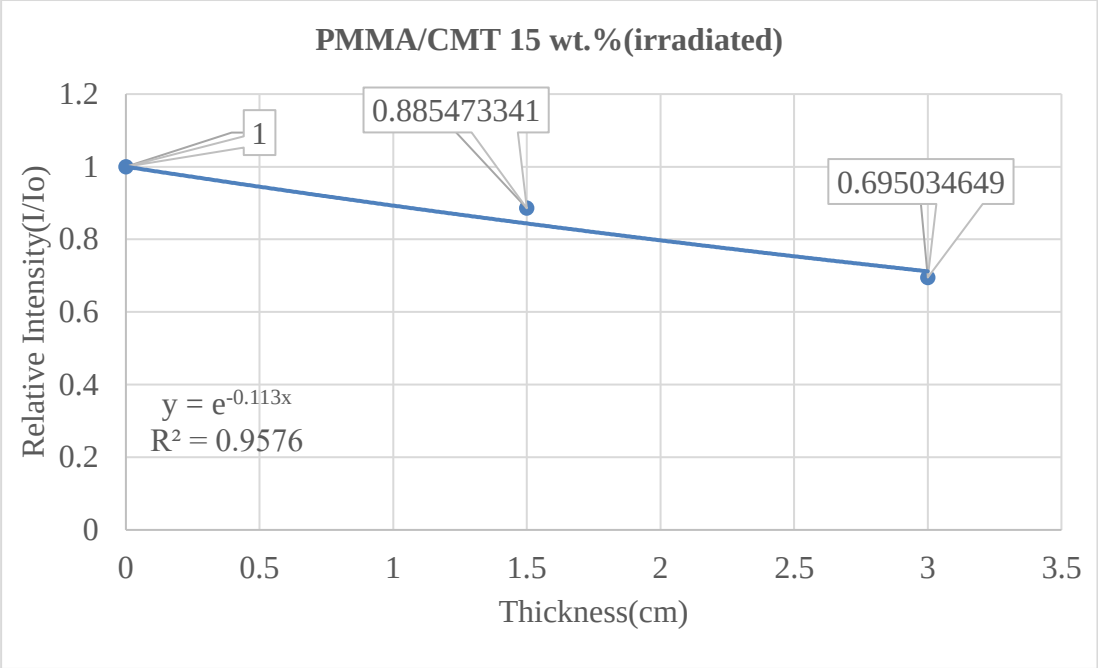

Figure 4.12 : The changes of the relative intensity with thickness for irradiated PMMA/CMT 15 wt.% for 0.662 MeV.

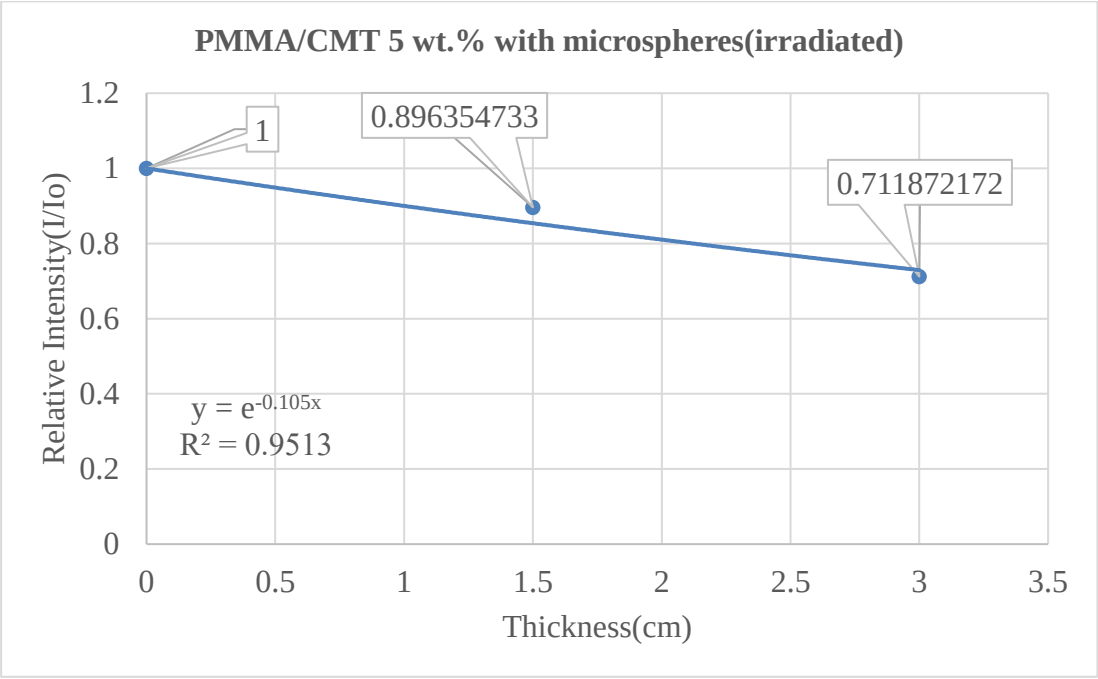

Figure 4.13 : The changes of the relative intensity with thickness for irradiated PMMA/CMT 5 wt.% with microspheres for 0.662 MeV.

The obtained HVL values of the irradiated samples for 0.662 MeV can be seen in Figure 4.14. As the amount of colemanite in the structure of the composite increased, the HVL value has decreased. However, there is no difference between the HVL values of PMMA/Colemanite 5 wt.% and PMMA/Colemanite 5 wt.% with microspheres samples for Cs-137.

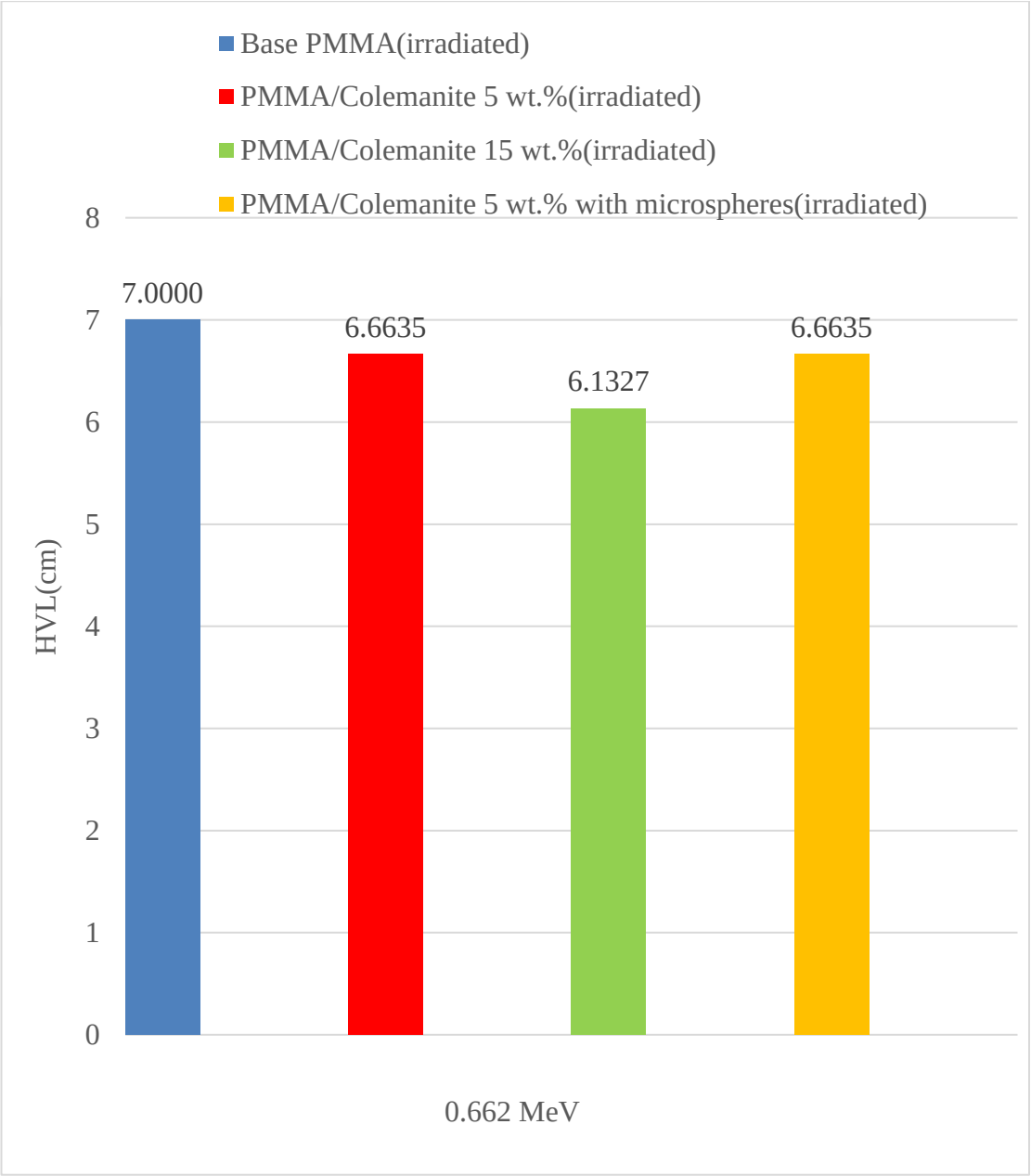

Figure 4.14 : The HVL values of the irradiated samples for 0.662 MeV.

HVL values of base PMMA, PMMA/Colemanite 5 wt.%, PMMA/Colemanite 15 wt.% and PMMA/Colemanite 5 wt.% with microspheres has calculated as 7, 6.66, 6.13 and 6.66 respectively for 0.662 MeV in terms of cm unit.

4.2.2 Comparison of irradiated and unirradiated sample for Cs-137

Figure 4.15 shows the difference between the relative intensity with thickness for both irradiated and unirradiated sample.Linear attenuation coefficient of unirradiated PMMA/Colemanite 15 wt.% has calculated as 0.112 cm^{-1} while irradiated sample has calculated as 0.113 cm^{-1}. HVL values of unirradiated and irradiated PMMA/Colemanite 15 wt.% has calculated as 6.18 and 6.13 respectively for 0.662 MeV in terms of cm unit in Figure 4.16.

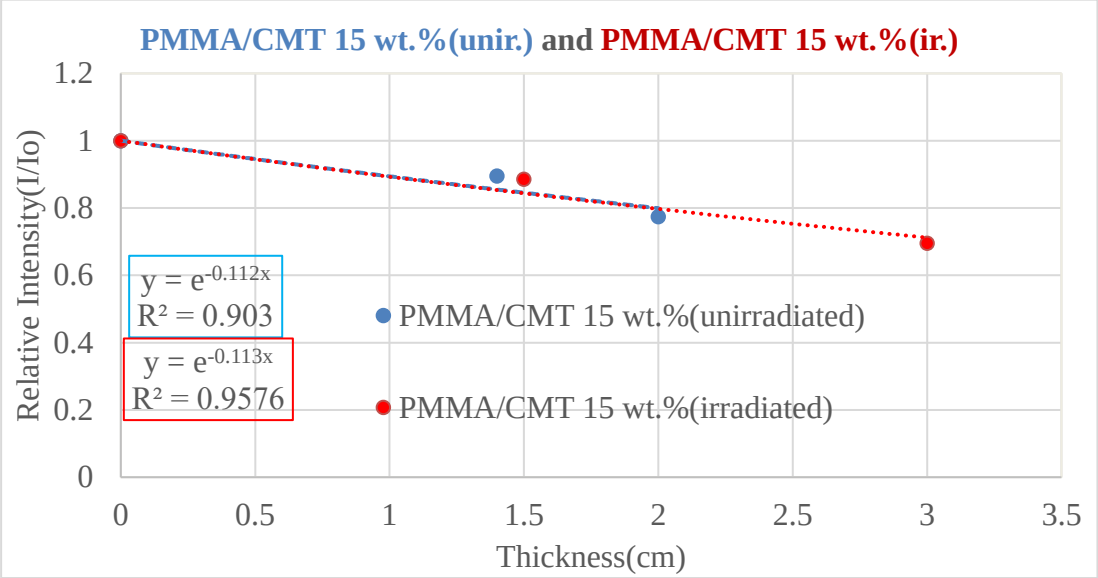

Figure 4.15 : The comparison of the relative intensity with thickness for irradiated and unirradiated PMMA/CMT 15 wt.% for 0.662 MeV.

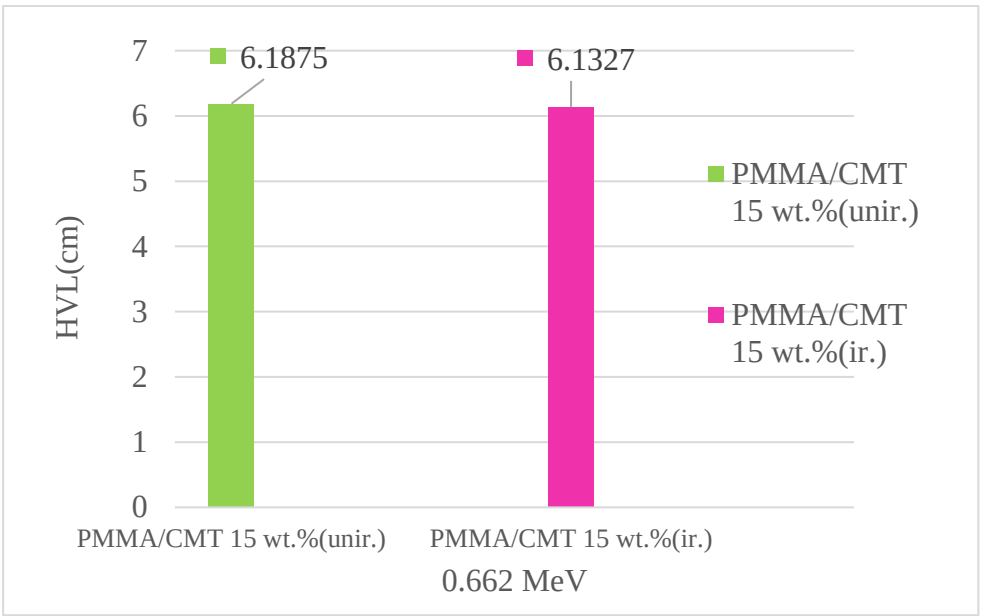

Figure 4.16 : The HVL values of the irradiated and unirradiated PMMA/CMT 15 wt.% for 0.662 MeV.

4.2.3 Gamma transmission measurements via Co-60 for 1.1732 MeV

Figure 4.17 and Figure 4.18 show the intensity drop as a function of the penetration depth for irradiated base PMMA and PMMA/Colemanite 5 wt.% respectively. Linear attenuation coefficients of the relevant samples were calculated as 0,080 cm^{-1} and 0,083 cm^{-1} in turn.

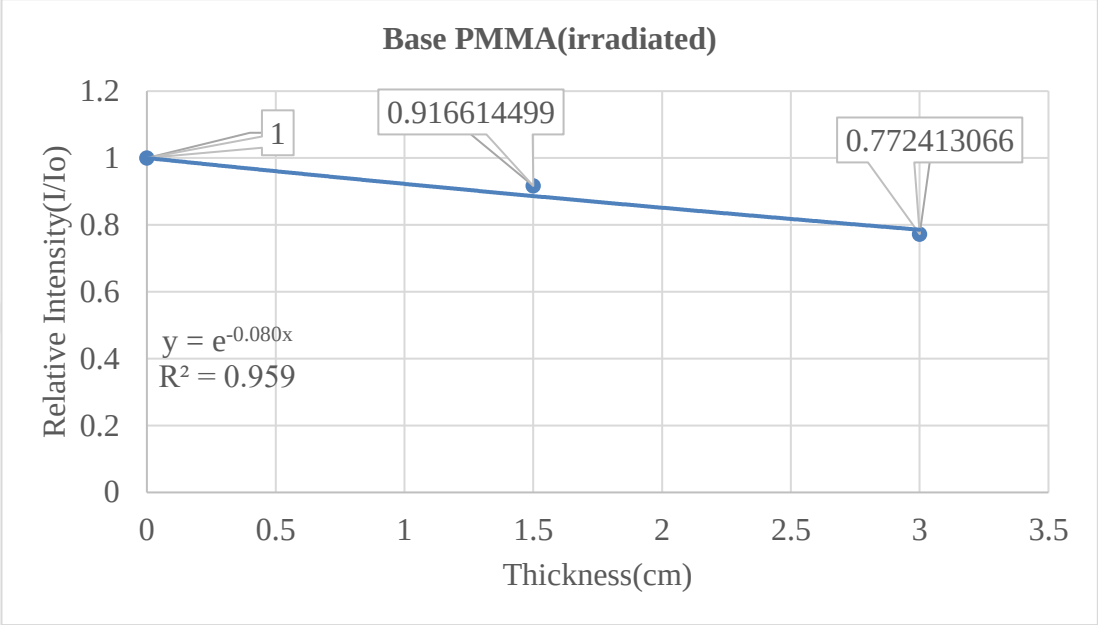

Figure 4.17 : The changes of the relative intensity with thickness for irradiated base PMMA for 1.1732 MeV.

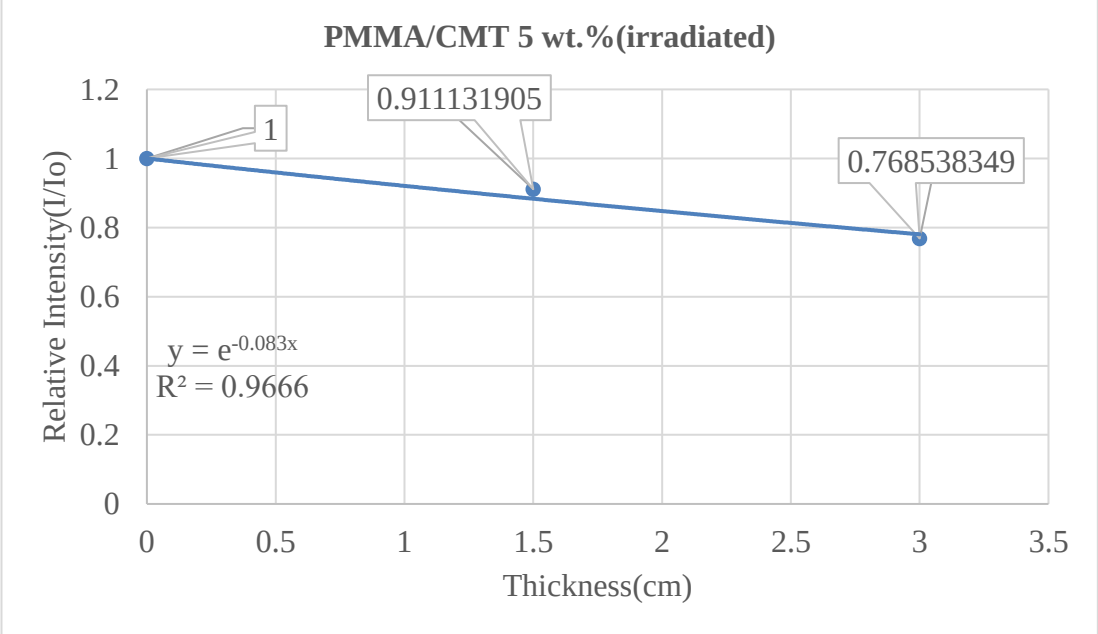

Figure 4.18 : The changes of the relative intensity with thickness for irradiated PMMA/CMT 5 wt.% for 1.1732 MeV.

Figure 4.19 and Figure 4.20 have explained the intensity drop as a function of the penetration depth for irradiated PMMA/Colemanite 15 wt.%. and PMMA/Colemanite 5 wt.% with microspheres respectively. Linear attenuation coefficients of the relevant samples were calculated as 0,089 cm^{-1} and 0,083 cm^{-1} in turn.

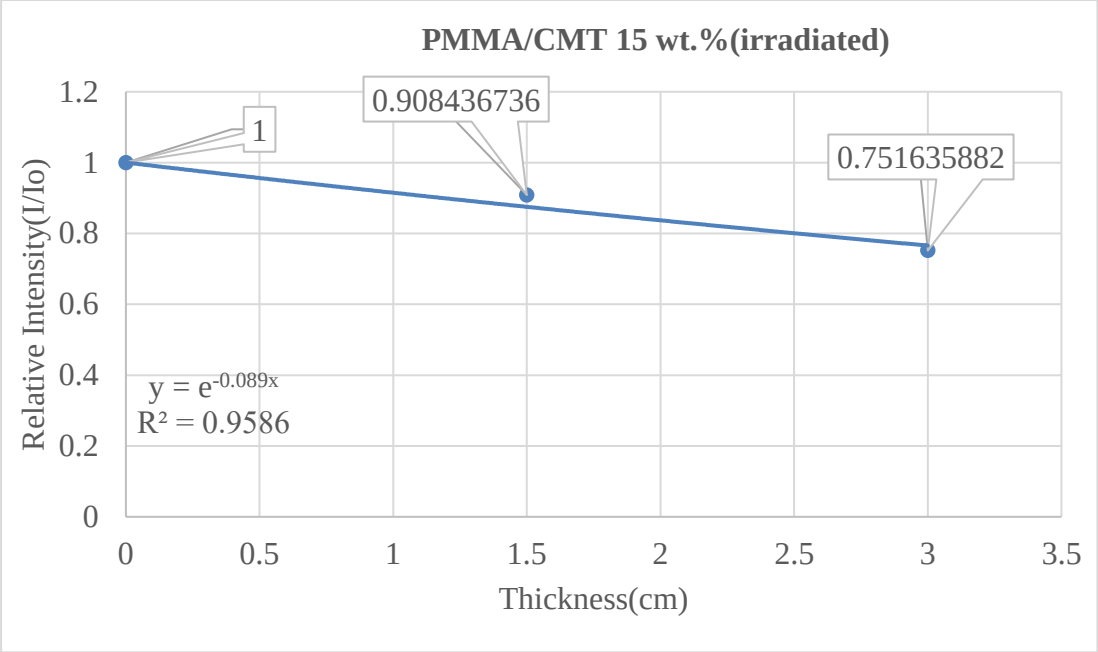

Figure 4.19 : The changes of the relative intensity with thickness for irradiated PMMA/CMT 15 wt.% for 1.1732 MeV.

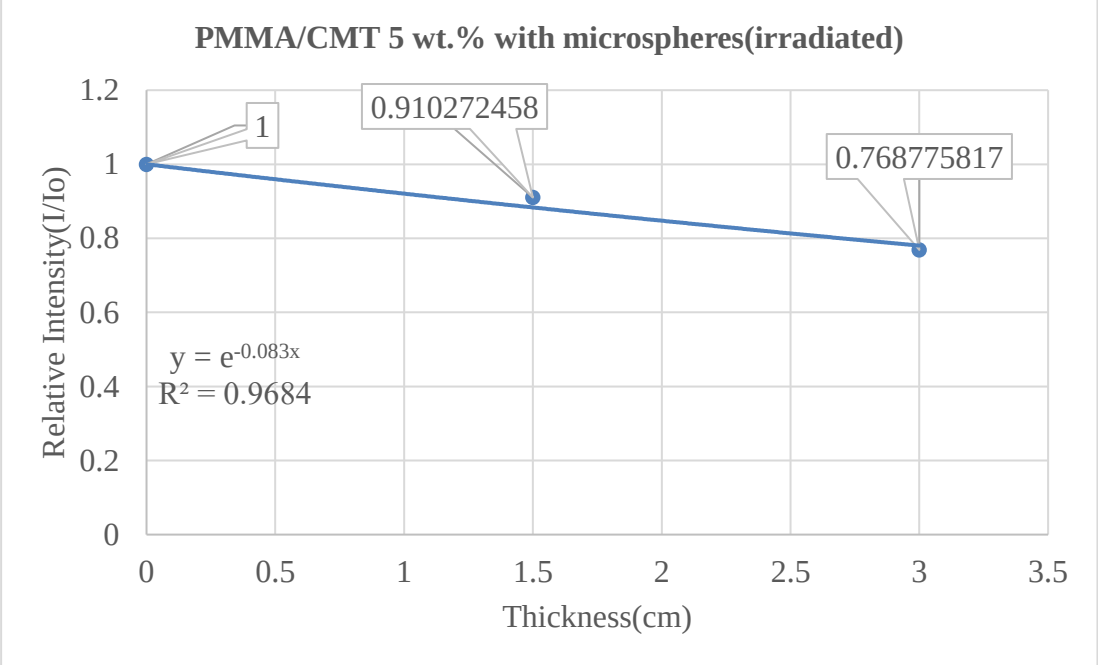

Figure 4.20 : The changes of the relative intensity with thickness for irradiated PMMA/CMT 5 wt.% with microspheres for 1.1732 MeV.

4.2.4 Gamma transmission measurements via Co-60 for 1.3325 MeV

Figure 4.21 and Figure 4.22 have explained the intensity drop as a function of the penetration depth for irradiated base PMMA and PMMA/Colemanite 5 wt.% respectively. Linear attenuation coefficients of the relevant samples were calculated as 0,074 cm^{-1} and 0,077 cm^{-1} in turn.

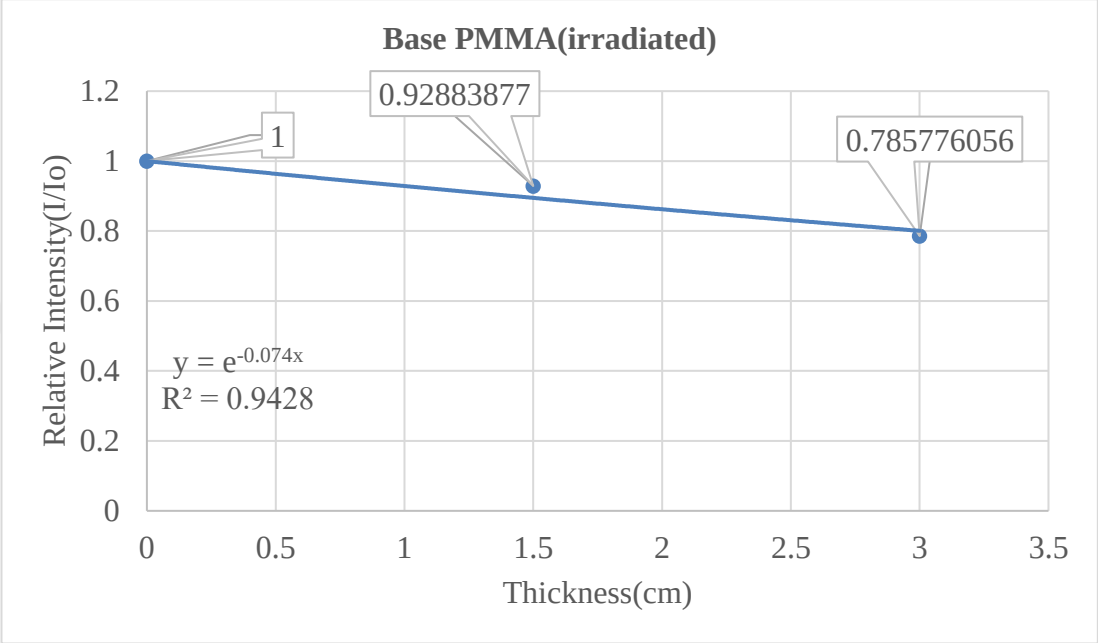

Figure 4.21 : The changes of the relative intensity with thickness for irradiated base PMMA for 1.3325 MeV.

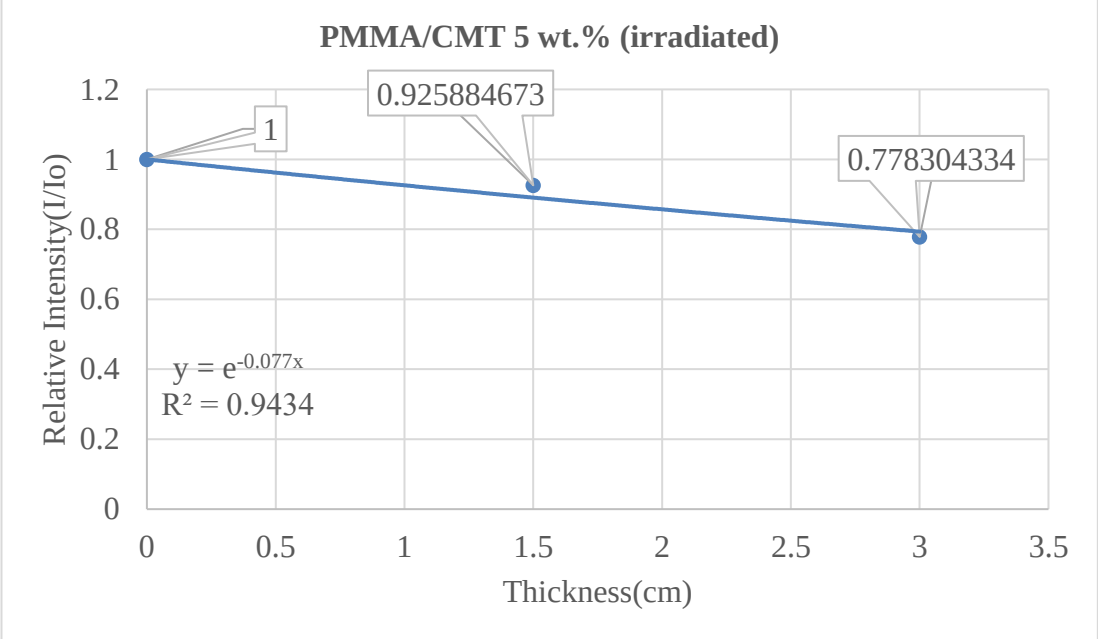

Figure 4.22 : The changes of the relative intensity with thickness for irradiated PMMA/CMT 5 wt.% for 1.3325 MeV.

Figure 4.23 and Figure 4.24 have explained the intensity drop as a function of the penetration depth for irradiated PMMA/Colemanite 15 wt.%. and PMMA/Colemanite 5 wt.% with microspheres respectively. Linear attenuation coefficients of the relevant samples were calculated as 0,084 cm^{-1} and 0,078 cm^{-1} in turn. Figure 4.25 and Figure 4.26 show the HVL values of the irradiated samples

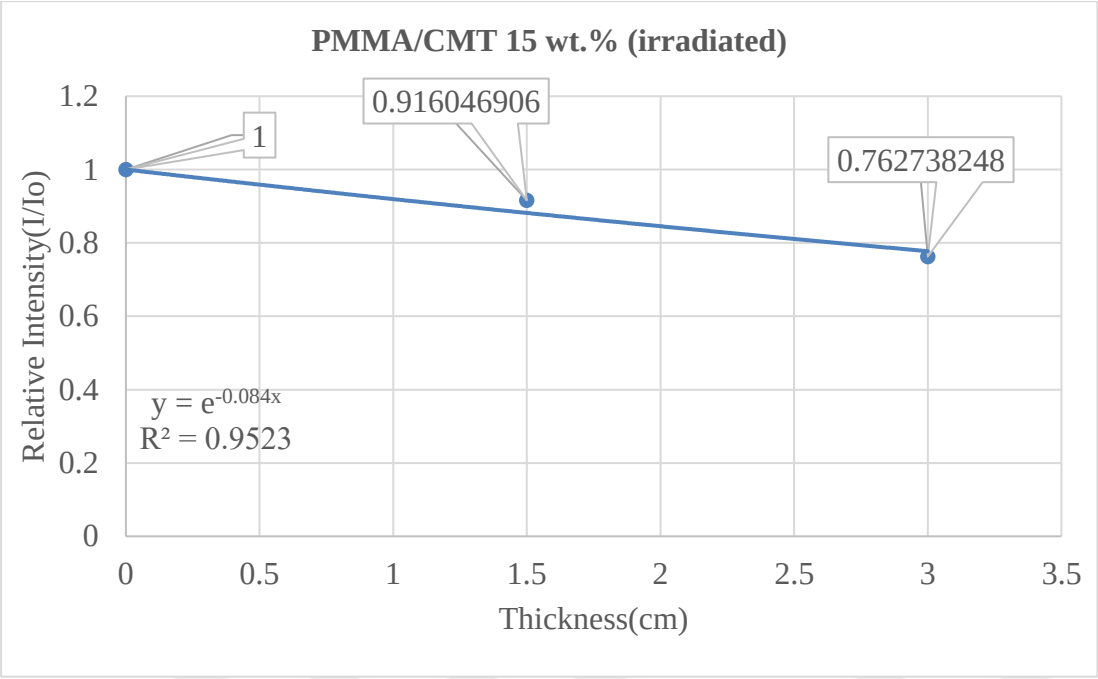

Figure 4.23 : The changes of the relative intensity with thickness for irradiated PMMA/CMT 15 wt.% for 1.3325 MeV.

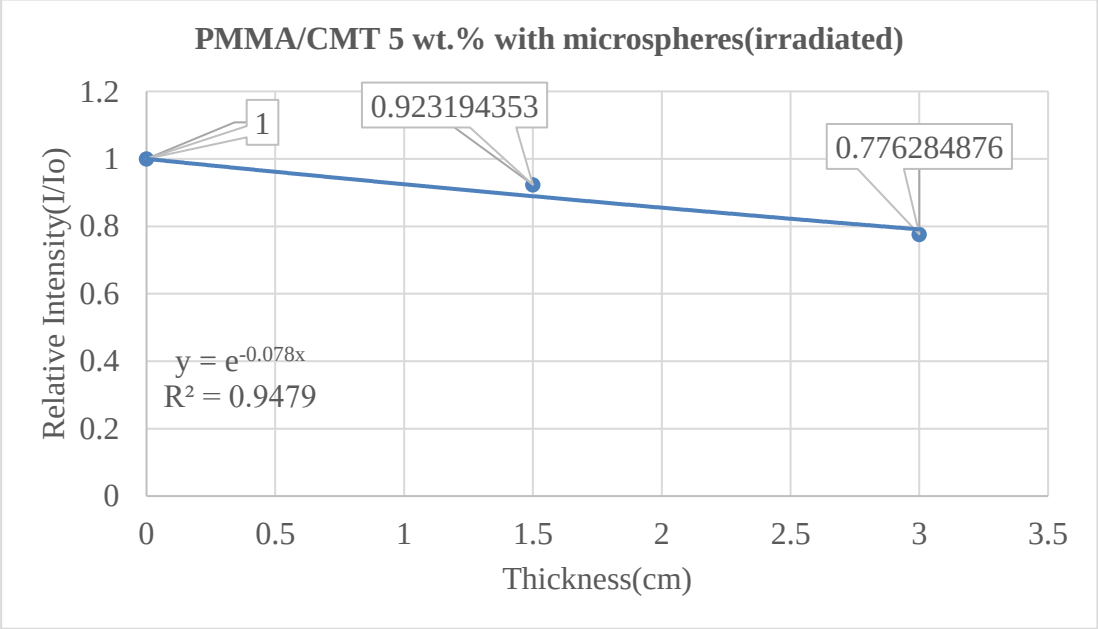

Figure 4.24 : The changes of the relative intensity with thickness for irradiated PMMA/CMT 5 wt.% with microspheres for 1.3325 MeV.

4.2.5 Comparison of HVL values for 1.1732 MeV and 1.3325 MeV

HVL values of the irradiated samples obtained from both energy level of Co-60 were calculated in terms of cm unit.

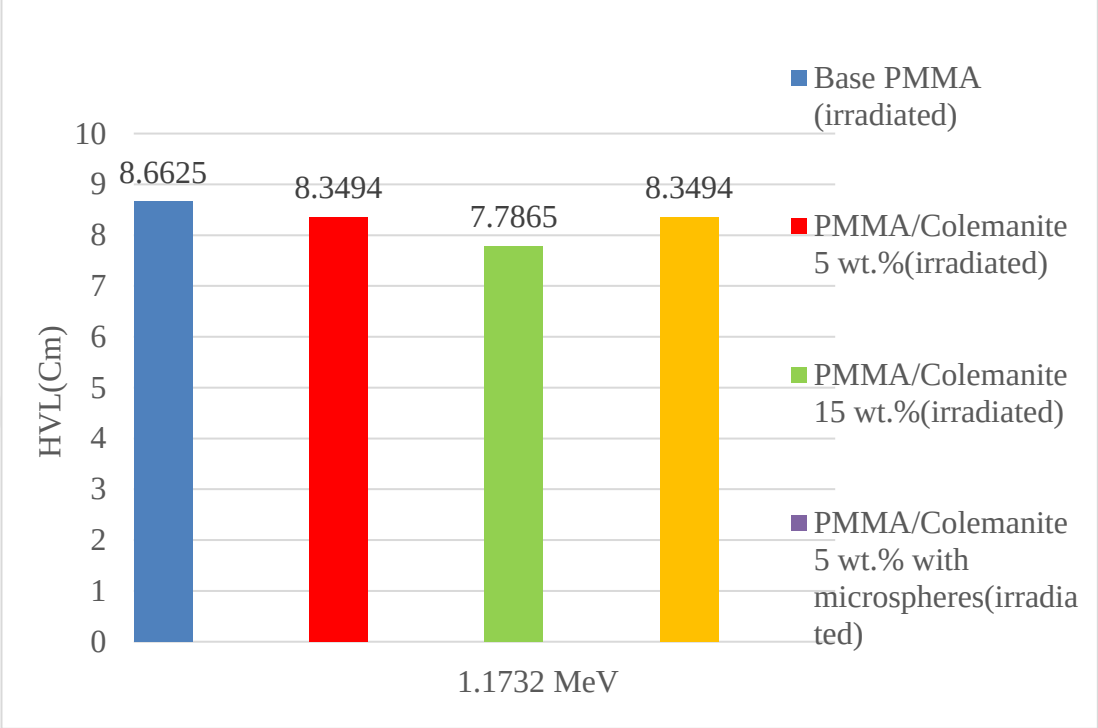

Figure 4.25 : The HVL values of the irradiated samples for 1.1732 MeV.

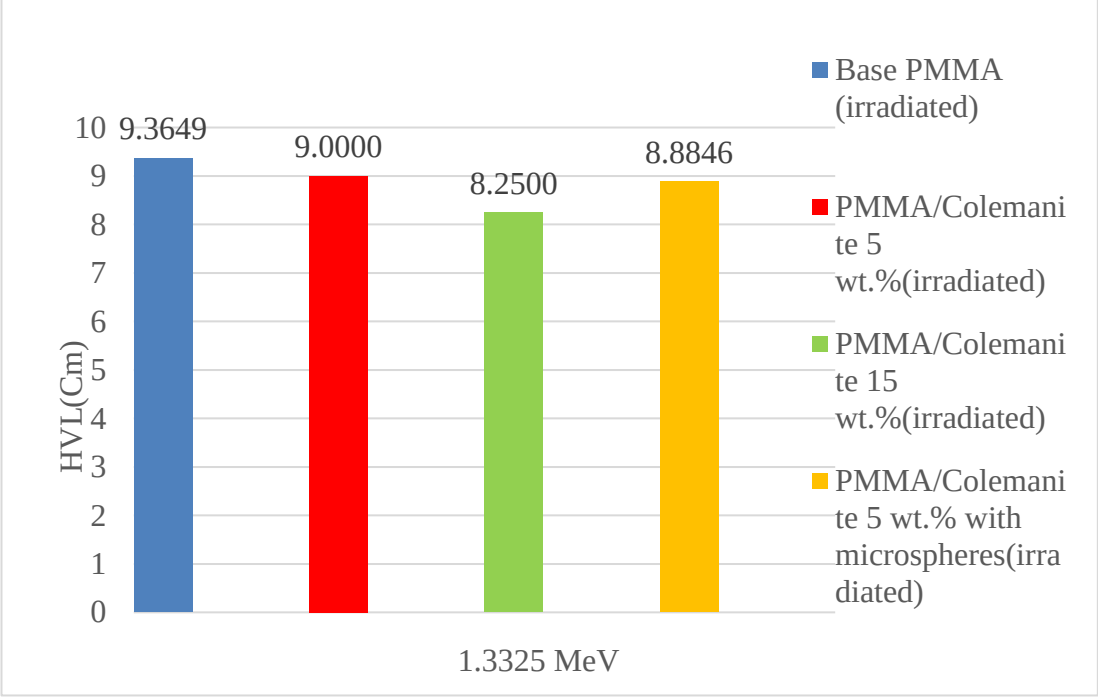

Figure 4.26 : The HVL values of the irradiated samples for 1.3325 MeV.

4.2.6 Comparison of irradiated and unirradiated sample for Co-60

Figure 4.27 and 4.28 shows the difference between the relative intensity with thickness for both irradiated and unirradiated sample for 1.1732 MeV and 1.3325 MeV respectively. Linear attenuation coefficient of unirradiated PMMA/Colemanite 15 wt.% has calculated as 0.087 and irradiated sample has calculated as 0.089 for 1.1732 MeV while 0.080 and 0.084 has calculated for 1.3325 MeV in turn.

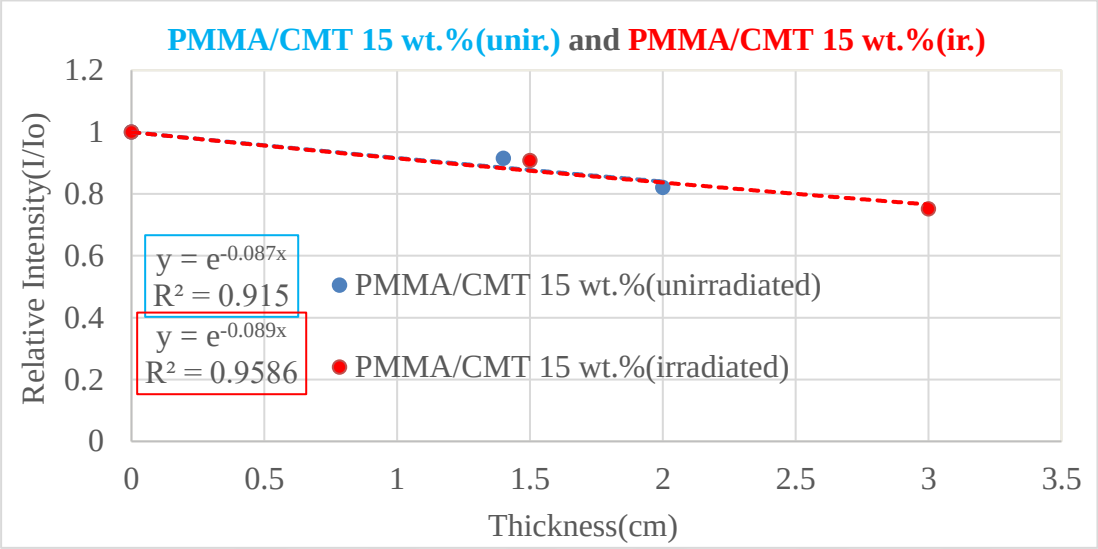

Figure 4.27 : The comparison of the relative intensity with thickness for irradiated and unirradiated PMMA/CMT 15 wt.% for 1.1732 MeV.

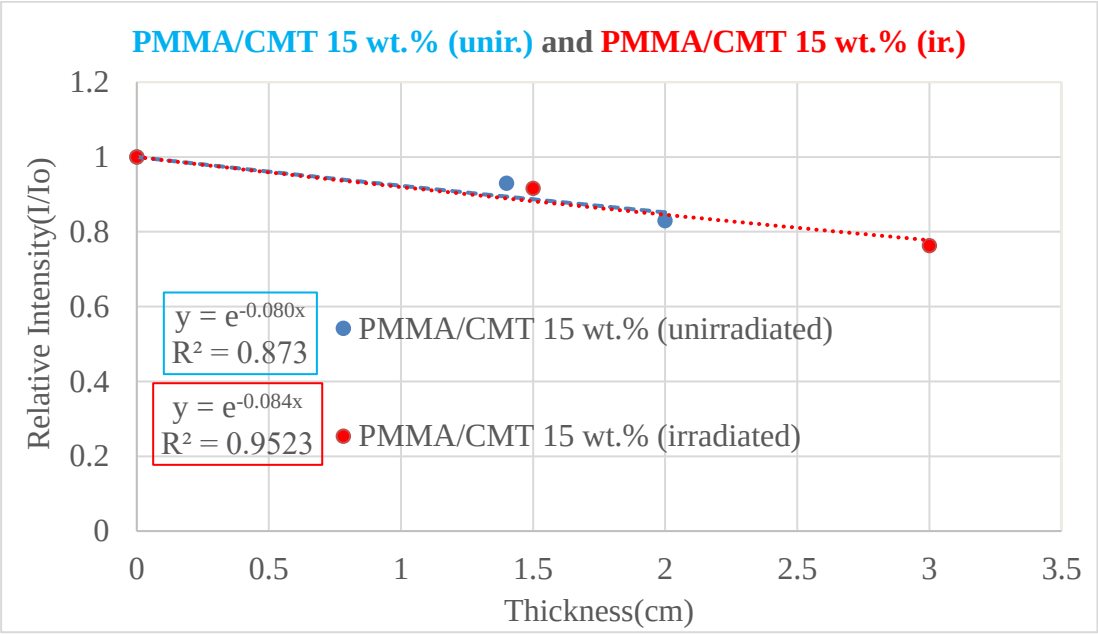

Figure 4.28 : The comparison of the relative intensity with thickness for irradiated and unirradiated PMMA/CMT 15 wt.% for 1.3325 MeV.

HVL values of the irradiated and unirradiated PMMA/Colemanite 15 wt.%. for 1.1732 MeV can be seen in Figure 4.29 while for 1.3325 MeV can be seen in Figure 4.30. HVL values of the regarding samples are close to each other for both energy peaks. HVL values of unirradiated and irradiated PMMA/Colemanite 15 wt.% has calculated as 7.96 and 7.78 respectively for 1.1732 MeV in terms of cm unit while has calculated as 8.66 and 8.25 respectively for 1.3325 MeV in terms of cm unit.

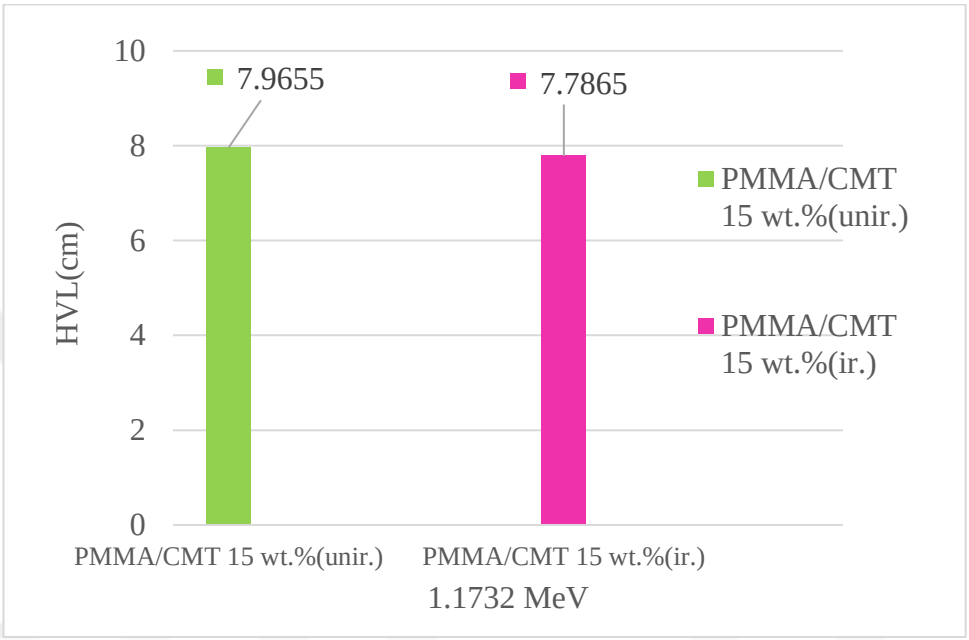

Figure 4.29 : The HVL values of the irradiated and unirradiated PMMA/CMT 15 wt.% for 1.1732 MeV.

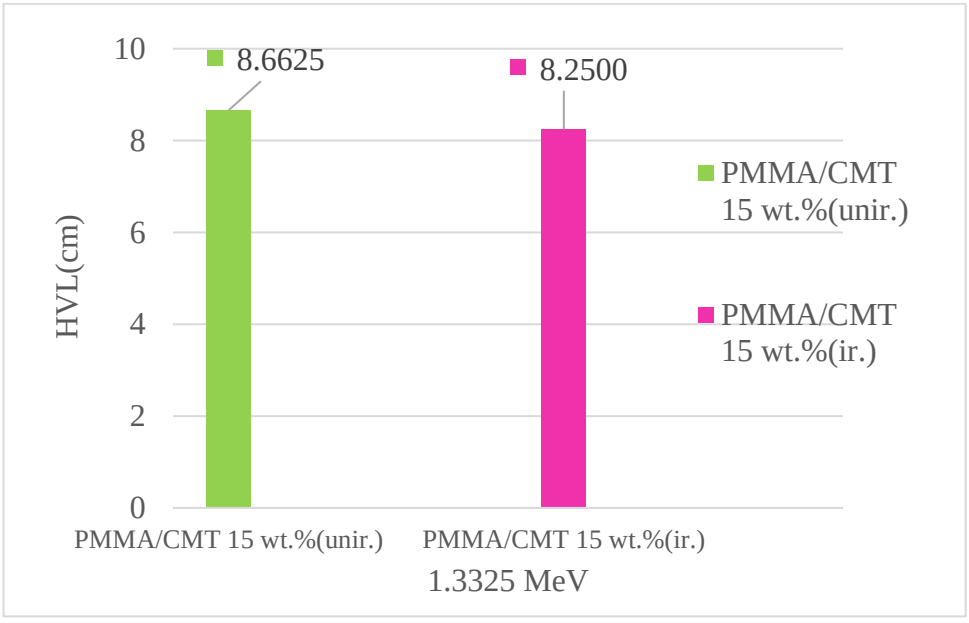

Figure 4.30 : The HVL values of the irradiated and unirradiated PMMA/CMT 15 wt.% for 1.3325 MeV.

4.3 Neutron Transmission Measurements

Figure 4.31 and Figure 4.32 have explained the intensity drop as a function of the penetration depth for irradiated base PMMA and PMMA/Colemanite 5 wt.% respectively. Linear attenuation coefficients of the relevant samples were calculated as 0,066 cm^{-1} and 0,070 cm^{-1} in turn.

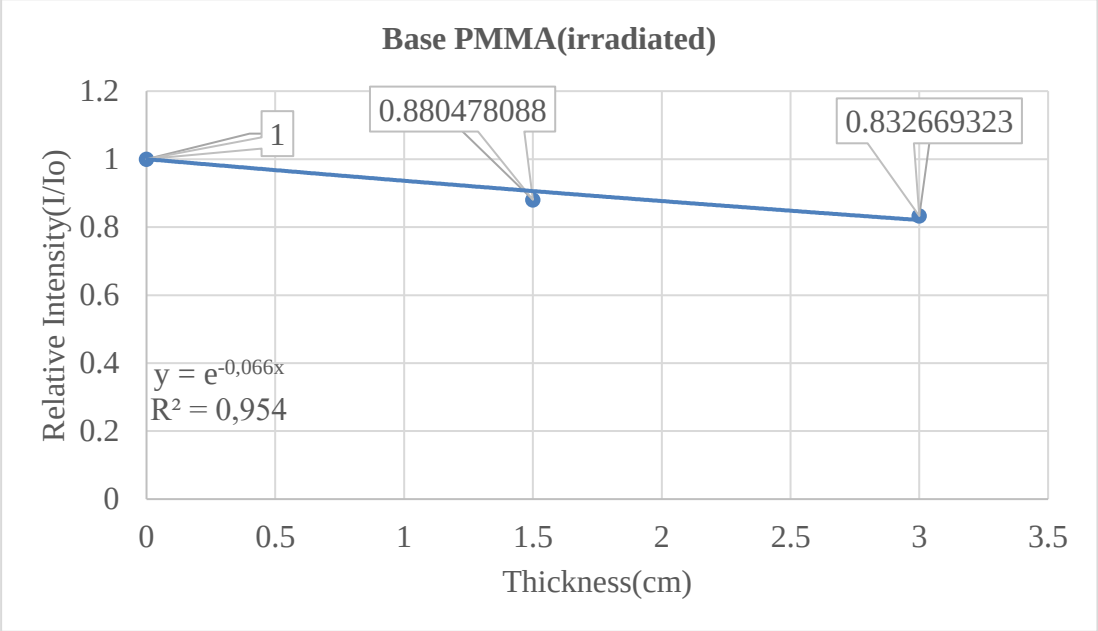

Figure 4.31 : The changes of the relative intensity with thickness for irradiated base PMMA for ~5 MeV.

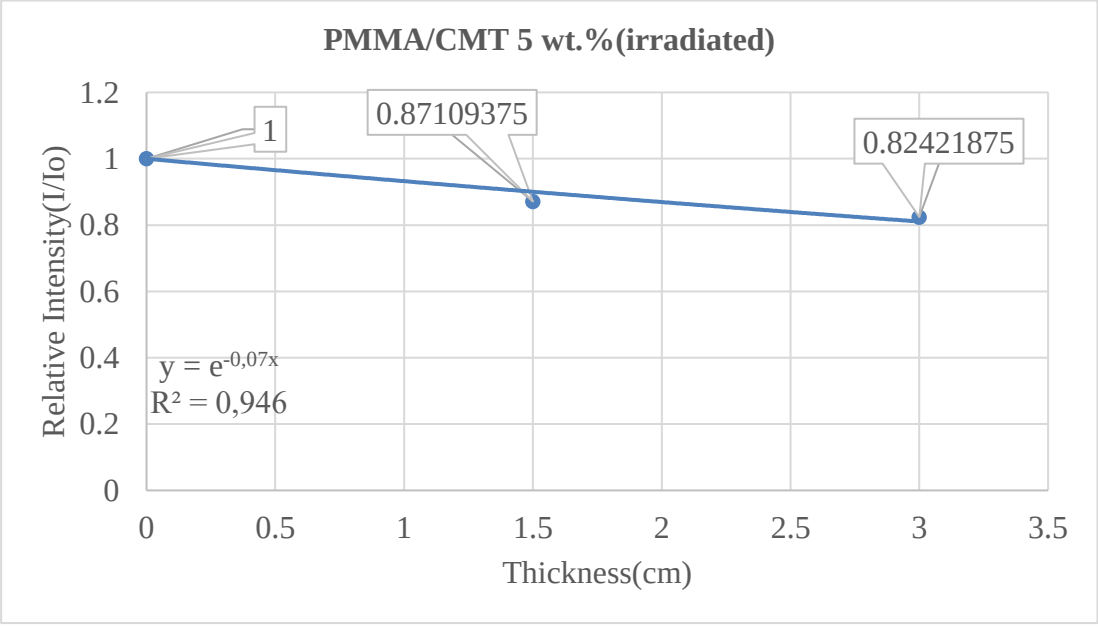

Figure 4.32 : The changes of the relative intensity with thickness for irradiated PMMA/CMT 5 wt.% for ~5 MeV.

Figure 4.33 and Figure 4.34 have explained the intensity drop as a function of the penetration depth for irradiated PMMA/Colemanite 15 wt.%. and PMMA/Colemanite 5 wt.% with microspheres respectively. Linear attenuation coefficients of the relevant samples were calculated as 0,078 cm^{-1} and 0,070 cm^{-1} in turn.

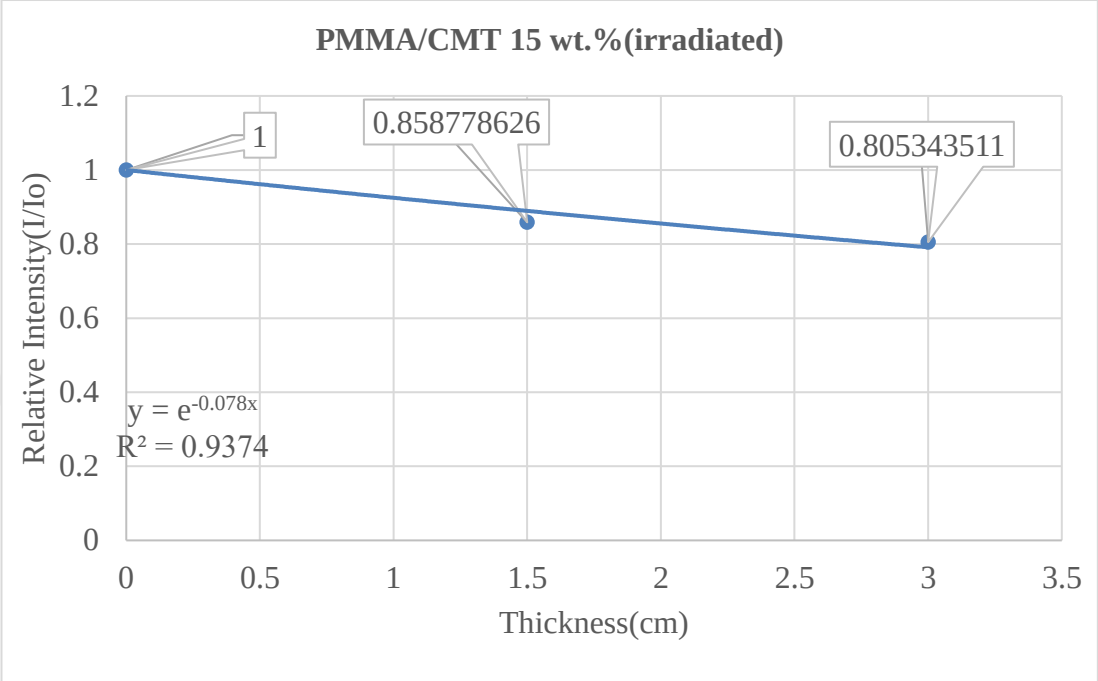

Figure 4.33 : The changes of the relative intensity with thickness for irradiated PMMA/CMT 15 wt.% for ~5 MeV.

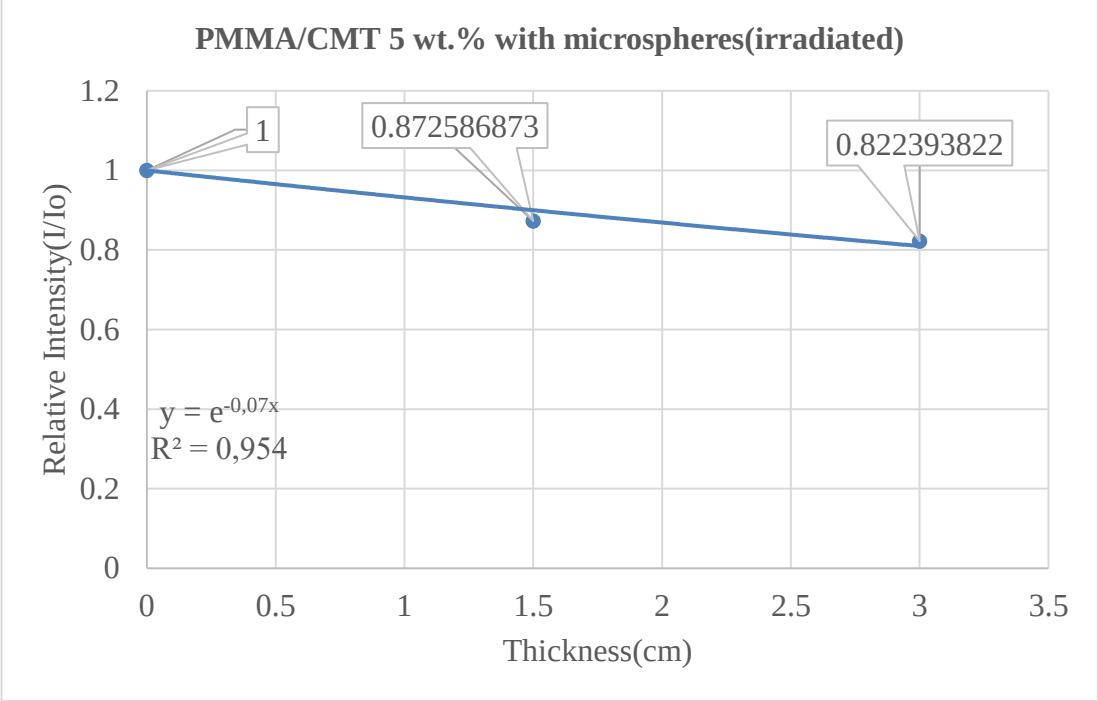

Figure 4.34 : The changes of the relative intensity with thickness for irradiated PMMA/CMT 5 wt.% with microspheres for ~5 MeV.

HVL values of the irradiated samples can be seen in Figure 4.35. As the amount of colemanite in the structure of the composite increased, the HVL value has decreased. However, there is no difference between the HVL values of PMMA/CMT 5 wt.% and PMMA/CMT 5 wt.% with microspheres samples.

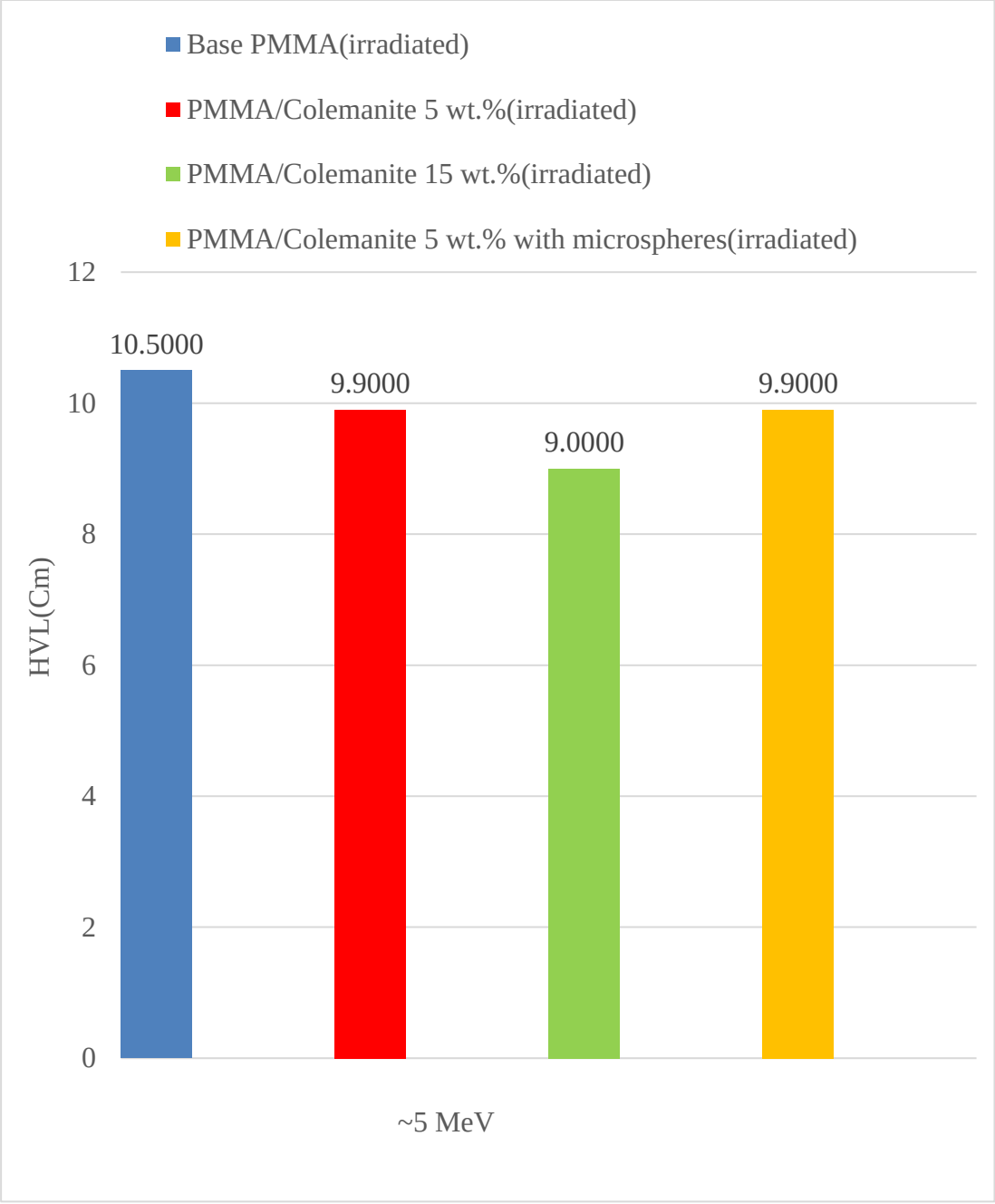

Figure 4.35 : The HVL values of the irradiated samples for ~5 MeV.

HVL values of base PMMA, PMMA/CMT 5 wt.%, PMMA/CMT 15 wt.% and PMMA/CMT 5 wt.% with microspheres has calculated as 10.5, 9.9, 9 and 9.99 in terms of cm unit respectively for average ~ 5 MeV neutrons.

4.3.1 Comparison of irradiated and unirradiated sample for ^{239}Pu-Be

Figure 4.36 has explained the difference between the relative intensity with thickness for both irradiated and unirradiated sample. The total macroscopic cross-sections of unirradiated PMMA/CMT 15 wt.% has calculated as 0.077 cm^{-1} while irradiated sample has calculated as 0.078 cm^{-1}. HVL values of unirradiated and irradiated PMMA/CMT 15 wt.% has calculated as 9 and 8.88 respectively for ~5 MeV in terms of cm unit which can be seen in Figure 4.37.

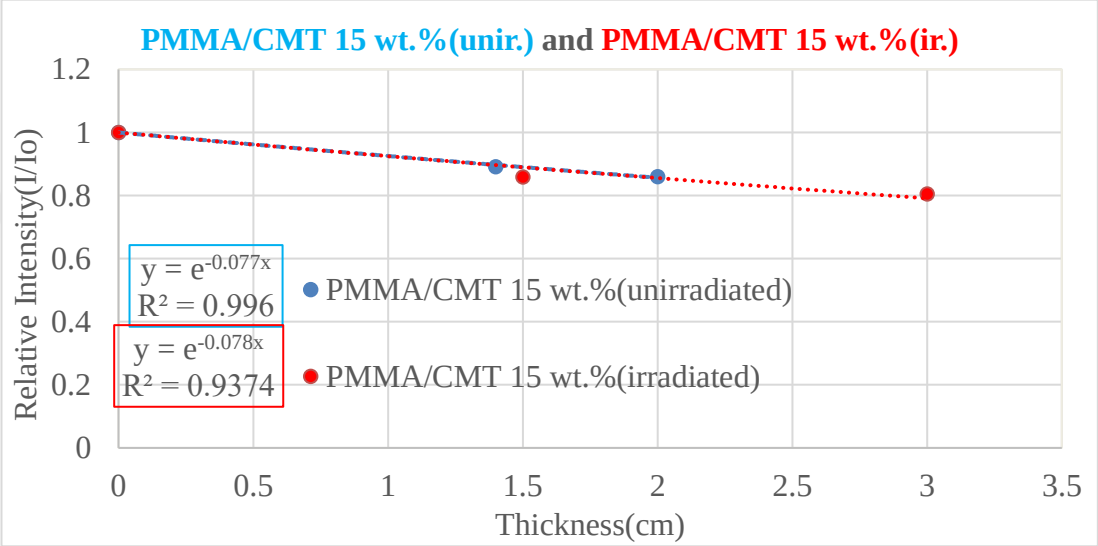

Figure 4.36 : The comparison of the relative intensity with thickness for irradiated and unirradiated PMMA/CMT 15 wt.% for ~5 MeV.

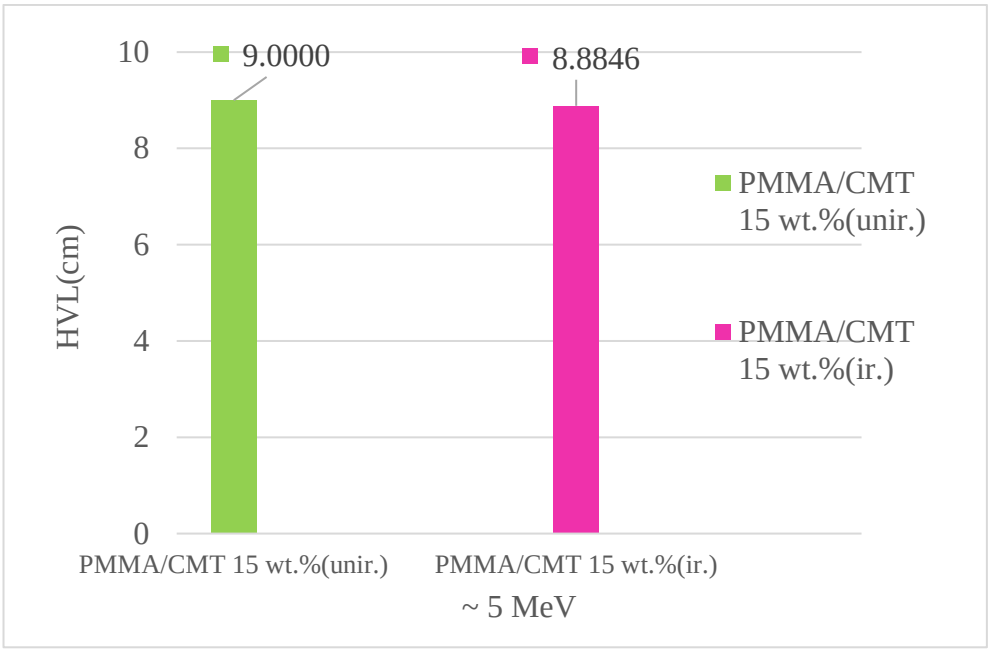

Figure 4.37 : The HVL values of the irradiated and unirradiated PMMA/CMT 15 wt.% for ~5 MeV.

4.4 Comparison of Attenuation Properties

Comparison of the linear attenuation coefficients of the regarding samples against negative beta particles emitted from Sr-90 can be found in Table 4.1.

Table 4.1 : Linear attenuation coefficients of the samples against beta particles at energy 0.546 MeV / 2.28 MeV.

Material	Linear Attenuation Coefficient(mm^{-1})
Base PMMA (irr.)	0.198
PMMA/CMT 5 wt.% (irr.)	0.201
PMMA/CMT 5 wt.% with microspheres(irr.)	0.201
PMMA/CMT 15 wt.% (irr.)	0.209
PMMA/CMT 15 wt.% (unirr.)	0.206

The change of the linear attenuation coefficients with the CMT ratio is shown numerically in Table 4.1 for all samples against β^- at 0.546 MeV / 2.28 MeV. The results clearly reveal the linear relationship between the proportional increase of CMT in the composite structure and the linear attenuation coefficient. Especially when a high level of radiation shielding was achieved against specifically for betas where it would be more useful to share the results in mm instead of cm. I/I_0 value has dramatically dropped to 0.032 with 15 mm thickness of PMMA/CMT 15 wt.% which means that broadly almost all negative beta particles emitted from Sr-90 were shielded with the sample.

Although it appears numerically that the base PMMA is also quite effective, the results reveal that a very high linear attenuation coefficient is obtained in terms of radiation shielding against betas together with the CMT reinforcement. In addition to all these, since the irradiated PMMA/CMT 15 wt.% has a higher linear attenuation coefficient than the unirradiated PMMA/CMT 15 wt.%, the irradiated sample will provide more effective radiation shielding against betas as it continues to be used in any space mission where space radiation exposure may occur.

Comparison of the linear attenuation coefficients of the regarding samples against γ rays at 0.662 MeV emitted from Cs-137 radioisotope can be found in Table 4.2.

Table 4.2 : Linear attenuation coefficients of the samples against gamma photons at energy 0.662 MeV.

Material	Linear Attenuation Coefficient(cm^{-1})
Base PMMA (irr.)	0.099
PMMA/CMT 5 wt.% (irr.)	0.104
PMMA/CMT 5 wt.% with microspheres(irr.)	0.104
PMMA/CMT 15 wt.% (irr.)	0.113
PMMA/CMT 15 wt.% (unirr.)	0.112

Unlike betas, there is no such an experimental result that shows shielding of almost all the gamma photons released from Cs-137 by the regarding samples for 15 mm and 30 mm. However, the most remarkable results have obtained in terms of gamma attenuation via the irradiated PMMA/CMT 15 wt.%. I/I_0 value has decreased to ~0.885 and ~0.695 in measurements took place with 15 mm and 30 mm respectively.

Comparison of the linear attenuation coefficients of the regarding samples against photons emitted from Co-60 at 1.1732 MeV and 1.3325 MeV can be found in Table 4.3. and 4.4 respectively.

Table 4.3 : Linear attenuation coefficients of the samples against gamma photons at energy 1.1732 MeV.

Material	Linear Attenuation Coefficient(cm^{-1})
Base PMMA (irr.)	0.080
PMMA/CMT 5 wt.% (irr.)	0.083
PMMA/CMT 5 wt.% with microspheres(irr.)	0.083
PMMA/CMT 15 wt.% (irr.)	0.089
PMMA/CMT 15 wt.% (unirr.)	0.087

Table 4.4 : Linear attenuation coefficients of the samples against gamma photons at energy 1.3325 MeV.

Material	Linear Attenuation Coefficient(cm^{-1})
Base PMMA (irr.)	0.074
PMMA/CMT 5 wt.% (irr.)	0.077
PMMA/CMT 5 wt.% with microspheres(irr.)	0.078
PMMA/CMT 15 wt.% (irr.)	0.084
PMMA/CMT 15 wt.% (unirr.)	0.080

The most remarkable results were obtained from irradiated PMMA/CMT 15 wt.% for both 1.1732 and 1.3325 MeV. While I/I_0 value has decreased to ~0.908 and ~0.751 for 15mm and 30mm respectively for 1.1732 MeV, ~0.916 and ~0.762 were observed at 1.3325 MeV for same thickness. In contrast to the results obtained from Cs-137, the difference between the linear attenuation coefficients of the irradiated and unirradiated sample is slightly higher for Co-60 which gives the clearer results to understand the effects of space radiation on the gamma attenuation behavior.In addition, comparison of the experimental results and theoretical outputs can be seen in Table 4.5. Theoretical outputs were obtained from the XCOM for Cs-137 and Co-60 for the unirradiated form of PMMA/CMT 15 wt.%.

Table 4.5 : Comparison of the experimental and theoretical results.

Sample	0.662 MeV	1.1732 MeV	1.3325 MeV
PMMA/CMT 15 wt.% (theoretical)	0.113	0.087	0.081
PMMA/CMT 15 wt.% (experimental)	0.112	0.087	0.080

The results clearly show that the experimental and theoretical results are quite close to each other.

Neutrons are another radiation type in a particle form that used in this study apart from β particles. The interaction of relatively high energy particles with nearly 5 MeV and the relevant samples is also important to expand the potential applications of samples. Just like β and γ attenuation results, it is observed that total macroscopic cross-section values linearly increase with the increasing ratio of CMT that contains various elements such as boron which is known as a reasonable neutron absorber. It is also worth noting that similar results were found for neutrons in terms of assessing the attenuation properties regarding the differences between irradiated and unirradiated samples just like the gamma attenuation results against Cs-137 since total macroscopic cross-sections values of the irradiated and unirradiated PMMA/CMT 15 wt.% are very close to each other.

The most effective results in terms of neutron attenuation were obtained from the PMMA/CMT 15 wt.% samples. It can be concluded that the irradiated sample is the most striking sample among all others when the uncertainty from experimental studies is neglected. I/I_0 value of irradiated PMMA/CMT 15 wt.% has calculated as 0.858 for 15 mm and 0.805 for 30 mm. It is very conspicuous that samples exposed to high doses of radiation for 363 days in space still has same attenuation behavior against neutrons in the most pessimistic approach.

Comparison of the total macroscopic cross-sections of the regarding samples against neutrons at ~5 MeV obtained via neutron howitzer NH3 (^{239}Pu-Be) produced by Nuclear Chicago Corporation can be found in Table 4.6

Table 4.6 : Total macroscopic cross-sections of the samples against neutron particles at energy ~5 MeV.

Material	Total macroscopic cross-sections (cm^{-1})
Base PMMA (irr.)	0.066
PMMA/CMT 5 wt.% (irr.)	0.070
PMMA/CMT 5 wt.% with microspheres(irr.)	0.070
PMMA/CMT 15 wt.% (irr.)	0.078
PMMA/CMT 15 wt.% (unirr.)	0.077

Comparison of the shielding percentage of incident radiation for the measured maximum thicknesses can be found in table 4.7. The comparison includes irradiated samples of different compositions PMMA/CMT composites. Shielding percentage of the materials were calculated with the following equation;

$$\text{Shielding percentage (\%): } [\ (1) - (I/I_{0max})\ x\ 100] \quad (4.1)$$

Table 4.7 : Comparison of the attenuation of the samples in percentage

Sample	0.546/2.28 MeV	0.662 MeV	1.1732 MeV	1.3325 MeV	~5 MeV
Base PMMA (irradiated)	96.6%	27.2%	22.8%	21.5%	16,8%
PMMA/CMT 5 wt.% (irradiated)	96.7%	28.5%	23.2%	22.2%	17.6%
PMMA/CMT 5 wt.%with microspheres(irradiated)	96.7%	28.9%	23.2%	22.4%	17.8%
PMMA/CMT 15 wt.% (irradiated)	97%	30.5%	24.9%	23.8%	19.5%

Results shows that irradiated form of PMMA/CMT 15 wt.% can stop 97% of the beta particles with the energy of 0.546 MeV and 2.28 MeV while 30.5%, 24.9% and 23.8% of the photons emitted from the Cs-137 and Co-60. In addition, 19.5% of the thermal neutrons with an energy of ~5 MeV can be shielded with 30mm thickness of the irradiated PMMA/CMT 15 wt.% composite.

It is clear that required thickness to shield the all the types of the radiations tested in this study is not possible with current thicknesses to operate a mixed radiation environment. However, it may be used in the mixed radiation environment depending on the radiation energies and intensities.

Therefore, the relevant sample can also be used in a mixed radiation environment where betas are densely present as it can also provide some shielding against gamma rays at different energies and neutrons with ~5 MeV energy.

4.5 The Approach for Experimental Study

The necessity of radiation shielding within the scope of space missions that might be planned to be carried out in various locations in the universe are explained in detail in the introduction chapter. However, it should not be ignored that the target location in space to be shielded from radiation directly effects radiation and material interactions due to the intensities and energies of different types of radiation in space strictly vary.

For this reason, the characteristics of the relevant target radiation/field must be specifically taken into account in various physical experiments or simulations about the shielding studies against space radiation. In addition, it is possible to say that a homogeneous radiation environment is not common in space. Mostly, the radiation cluster with different radiation components such as heavy nuclei and photons at different energies can be observed in space.

Therefore, it is necessary to focus on research by examining the radiation types in the relevant radiation cluster in the area to be shielded, rather than a specific type of radiation. However, there are differences in evaluating of the effects of different types of radiation separately and simultaneously. This simultaneous exposure of the samples against to high-energy and intense radiation is an important challenge that humanity faces and must be overcome in shielding studies against different components of space radiation.

The actual representation of harsh space radiation environment on Earth is an extremely crucial obstacle to conduct space research via ground-based experiments. Although the release of different photons and different high-energy particles at excessive energies to the target are not achieved simultaneously, it is possible to experimentally observe the exposure of different types of radiation to a target material in very short time intervals that can be considered as close to simultaneous action in experimental studies carried out on Earth.

To sum up, considering the operational applicability of the mixed radiation environment that can fully represent space radiation, the attenuation properties of the samples were examined separately for discrete radiation types and energies. Therefore, the obtained experimental results against beta, gamma and neutrons can be used more reasonably via local field approach principle for space studies.

4.6 The Approach for Shielding Study

All these challenges about working on space radiation somehow have caused the creation of alternative classifications. In other words, some research processes have been divided into simpler parts by the development of different understandings about approaching the topic. An example of this is the external field and local field approaches for the interpretation of incoming radiation. At this stage, since humanity has already collected the data such as the dose received inside the ISS, researchers have the opportunity to conduct various studies using the local field approach instead of the external one.

Although the external field approach might be preferable in some studies, it is still an extremely difficult scenario to experimentally simulate the entire space environment on Earth with a ground-based experiment. However, it should be noted that in some studies, external field approach is an inevitable reality and should be tried as much as possible instead of internal field for some specific studies within the scope of the laboratory facilities. On the other hand, since it is not necessary to systematically use external or internal field approaches, there is a possibility to make a series of independent comments via interpreting the data.

Active/passive shielding and their advantages were mentioned in detail in the introduction section. Operational restrictions for the space missions that carried out under the technological opportunities as of the first quarter of the 21st century show that the use of active shielding is not as feasible as passive shielding in space missions that are going to be performed in short term. However, increasing operational opportunities, developments in superconductor technology or possible developments in battery technologies reserve the opportunity to open a door for active shielding.

To sum up, it should be clearly stated that it is possible to see that active shielding to take an important place in space studies with the development of various technologies such as superconductor in the future. However, until achieve this goal in the future, passive shielding approach still has been using for various experiments carried out in space. Although there is a brief mention about active shielding in introduction section within the scope of this thesis, the study was completed by considering the passive shielding applications.

4.7 The Approach for Material Study

When the interpretation step is focused on a material basis approach rather than a radiation physics basis approach, it is possible to mention a number of factors in terms of suitability of the developed materials for use in the space environment. A number of obstacles such as the weight, mechanical strength and operational capability limitation which is the major factor preventing the use of active shielding in space also effects material design and development stages.

As a result of a rough evaluation at this point, it is possible to make an estimation about how very promising polymer-based materials are in terms of many properties such as cost, lightness, mechanical strength, radiation attenuation etc. In addition, it is not rational to expect polymers to provide sufficient functionality without any reinforcement in an environment like space where hosts a lot of independent operating conditions such as temperature, load, vibration, and radiation etc. For this very reason, it can be concluded that composite structures may be more advantageous than base polymer materials in terms of different expectations from the materials such as mechanical or radiation protection in space applications. Especially with the addition of different reinforcement agents to the polymer-based materials, an optimum level of structure that meets a great variety of demands can be obtained.

On the other hand, it would be extremely unfair to limit the place of polymers in space applications only as a matrix in composite structure. Polymers offer the wide opportunities to be produced in various structures with many alternative production methods. Moreover, when polymer-based materials are examined in terms of operationality in space studies and the functionality expected from a material such as recycling, and reforming can be found in the nature of a number of promising polymer materials. Finally, it should be noted that the lifetime of the relevant materials also appears as a critical parameter for long-term space missions. It is aimed to have a long effective lifespan of the materials in order to avoid permanent cargo costs in the space environment. The fact that the irradiated sample gives much better results in terms of attenuation against all radiation types that experimentally studied in this thesis which is an inevitably positive development in this sense for the long-term usage of the PMMA/CMT composites.

4.8 The Approach for PMMA/CMT Composites

However, some differences can be observed in the bonding of the structure that have been exposed to high doses in harsh radiation environment of the space. Deterioration of the homogeneous structure of the material can be observed as well as chemical bonding can be evaluated as positive or negative within the scope of the relevant purpose. The changes in the structure of the PMMA/CMT composites used in this thesis study as a result of exposure to open space radiation for approximately 1 year can also be evaluated positively or negatively within the framework of this logical approach. It is possible to observe that PMMA/CMT composites move away from the homogeneous structure even at the macro level. However, the changes in the bond structure with the dose received in low earth orbit can be evaluated as quite positive from the perspective of radiation shielding. As a matter of fact, the results show that there is a slight increase in beta, gamma, and neutron attenuation properties of the regarding samples.

'H', 'C' and 'O' in the structure of PMMA have relatively low atomic numbers and it is known that material compositions consisting of elements with low atomic numbers are more convenient against beta particles due to the elimination the risk of Bremsstrahlung formation. On the contrary, H, O, B and Ca that can be found in the chemical structure of CMT might be preferable elements against shielding gammas and neutrons as well as betas. Although it is inevitable to say that it is not entirely feasible to make a comprehensive interpretation from the chemical structure alone, it should be noted that both the experimental results of PMMA/CMT samples exposed to open space radiation in the ISS and samples that were not exposed to any radiation are also promising in terms of radiation shielding.

All things considered, the radiation attenuation properties of PMMA/CMT composites have interpreted with using passive shielding principles for local field approaches. The thesis study was carried out by taking into account the effects of the harsh radiation environment to the samples that exposed open space radiation in low earth orbit. It will be possible to make various interpretations, by considering the effects of exposure in on the attenuation properties of samples for the upcoming space research.

5. CONCLUSION

Space studies are steeply important for the future of humanity and the necessity of radiation shielding applications in space is inevitably obvious. Therefore, a great variety of scientific studies have been carried out and theories have been put forward for the shielding against space radiation. It is possible to say that PMMA/CMT composites in different compositions produced with the ATRP technique can be a critical milestone in space studies due to the basic principles of ATRP. CMT addition to PMMA has increased the attenuation properties of the composites against all the radiation types studied in this thesis which are beta, gamma and neutron radiations. The fact remains that, there is no scientific evidence that has been found regarding the direct effect of microspheres on the attenuation coefficients.

Moreover, the increase in the attenuation properties of the PMMA/CMT 15 wt.% sample after exposure to space radiation is an astonishing output for the long-term use of related materials in space applications. PMMA/CMT composites have provided outstanding results even with relatively low thickness values against beta radiation. On the other hand, regarding PMMA/CMT composites synthesized by ATRP technique can be considered as promising material for the future against gamma and neutron radiations.

The reason for the improvement of the attenuation properties of the relevant composites can be considered as the technique preferred for the production of the samples. It can be deducted that new reactive end groups and free radicals occurred as a result of exposure to space radiation. Furthermore, formation of molecular cross-links can be stated by the formation of new reactive end groups and free radicals. Hence, the network structure of the material can be compressed and strengthened via the formation of cross-links.

In conclusion, PMMA/CMT composites synthesized by ATRP technique can be used for several long-term space applications due to the improved attenuation capabilities as a result of the exposure to space radiation in low earth orbit.

REFERENCES

[1] Obodovskiy, I. (2019). The early history of Radiation Damage. Radiation, 505–511.

[2] Podgorsak, E. B. (2010). Radiation physics for medical physicists. 2. enl.

[3] Zhang, J., Traylor, K. S., & Mountz, J. M. (2020, December). PET and SPECT imaging of brain tumors. In Seminars in Ultrasound, CT and MRI (Vol. 41, No. 6, pp. 530-540). WB Saunders

[4] Martin, J. E. (2006). Physics for radiation protection: a handbook. John Wiley & Sons.

[5] Barthel, J., & Sarigul-Klijn, N. (2019). A review of radiation shielding needs and concepts for space voyages beyond Earth's magnetic influence. Progress in Aerospace Sciences, 110, 100553.

[6] Cucinotta, F. A. (2014). Space radiation risks for astronauts on multiple International Space Station missions. PloS one, 9(4), e96099.

[7] Kilifarska, N. A., Bakmutov, V. G., & Melnyk, G. V. (2020). The hidden link between Earth's magnetic field and climate. Elsevier.

[8] L'Annunziata, M. F. (2016). Cosmic radiation. Radioactivity, 495–518.

[9] Dyer, C. S., Truscott, P. R., Evans, H., Sims, A. J., Hammond, N., & Comber, C. (1996). Secondary radiation environments in heavy space vehicles and instruments. Advances in Space Research, 17(2), 53-58.

[10] Bond, D. K., Goddard, B., Singleterry Jr, R. C., & y León, S. B. (2019). Evaluating the effectiveness of common aerospace materials at lowering the whole body effective dose equivalent in deep space. Acta Astronautica, 165, 68-95.

[11] Dobynde, M. I., & Shprits, Y. Y. (2020). Radiation environment created with GCRs inside a spacecraft. Life Sciences in Space Research, 24, 116-121.

[12] Bartlett, D. T., Hager, L. G., & Tanner, R. J. (2003). The determination of the neutron component of cosmic radiation fields in spacecraft. Radiation measurements, 36(1-6), 439-443.

[13] Litvak, M. L., Mitrofanov, I. G., Sanin, A. B., Bakhtin, B., Golovin, D. V., & Zeitlin, C. (2021). Observations of neutron radiation environment during Odyssey cruise to Mars. Life Sciences in Space Research, 29, 53-62.

[14] Armstrong, T. W., & Colborn, B. L. (2001). Predictions of secondary neutrons and their importance to radiation effects inside the International Space Station. Radiation measurements, 33(3), 229-234.

[15] Mary, H., Brian, K., Hans, M., Thiago, B., Feifei, C., & Yuri, S. (2009). Relationship of the van Allen radiation belts to solar wind drivers. In Geodetic and Geophysical Research Institute of the Hungarian Academy of Sciences (Ed.). International Association of Geomagnetism and Aeronomy IAGA 11 Scientific Assembly, (p. 1212).

[16] Sforza, P. M. (2016). The space environment. Manned Spacecraft Design Principles, 47–58.

[17] G.M. Studios, (2013). Van Allen Probes Find Storage Ring in Earth's Outer Radiation Belt [Online image]. accessed April 21, 2024 https://svs.gsfc.nasa.gov/vis/a010000/a011200/a011212/Mona_2.jpeg.

[18] Spillantini, P., Casolino, M., Durante, M., Mueller-Mellin, R., Reitz, G., Rossi, L., ... & Sorbi, M. (2007). Shielding from cosmic radiation for interplanetary missions: Active and passive methods. Radiation measurements, 42(1), 14-23.

[19] Tripathi, R. K. (2016). Meeting the Grand Challenge of Protecting Astronauts Health: Electrostatic Active Space Radiation Shielding for Deep Space Missions (No. HQ-E-DAA-TN33876).

[20] Spillantini, P. (2014). Manned exploration and exploitation of solar system: Passive and active shielding for protecting astronauts from ionizing radiation—A short overview. Acta Astronautica, 104(2), 509-515**.**

[21] Fry, D., Madzunkov, S., Simcic, J., & Hunt, A. W. (2021). Application of scaling methods to foster ground development of active shielding concepts for space exploration. Acta Astronautica, 178, 296-307.

[22] Vana, N., Hajek, M., Berger, T., Fugger, M., & Hofmann, P. (2006). Novel shielding materials for space and air travel. Radiation protection dosimetry, 120(1-4), 405-409.

[23] Cataldo, F., & Prata, M. (2020). Neutron radiation shielding composites for deep space exploration: an introduction. In Micro and nanostructured composite materials for neutron shielding applications (pp. 263-285). Woodhead Publishing.

[24] Norbury, J. W., Schimmerling, W., Slaba, T. C., Azzam, E. I., Badavi, F. F., Baiocco, G., ... & Zeitlin, C. J. (2016). Galactic cosmic ray simulation at the NASA Space Radiation Laboratory. Life sciences in space research, 8, 38-51.

[25] Slaba, T. C., Blattnig, S. R., Norbury, J. W., Rusek, A., La Tessa, C., & Walker, S. A. (2015). GCR simulator reference field and a spectral approach for laboratory simulation (No. NASA/TP-2015-218698).

[26] Callister Jr, W. D. (2007). Materials science and engineering an introduction.

[27] Carraher Jr, C. E. (2017). Carraher's polymer chemistry. CRC press.

[28] Dodiuk, H., & Goodman, S. H. (2014). Introduction. Handbook of Thermoset Plastics, 1–12. https://doi.org/10.1016/b978-1-4557-3107-7.00001-4

[29] Wang, M., Guo, L., & Sun, H. (2019). Manufacture of biomaterials. Encyclopedia of Biomedical Engineering, 116–134.

[30] Hasirci, V., Yilgor, P., Endogan, T., Eke, G., & Hasirci, N. (2011). 1.121-polymer fundamentals: polymer synthesis (pp. 349-371). Oxford, Elsevier.

[31] More, C. V., Alsayed, Z., Badawi, M. S., Thabet, A. A., & Pawar, P. P. (2021). Polymeric composite materials for radiation shielding: a review. Environmental chemistry letters, 19, 2057-2090.

[32] Chang, L., Zhang, Y., Liu, Y., Fang, J., Luan, W., Yang, X., & Zhang, W. (2015). Preparation and characterization of tungsten/epoxy composites for γ-rays radiation shielding. Nuclear Instruments and Methods in Physics Research Section B: Beam Interactions with Materials and Atoms, 356, 88-93.

[33] Durante, M. (2014). Space radiation protection: destination Mars. Life sciences in space research, 1, 2-9**.**

[34] Takahashi, Y., & Tanaka, K. (1992). Material recycling in a regenerative life support system for space use: its issues and waste processing. Advances in Space Research, 12(5), 65-73.

[35] Webb, J. C. J., & Spencer, R. F. (2007). The role of polymethylmethacrylate bone cement in modern orthopaedic surgery. The Journal of Bone & Joint Surgery British Volume, 89(7), 851-857.

[36] Wypych, G. (2016). PMMA polymethylmethacrylate. Handbook of Polymers, 467–471.

[37] Goseki, R., & Ishizone, T. (2014). Poly(methyl methacrylate) (PMMA). Encyclopedia of Polymeric Nanomaterials, 1–11.

[38] Ali, U., Karim, K. J. B. A., & Buang, N. A. (2015). A review of the properties and applications of poly (methyl methacrylate)(PMMA). Polymer Reviews, 55(4), 678-705.

[39] Cataldo, F., & Prata, M. (2019). New composites for neutron radiation shielding. Journal of Radioanalytical and Nuclear Chemistry, 320(3), 831-839.

[40] Cao, D., Yang, G., Bourham, M., & Moneghan, D. (2020). Gamma radiation shielding properties of poly (methyl methacrylate)/Bi2O3 composites. Nuclear Engineering and Technology, 52(11), 2613-2619.

[41] Li, Z., Chen, S., Nambiar, S., Sun, Y., Zhang, M., Zheng, W., & Yeow, J. T. (2016). PMMA/MWCNT nanocomposite for proton radiation shielding applications. Nanotechnology, 27(23), 234001.

[42] Bel, T., Mehranpour, S., Şengül, A. V., Camtakan, Z., & Baydogan, N. (2021). Electron beam penetration of poly (methyl methacrylate)/colemanite composite irradiated at low earth orbit space radiation environment. Journal of Applied Polymer Science, 138(45), 51337.

[43] Haldar, S. K. (2020). Minerals and rocks. Introduction to Mineralogy and Petrology, 1–51.

[44] Al-Omari, S., Afaneh, F., Alsaif, N. A., Al-Ghamdi, H., Rammah, Y. S., & Khattari, Z. Y. (2024). Optimization radiation shielding properties of aluminum-based spinel minerals through the crystal tetrahedral and octahedral voids and their ions composition. Radiation Physics and Chemistry, 217, 111527.

[45] Aygün, B. (2019). Neutron and gamma radiation shielding properties of high-temperature-resistant heavy concretes including chromite and wolframite. Journal of Radiation Research and Applied Sciences, 12(1), 352-359.

[46] Frost, R. L., Xi, Y., Scholz, R., Belotti, F. M., & Cândido Filho, M. (2013). Infrared and Raman spectroscopic characterization of the borate mineral colemanite–CaB3O4 (OH) 3· H2O–implications for the molecular structure. Journal of Molecular Structure, 1037, 23-28.

[47] Okuno, K. (2005). Neutron shielding material based on colemanite and epoxy resin. Radiation protection dosimetry, 115(1-4), 258-261.

[48] Abdulrahman, S. T., Ahmad, Z., Thomas, S., & Rahman, A. A. (2020). Introduction to neutron-shielding materials. In Micro and nanostructured composite materials for neutron shielding applications (pp. 1-23). Woodhead Publishing.

[49] Bevelacqua, J. J., & Mortazavi, S. M. J. (2020). Neutron shielding concrete in medical applications. In Micro and Nanostructured Composite Materials for Neutron Shielding Applications (pp. 219-237). Woodhead Publishing.

[50] Bel, T., Arslan, C., & Baydogan, N. (2019). Radiation shielding properties of poly (methyl methacrylate)/colemanite composite for the use in mixed irradiation fields of neutrons and gamma rays. Materials Chemistry and Physics, 221, 58-67.

[51] Chowdhury, M. J., & Blust, R. (2011). Strontium. Fish physiology, 31, 351-390.

[52] Ashraf, M. A., Akib, S., Maah, M. J., Yusoff, I., & Balkhair, K. S. (2014). Cesium-137: radio-chemistry, fate, and transport, remediation, and future concerns. Critical reviews in environmental science and technology, 44(15), 1740-1793.

[53] Cámara-Martos, F., & Moreno-Rojas, R. (2016). Cobalt: Properties and determination. Encyclopedia of Food and Health, 166–171. https://doi.org/10.1016/b978-0-12-384947-2.00175-6

[54] Topuz, A.I., & Reyhancan, I.A. (2018). Neutronic Analysis of a Nuclear-Chicago NH3 Neutron Howitzer. arXiv: Instrumentation and Detectors**.**

CURRICULUM VITAE

Name Surname **:** Mehmet Orhan **ŞIRIN**

EDUCATION

- **B.Sc.** **:** 2021, Yildiz Technical University, Department of Metallurgical and Materials Engineering

PUBLICATIONS, PRESENTATIONS AND PATENTS ON THE THESIS:

- Baydogan, N., **Sirin, M.O.** 2024: Investigation of the Effects of the Exposure to Space Radiation in ISS on Gamma Attenuation Properties of PMMA/CMT Composites via Co-60. International Congress - SMARTINDUSTRY, April 18-20, 2024, Lviv, Ukraine.
- Baydogan, N., **Sirin, M.O.** 2024: Comparison of Gamma Attenuation Properties of Poly (methyl methacrylate) / Colemanite Composites via Cs-137 Before and After the Exposure to Space Radiation in Low Earth Orbit. International Congress - IGRS, May 8-10, 2024, Istanbul, Turkey.